Wesleyan University

GEOMETRIES OF MARTIAN HILLSIDE GULLIES IN THE NORTHERN HEMISPHERE: EVIDENCE FOR AN INSOLATION-DRIVEN MECHANISM OF FORMATION

By

Nina Lanza

Faculty Advisor: Dr. Martha Gilmore

A Thesis submitted to the Faculty of Wesleyan University in partial fulfillment
of the requirements for the Degree of Master of Arts in
Earth and Environmental Sciences

Middletown, Connecticut May 2006

Table of Contents

Table of contents……………………………………………………………………ii
List of Tables……………………………………………………………………iv
List of Figures…...…………………………………………………………………iv
Acknowledgements…..……………………………………………………………...vii

I. Introduction………………………………………………………………….…1
Definition of a gully
Significance of gullies on Mars
Goal of the study
Limitations of the study
Summary of results and conclusion
II. Background…………………………………………………………………….6
1. Morphologic and geometric observations of gullies………………………6
2. Proposed formation mechanisms…………………………………………...8
a. Dry flow……………………………………………………………….8
b. Formation by CO_2………………………………………………………11
c. Formation by H_2O………………………………………………………14
i. Subsurface ice and liquid…………………………………..14
ii. Melting of surface ice……………………………………..17
3. Stability and placement of water…………………………………………..19
a. The surface environment today……………………………….…19
b. Changes in obliquity……………………………………………...20
c. The effect of insolation and slope angle…………..………………22
III. Methods………………………………………………………………………24
1. Data sets…………………………………………………………………..24
a. Images from the Mars Orbiter Camera (MOC)……………………24
b. Topography from the Mars Orbiter Laser Altimeter (MOLA)……25
c. Gully locations………………………………………………………25
2. Measurement technique…………………………………………………...26
a. Creating digital elevation models from MOLA data……………...26
i. Interpolating with GMT……………………………………26
ii. Creating ArcMap compatible files using Perl…………….27
iii. Putting data into ArcMap………………………………...29
b. Processing MOC images with ISIS and Perl……………………...29
c. MOC and MOLA in ArcMap……………………………………...31
d. Digitizing features in ArcMap…………………………………….32
IV. Results…………………………………………………………………………...33
1. Slope…………………………………………………………………………33
2. Depths………………………………………………………………………..33
3. Orientations…………………………………………………………………..33

4. Insolation……………………………………………………………..35
a. Present obliquity 25.2°…………………………………………….35
b. Other obliquities (5° and 60°)……………..………………………43
5. Slope temperatures…………………………………………………...47
a. Blackbody…………………………………………………………48
b. Basalt………………………………………………………………50
c. Sand………………………………………………………………..52
6. Summary of results…………………………………………………..53
V. Discussion……………………………………...……………………57
1. Gully slopes…………………………………………………………57
2. Gully depths………………………………………………………...59
3. Gully orientation……………………………………………………..61
4. Insolation modeling…………………………………………………63
5. Constraints on gully formation……………………………………68
a. Water emplacement at high obliquity……………………………..68
b. Insolation differences at varying obliquities………………………69
i. Thermal heating and water stability………………………..69
ii. Development of gullies by release of subsurface water…..71
6. Model Constraints……………………………………………………73
a. Subsurface ice, aquicludes, and shallow aquifers…………………73
b. Snowmelt……………………………………………………………76
7. Summary of discussion………………………………………………78
VI. Conclusions and recommendations…………………………………..80
VII. References…………………………………………………………...87

List of Tables

1. Orientation of gullied slopes binned by orientation……………………………….……34
2. Averages and ranges of irradiance on gullied and nongullied slopes at 25.2° obliquity…………………………………………………………………………...42

List of Figure Captions (by figure number)

Background

B1. Gullies and associated landforms. The three main elements are the alcove, the channel, and the apron. From Malin and Edgett (2000).

B2. Examples of various gully morphologies. From Malin and Edgett (2000).

B3. MOC images containing gullies binned by latitude in the southern hemisphere. The majority of the gullies are found in the midlatitudes, although there is also a cluster found in the polar region ~70°S. From Heldmann and Mellon (2004).

B4. Depths of gully alcoves in relation to the surface topography of the southern hemisphere. From Heldmann and Mellon (2004).

B5. Depths of gully alcoves from the surface by latitude, for southern hemisphere gullies. From Heldmann and Mellon (2004).

B6. Southern hemisphere gullies binned by orientation. In the lower latitudes (30°S-44°S), gullies face poleward, while in mid to high latitudes (44°S-58°S), gullies face equatorward. From Heldmann and Mellon (2004).

B7. Southern and northern hemisphere gullies binned by orientation. Gullies appear in all orientations. From Edgett et al. (2003).

B8. The temperature-pressure environment at southern hemisphere gully alcove depth in relation to CO_2 stability. Triangles represent a dry overburden and diamonds represent an icy overburden. In either case, the majority of gullies fall outside of the field of liquid CO_2 stability. From Heldmann and Mellon (2004).

B9. The temperature-pressure environment at southern hemisphere gully alcove depth in relation to H_2O stability. Triangles represent a dry overburden and diamonds represent an icy overburden. If an dry overburden is assumed, ~80% of the

gullies will be within the stability field of liquid water. From Heldmann and Mellon (2004).

B10. Insolation variation with solar zenith angle. As the zenith angle approaches 90°, the insolation goes to 0. From Hecht (2002).

Results

1. Slope orientations by latitude.
   a) Orientation from 0-359°.
   b) Orientation binned by facing direction. Values above 360 represent orientations between 0-90° (orientation + 360).
2. Slope angles of gullies and nongullies.
3. Depths
   a) Depths of gullies below the surface by latitude. Error bars = 86 m.
   b) Absolute depth from the aeroid of gullies and nongullies by latitude. Error bars = 86 m.

..

5. Maximum noontime irradiance at current obliquity = 25.2°
   a) nongullied slopes by latitude
   b) nongullied slopes by orientation
   c) gullied slopes by latitude
   d) gullied slopes by orientation.
6. Daily average irradiance at current obliquity = 25.2°
   a) nongullied slopes by latitude
   b) nongullied slopes by orientation
   c) gullied slopes by latitude
   d) gullied slopes by orientation.
7. Maximum noontime irradiance at obliquity = 5°
   a) gullied slopes by latitude
   b) gullied slopes by orientation
   c) nongullied slopes by latitude,
   d) nongullied slopes by orientation.
8. Maximum noontime irradiance at obliquity = 60°
   a) nongullied slopes by latitude
   b) nongullied slopes by orientation
   c) gullied slopes by latitude
   d) gullied slopes by orientation.
9. Difference in insolation between gullied and nongullied slopes
   a) at obliquity = 5° by latitude
   b) at obliquity = 5° by orientation
   c) obliquity = 25.2° by latitude

d) at obliquity = 25.2° by orientation
e) at obliquity = 60° by latitude
f) at obliquity = 60° by orientation. Difference computed as gully – nongully for binned average values for latitude bins = 5°, orientation bins = 45°.

10. Maximum noontime temperatures on gullied slopes by latitude at
a) obliquity = 5°
b) obliquity = 25.2°
c) obliquity = 60°
by orientation at
d) obliquity = 5°
e) obliquity = 25.2°
f) obliquity = 60°

11. Maximum noontime temperatures on nongullied slopes by latitude at
a) obliquity = 5°
b) obliquity = 25.2°
c) obliquity = 60°
by orientation at
d) obliquity = 5°
e) obliquity = 25.2°
f) obliquity = 60°

12. Temperatures on basalt slopes (ε = 0.72) at obliquity = 25.2° for gullied slopes
a) by latitude
b) by orientation
for nongullied slopes
c) by latitude
d) by orientation.

13. Temperatures on sand slopes (ε = 0.9) at obliquity = 25.2° for gullied slopes
a) by latitude,
b) by orientation
for nongullied slopes
c) by latitude
d) by orientation

X. Difference in insolation between gullied and nongullied slopes by season at different obliquities. By latitude
1) spring, 3) summer, 5) fall, 7) winter; by orientation 2) spring, 4) summer, 6) fall, 8) winter.

Z. Difference in temperature between gullied and nongullied slopes by season at different obliquities. By latitude 1) spring, 3) summer, 5) fall, 7) winter; by orientation 2) spring, 4) summer, 6) fall, 8) winter.

Acknowledgements

Much thanks must be given to my friends, who made finishing this work possible by bringing me food, catching my mistakes, and listening to me work out my ideas aloud. This work would not be possible without the contributions of Heather Olins, Astrid Hesse, Jennifer Connelly, Ethan De Seif, Dave Carlsson, Anne Rhodes, my parents Richard and Sylvia Lanza, and many more who gave their time to ensure this work could be finished. I would also like to thank Barbara Ann Winter Schukoske for helping me navigate the labyrinth of the administrative side of graduate school as well as showing me a picture of her squirrel when she knew my life was at its most chaotic.

I would also like to thank my advisor, Dr. Marty Gilmore, for her guidance these past two years. She has helped me to accomplish tasks I never imagined I could be capable of, and she has prepared me well for my future graduate work.

Most of all, I would like to thank Mouser Williams, who convinced me that I could go to graduate school in the first place, and who has offered unending support and kindness when I have needed them most.

I. Introduction

On Earth, a gully has been defined as a steep sided channel that is formed by surface or subsurface flow (Higgins et al, 1990). Gullies vary greatly in size, but tend to have "a width greater than about 1 foot, and a depth greater than about 2 feet" (Brice 1966, as quoted in Higgins et al, 1990). However, gullies are fairly small features when seen in a global context. Gullies are formed when near-surface liquid undermines the surface and causes it to collapse (Higgins et al, 1990). Often, this collapse creates a steep slope above the region of output, and significant undercutting will occur. The collapse is contingent upon the surface being composed of unconsolidated materials such as soil; gullies will not form in solid rock.

Gully-like features on Mars were first detected by the Mars Orbiter Camera (MOC) on the Mars Global Surveyor (MGS) spacecraft, which was launched in 1996 and began returning data in 1998. This instrument can photograph the surface of Mars at resolutions of 1.4-1.6 m/pixel (Malin et al, 2004). This resolution was a significant improvement on past instruments' resolutions, and it allowed small scale features like the gullies to be resolved and observed. Malin and Edgett (2000) were the first to describe these features. Both they and Edgett et al. (2003) observed that gullies are only observed poleward of 30° in both hemispheres. Malin and Edgett (2000) suggest that this latitudinal dependence indicates a relationship between insolation and gullies, which in turn suggests a thermal control on their formation.

Malin and Edgett (2000) also inferred the relative ages of the gullies by cross cutting relationships. They note that gullies are seen to overlay features such as dunes, which are young, transient landforms. Gullies also have sharp relief, which is not expected in older features that have had time to erode by either mass wasting or aeolian processes. Gullies also have not been observed with impact craters layered on top of them, again point to their relative youth.

On Earth, gullies indicate the presence of liquid water. Thus, their possible existence on Mars is significant. Currently, liquid water is not stable on the surface. If liquid water has been present on the surface in the recent past, then our understanding of fundamental martian surficial processes would be greatly altered. In addition, Mars and Earth have similar origins; we can learn much about the origins of life on Earth from life—or the lack thereof—on Mars. Water is a necessary ingredient for life, and its presence on Mars leaves open the possibility for life's existence.

Today, erosion on Mars is dominated by aeolian processes (Greeley et al., 1992). However, large scale fluvial features indicate that water once played a larger role in shaping the surface. Baker et al. (1992) examined large scale channels (~30 km) and valley networks, and found that these features exhibit signs of formation by a liquid, such as streamlining and sedimentation. They point to the morphologic similarities between these features and the Channeled Scabland in the western U.S., and note that flow of water provides the simplest explanation for these features. Other possible liquids, such as lava, do not generally form both streamlined features and incised channels. However, liquid water is not presently stable on the surface. This suggests that the process that created these features occurred sometime in the past, when the temperature-pressure environment was significantly different. Models of Mars' early atmosphere suggests that it may have been thicker in the past, and that it was likely primarily CO_2 as it is today (Fanale et al., 1992). A thicker CO2 atmosphere could lead to increased thermal heating on the surface due to a greenhouse effect, in which thermal energy from insolation is retained by the atmosphere. This would act not only to increase temperatures, but also pressures on the surface. Additionally, the heat flow in the past was likely several times its current value (Fanale et al., 1992). Fanale et al. (1992) note that the valley networks are almost entirely confined to the most heavily cratered terrain, which points to the older ages of the networks. However, they caution that these networks may simply develop over older terrains. In any case, it is clear that these features could not have formed in the recent history of the planet, given the unfavorable temperature-pressure environment on the surface today.

Gullies provide evidence for geologically recent liquid on the surface. Since gullies have only been discovered within the past 6 years, relatively few studies have described their basic characteristics, such as location, orientation, depth, and slope. One reason for this is that examining the images for gullies is a time consuming endeavor. Additionally, MOC is still returning data; new images continue to be added to the dataset, and this increases the chances for more gullies to be discovered.

Finally, values for slope and depth cannot be obtained from MOC data alone, since it requires knowledge of topographic information. The most comprehensive study measuring gully characteristics to date has been Heldmann and Mellon's (2004) study of gullies in the southern hemisphere. Edgett et al. (2003) examined ~10,000 gullies in both hemispheres, but their study focused primarily on the geologic setting and morphology of the features. Other notable studies include Gilmore and Phillips (2002), who examined a smaller subset of southern hemisphere gullies, and Gilmore and Goldenson (2004), who examined 23 gully systems in the northern hemisphere.

At present, there have been few basic measurements made on northern hemisphere gullies. The goal of this study is to measure the basic geometries of the martian gullies in the northern hemisphere, and to determine or constrain the controls on their formation. Previous studies have shown that southern hemisphere gullies appear to occur in specific locations, with specific orientations (Malin and Edgett 2000, Heldmann and Mellon 2004). Our aim is to confirm whether these observations hold true for the northern hemisphere gullies. In addition, we attempted to constrain the gullies' mechanism of formation based on their physical characteristics. Gullies do not form on all slopes; thus, the slopes they do form on may have special qualities. This study does not, for the most part, take into account factors such as local geology or surface composition. However, we can constrain other models of gully formation that do take these factors into account using the measurements that we make.

The methods used to measure the gullies were developed specifically for this project. These methods allowed us to make good measurements of orientation, slope, and depth for 153 individual gullies using data from both the Mars Orbiter Camera and the Mars Orbiter Laser Altimeter. In addition, we also measured the same quantities on ~200 slopes without gullies in order to determine whether the gullied slope characteristics were distinct. We found that gullies do indeed have specific geometries that result in a specific range of solar insolation for a range of obliquities. This implies that specific temperatures are required to form gullies.

We conclude that gullies may have formed as the result of a change from high obliquity to low obliquity. A source for liquid water can be found in subsurface ice that was emplaced during a period of higher obliquity than present. This ice could have melted due to long-term fluxuations in the obliquity cycle, which can affect temperatures at depth. Alternatively, melt from surface ice may percolate into the regolith and collect on impermeable layers, where liquid water is stable at depth due to increased pressures and temperatures. We propose that already-liquid water at depth can supply the surface with a source of transient water. If this water is released in locations where the surface temperature is ~273 K, the liquid water may persist long enough to flow and form a gully. Our estimates of surface temperature confirm that this scenario is plausible.

II. Background

1. Morphologic and geometric observations of gullies

Malin and Edgett (2000) first described the martian gullies. They determined that the martian gullies can be recognized by three distinct landforms (Figure B1). The gullies have a head alcove that tapers downslope into a v-shaped channel, which follows local topography. At the bottom of the channel is a triangular depositional apron. Malin and Edgett (2000) have also categorized several gully types. (Figure B2) shows several different types of alcoves found in the gully systems. They note that the martian gullies closely resemble similar terrestrial features that were formed by liquid water, and they suggest that the martian features have a similar genesis.

Malin and Edgett (2000) observed that gullies appear to be latitude dependent, appearing only in the midlatitudes. Heldmann and Mellon (2004) and Edgett et al. (2003) confirmed that the majority of gullies fall within the midlatitudes (Figure B3, southern hemisphere only). Heldmann and Mellon's (2004) study focuses on the characteristics of gullies in the southern hemisphere only. They find that absolute gully depths tend to follow local topography until ~40°S, where there is a larger range of values (Figure B4). The starting depths of the gully alcove bases from the surface tends to be deeper as the latitude decreases, with a maximum of ~1900 m and most values between 0-400 m (Figure B5). Gilmore and Phillips (2002) found similar values for gully depths. They measured the alcove depths of 49 gullies in the southern hemisphere between 26°S-38°S, and found that their elevations ranged from ~70-800 m below the local surface. They found no correlation between depth and latitude, although this may be the result of the small sample size and latitude range. Similar ranges were found for northern hemisphere gullies by Gilmore and Goldenson (2004). They found that while the absolute depths of gullies tended to follow the local topography of their respective hemispheres, both northern and southern hemisphere gullies tend to start at the same depth from the surface, ~700 m or less.

Heldmann and Mellon (2004) also measured the angle of gullied slopes. They found that the slopes of the alcoves are on average ~21°, which Heldmann and Mellon point out is below the angle of repose. This implies that the gullies cannot have been formed by mass wasting.

Edgett et al. (2003) examined the orientations of ~10,000 gullies in both hemispheres, and found that gullies were found at all orientations (Figure B6). This finding was confirmed for the southern hemisphere by Heldmann and Mellon, who also determined that orientation is dependent on latitude (Figure B7). At lower latitudes (30°S-44°S), gullies tend to face south, or poleward. At midlatitudes (44°S-58°S), gullies tend to face north, or equatorward. In the highest latitudes (58°S-72°S), gullies again face towards the pole. Gilmore and Goldenson (2004) found that gullies in the northern hemisphere were oriented equally to the north (poleward) and south (equatorward). There were few gullies measured that had an east-west orientation, although they suggest that this may be due to the geometry of MOC images, which tends to exclude the east and west walls of craters.

Gullies have also been observed to coincide with specific landforms. Gilmore and Phillips (2002) found a relationship between mapped surface geology and gully location in the southern hemisphere. They observed that gullies are often seen emanating from cliff-forming layers, and they suggest that this is related to the location of source water. Gilmore and Goldenson (2004) confirmed that this observation holds true for northern hemisphere gullies as well. They examined 23 gully systems in the northern hemisphere between 35°N-64°N and found that in most cases, the gully heads coincide with a cliff-forming layer.

2. Proposed formation mechanisms

    a. Dry flow

The simplest explanation for the gully features is that they are the result of mass wasting. This is a gravity-driven process that requires no special temperature-pressure environment, nor does it require an agent such as a liquid or gas to occur. Treiman (2003) examined the morphologies, locations, and cross-cutting relationships of gullies in both hemispheres, and determined that dry flow of aeolian-deposited material was a feasible formation mechanism. He suggests that the similarities between the martian and terrestrial gullies are not significant; similar features may be formed by completely different mechanisms.

Firstly, Treiman (2003) points out that even though gullies appear to be geologically recent features, they may have in fact been forming throughout martian history. He points to several examples where new gullies are superimposed on older ones, or where gully features appear to be cut across by a fault or different terrain. Since few MOC images show large rocks making up the gully slope material, the material is likely to be relatively fine grained. As a result, older gullies could have easily been altered or erased by aeolian processes.

Next, Treiman (2003) observes that gullies form on slopes regardless of the local geology. Gullies are mostly found on crater walls, but are also seen on dunes, mesas, and on different types of patterned terrain. Using a global circulation model, Treiman found that in the southern hemisphere, the global wind patterns would deposit fine grained material in the midlatitudes, which is where the gullies are primarily found in both hemispheres. Once the material is in place, it need only avalanche under its own weight to form the gullies.

Treiman's model for gully formation is similar to that of Sullivan et al.'s (2001) explanation of dark streak features on martian hillsides. Like Treiman, Sullivan et al. (2001) have modeled these features after terrestrial dry flow features. These features usually begin at a steeper or more rugged part of the slope and narrowly fan outward on a less steep slope. They differ in albedo from the surrounding terrain, and are usually darker. Treiman points to these features as similar to the gully features;

however, there are significant differences between these features' morphologies. Most importantly, the topography of the dark streaks is entirely unlike that of the gullies. While the dark streaks appear to be mostly a coloration difference on the existing surface, the gullies cut into the slope to form levied channels. In addition, the streaks are fairly linear, and tend to form parallel to one another. Gullies, in contrast, can be quite sinuous. While Treiman's observations are sound, the dry flow model cannot easily explain the sinuous, levied channels of the gullies. Felix and Thomas (2004) have performed experiments on dry granular material flowing down an inclined plane, and they have found some evidence of levee formation. However, they did not produce sinuous features. Additionally, the experiment was kept between 50-55% humidity to avoid electrostatic effects between particles, and this may have introduced a water film into the material.

While Treiman's dry flow model does not invoke special circumstances per se, it is clear that it cannot fully explain the morphologies of all gullies. Gullies come in a variety of morphologies, and it is plausible that there is more than one mechanism of formation at work. However, Heldmann and Mellon (2004) found that the alcove slope angles averaged ~21°, which is well below the angle of repose of dry material on Mars. They determined that for mass wasting to occur, the slope angle must be at least 25°-35°. The majority of slopes they measured were well below this range. Given these findings, as well as the gullies' similarity to water-formed terrestrial gullies, the possibility of an agent of formation must be explored.

b. Formation by CO_2

CO_2 is extremely abundant on Mars, making up the majority of its atmosphere (Zurek, 1992). Present day temperatures and pressures on the surface allow for solid CO_2 to exist on the surface in the winter, but it is generally only stable in the gas phase. However, lithostatic pressure in the subsurface creates a higher pressure environment than the surface. Musslewhite et al (2001) have proposed a model for the presence and sudden outflow of liquid CO_2 in the near-surface regions. They cite Malin and Edgett's (2000) work when they start with the assumption that gullies in the southern hemisphere have a preferred pole facing orientation, although this has subsequently been determined not to be the case. At the current obliquity of ~25°, Musslewhite et al. (2001) determined that pole facing slopes receive less solar insolation in general, and are cooler than other regions as a result. They also point out that the southern hemisphere is higher in elevation than the northern hemisphere, which also contributes to the lower temperature of these slopes. They propose that these slopes are "cold traps," in which CO_2 (or a CO_2 and H_2O mixture) is able to condense in pore spaces and remain frozen throughout the majority of the year. As the ice condenses, it forms a barrier layer between the surface and the interior. With the continuing formation of this barrier, the lithostatic pressure is increased past the triple point of CO_2, and liquid CO_2 will form. As the pressure continues to rise, the ice barrier melts, until eventually the liquid will break though and very quickly drain out of the cliff face. As the CO_2 rapidly expands due to the decrease in pressure, it will bubble and behave fluidly as it boils, and it may be able to entrain particles and move them downslope. In this way, a gully could be formed in a single episode.

Hoffman (2002) also models gully formation as a result of CO_2 ice melt. However, in his model the CO_2 ice forms on the surface of the pre-gullied slopes. CO_2 snow and ice have been observed in the winter, and appear to sublime away during the summer. In the Hoffman model, a seasonal increase in solar insolation is the driving force behind gully formation. A thin snowcover over a low-albedo surface will melt from the bottom up due to secondary radiation. Solar radiation will penetrate a thin snow cover and be absorbed by the surface below. This in turn heats the snow from beneath and can cause melt. Thus, during the martian spring, pockets of CO_2 gas will form beneath the layer of snow. As these pockets of gas escape to the surface, snow avalanches are triggered, causing downward movement of material. Since the avalanche is a mixture of solids and quickly expanding gas, it will behave fluidly. Hoffman cites pyroclastic flow and slope failure as terrestrial analogs to this phenomenon. Both of these are density flows that form many of the same features that are observed in fluvial channels, such as levees and fan deposits.

While CO_2 is clearly a reasonable candidate, there are several unresolved issues surrounding its role in gully formation. Heldmann and Mellon (2004) point out that the subsurface is unlikely to be colder than the surface due to the geothermal gradient, making it unlikely that CO_2 ice would form in the near subsurface when it is unstable at the surface. Therefore, atmospheric CO_2 would not condense into the subsurface. In addition, Stewart and Nimmo (2002) find that the gully morphologies are indicative of relatively slow flow. They indicate that gullies on Earth are generally formed by water moving at ~1 m/s. In contrast, the exit velocity of the CO_2 is expected to be ~100 m/s in these models, which is several orders of magnitude higher. This is due to the rapid expansion of the CO_2 as the pressure is rapidly decreased. Given the high exit velocity, the CO_2 would likely be shot away from the surface for a significant distance before being deposited. However, the gullies show no indication of this type of jet; the channels and alcoves have no discontinuity, as would be expected if this had occurred. Stewart and Nimmo (2002) also point out that the surface pressures are not in the correct ranges to support liquid CO_2. The triple point of CO_2 is at ~5 bar, while the surface pressure is ~0.006 bar. In order for CO_2 to remain liquid on the surface for even a short amount of time, the pressure at the surface must be significantly higher.

The most compelling argument against CO_2 as the agent of gully formation is Heldmann and Mellon's calculation of the expected pressures and temperatures of the layers from which the gullies emanate. These were estimated using gully depths measured from pictures taken by the Mars Orbiting Camera (MOC). Figure B8 shows the CO_2 phase diagram with calculated temperatures and pressures at the gully forming layer. Data from the Thermal Emission Spectrometer (TES) were used to infer thermal conductivity of the near surface, and two different densities were used for the overburden (icy and dry). Even with a high density, icy overburden, it is clear that most of the gully alcove bases—the region from which the flow emanates—do not reside in the temperature-pressure regime needed for liquid CO_2.

c. Formation by H_2O

i. Subsurface ice and liquid

While water is not found on Mars in the same abundance as CO_2, there does exist a significant amount in the polar caps (Jakosky and Haberle, 1992). The surface conditions are generally at the triple point of water, which is significant because it would not take a large change in temperature or pressure to change the phase of water on the surface. Currently, water is only found in the gas and solid phases on the surface, much like CO_2. Several models have been proposed to examine the conditions necessary for liquid water on the surface and subsurface of Mars.

Mellon and Phillips (2001) have examined the obliquity cycles of Mars to determine whether liquid water could have existed at some time in the past given the current atmospheric pressure. They found that the mean annual surface temperatures never exceeded 222 K, which is below the freezing point of water. However, when they added salt to the water, they found that they could depress the freezing point to as low as 223 K if several salt species were used. In addition, they found that a briny permafrost could melt at lower temperatures and higher depths. Salts have been inferred on Mars by both the existence of duricrust, which is a layer of hardened sediments, as well as from a wealth of mineral studies.

In this model, the briny groundwater would undermine the surface through seepage, causing gullies to appear. This is supported by Heldmann and Mellon’s study of gully depth versus temperature with the H_2O phase diagram (Figure B9). They find that if a dry overburden is assumed, the majority of the gullies emanate from a region in which water is well within the liquid region. In addition, those gullies that do not lie in the liquid zone are in the solid zone, where a slight rise in temperature could move them into the liquid region. This stands in contrast to Figure B8, in which the majority of the gully layers are in the CO_2 gas phase.

Mellon and Jakosky (1995) modeled the emplacement and stability of near-surface ground ice and found that at obliquities around today’s value of ~25°, ice can be stable in the midlatitudes. Mellon and Phillips (2001) examined the possibility of this ice as a source for gullies. They determined that seasonal changes in temperature could cause near-surface ice to melt and allow the liquid to percolate deeper into the regolith. In this model, the liquid will collect on impermeable layers. If these layers encounter exposure to the surface, such as on a slope face, an icy plug will develop and prevent the liquid from sublimating into the atmosphere. As the seasonal cycle continues to emplace liquid on the impermeable layer, the fluid pressure will increase due to the continuing presence of the ice plug. Eventually the plug will fracture, allowing liquid to seep outwards.

If seasonal melt of near-surface ice is the primary control on gully formation, we would expect gully location to latitude dependent, since at today's obliquity permafrost is less abundant in the equatorial regions and more abundant near the poles. However, neither Heldmann and Mellon (2004) nor Malin and Edgett (2000) found that relationship. As was previously mentioned, they found that gullies tended to be in the mid latitudes of both hemispheres. Gilmore and Phillips (2002) point out that if gullies were controlled only by permafrost, we should expect to see deeper gullies closer to the equator, which has not been observed.

Head et al (2003) have suggested that large scale obliquity changes could cause water to be removed from the poles and redeposited as ice in the mid-latitudes. If the climate became warmer, the ice could melt and become a source of water for the formation of gullies. This could explain why the majority of gullies are found in mid-latitudes. The morphologies of the gullies are not consistent with surface runoff; however, the newly melted water could seep into the subsurface and remain stable there because of the increased pressure.

Malin and Edgett (2000) have suggested that the liquid water may be controlled by certain competent rock layers that act to contain the liquid in aquifers. They note that many gullies appear to emanate from a layer or layers within the slope on which the gullies are found. This work was continued by Gilmore and Phillips (2002); they determined that the average depth for the gully alcoves is 200-400m below the surface. They suggest that solar insolation will melt near-surface ice, forming subsurface liquid. This liquid will percolate through the subsurface until an impermeable layer is reached. If this layer dips towards a cliff face, the water could seep out along the impermeable layer and form gullies along the cliff. However, Heldmann and Mellon (2003) point out that many gully alcoves are above the highest cohesive strata.

Hartmann et al (2003) have also documented a similar phenomenon on Earth. They studied a glacial region in Iceland in which they observed a cliff face with water originating in a particular layer flowing down the face. While they did not see distinct gullies, they surmised that they would evolve over time due to erosion. If there were unconsolidated material present, features with gully-type morphologies could form.

ii. Melting of surface ice

Christensen (2003) notes that at high obliquities, water vapor will condense on the surface as well as within the regolith, as suggested by Mellon and Jakosky (1993). At high obliquities, these surface deposits could develop into a layer of snow that would be regionally widespread. As the obliquity lessens, these snow deposits will become less stable and will sublimate from all areas except for regions of shade. Christensen

(2003) also suggests that these patches may be protected from further sublimation by layers of dust or sediment. He notes that insolation absorption in the snowpack will occur at a depth below the snowpack surface, and that dust particles will increase this absorption. In this way, temperatures within the snowpack may be above the melting point of water even though the surface temperatures are well below it. The resultant liquid would be protected from sublimation by the overlying snowpack, and a gully could be formed on the underlying slope if it were made of unconsolidated material. Christensen (2003) suggests that emplacement of snow occurs at high obliquities, but melting would occur only at low obliquities, since this is the time when temperatures in the midlatitudes are the highest. The placement of snow is not limited to a particular placement along a slope, and so gullies may start at any depth so long as there is snow there.

Gullies forming in snow have been observed on Earth by Lee et al. (2006), who studied a region in the high arctic. They suggest that these gullies are analogous to the martian gullies due to their presence in a dry, cold region where liquid water is not always stable. However, these gullies only exist within the snowpack, and have not been observed to cut channels into the host slopes. Lee et al. (2006) suggest that this is due to the relative youth of the features, and that snow gullies might evolve into slope gullies if given unconsolidated material and enough time. As it stands, it is not entirely clear how snowmelt can create the type of gullies observed on Mars.

3. Stability and placement of water

   a. The surface environment today

Currently, water is not stable on most of the martian surface today due to the temperature-pressure environment. The atmospheric pressure at the surface is ~6 mbar, and the average surface temperature is ~210 K (Kieffer et al., 1992). This is within the stability field of ice; however, ice tends not to be stable on the surface due to diurnal and seasonal heating that allows the temperatures to rise above the average, which places the surface in the vapor stability field. Thus, long term surface ice is only observed at the poles, where there are cold temperatures throughout the year. The northern ice cap is primarily water, while the southern cap appears to be mostly CO_2 (Thomas et al., 1992). The northern cap greatly affects the amount of water vapor in the atmosphere during northern summer due to sublimation of a significant volume of the cap as a result of seasonal thermal heating (Haberle and Jakosky, 1990). This vapor can migrate to lower latitudes and condense in the regolith (Mellon and Jakosky, 1993). Mellon and Jakosky (1995) modeled the stability of subsurface ice at today's obliquity, and found that ice can be stable as low as 40° latitude in both hemispheres as long as it remains deep enough at lower latitudes (~100 m).

Liquid water has not been observed on the surface, and it is not generally expected to exist there given the current surface environment. However, calculations of maximum surface temperatures show that the low and mid latitudes can reach temperatures above 273 K (Paige, 1992). The triple point of water is at ~6 mbar of pressure—the current atmospheric pressure—and ~273 K temperature; liquid water may exist on the surface when these conditions are met. The morphologies of the gullies are highly suggestive of their formation by liquid (Malin and Edgett, 2000). Currently, water is only observed to exist in the polar caps and as a component in the atmosphere. However, if gullies are formed by water, their locations may help to constrain the distribution of subsurface water.

b. Changes in obliquity

Changes in obliquity lead to differences in the distribution of water on Mars. Jakosky and Haberle (1992) examined variation in atmospheric water vapor content as a measure of the martian water cycle at several obliquities. At today's obliquity, they found that the water vapor content varies significantly with season, indicating that insolation changes are driving the water cycle. During the summer, a portion of the ice caps will sublimate into the atmosphere, increasing the vapor amount. In the winter, most of this vapor is redeposited at the pole. However, some of it may also condense into the regolith. At high obliquities, they found that the elevated summer temperatures at the poles would cause all-CO_2 ice to sublime as well as a significant portion of the H_2O ice available there. They suggest that the atmosphere outside the polar regions might thus become saturated in water vapor, leading to nonpolar ice deposits in the lower latitudes. At lower obliquities, this ice would become unstable. Lower temperatures at the poles would allow for a permanent CO_2 frost covering, which would act as a cold trap for water, removing it from the atmosphere. Thus, in transitional obliquities from high to low water is in the process of being removed from the lower latitudes and emplaced in the higher latitudes.

Head et al. (2003) modeled past obliquity cycles and like Jakosky and Haberle (1992) found that at high obliquities, water ice could be emplaced in the lower latitudes. Using a climate model, they found that ice is moved from the polar regions into the midlatitudes due to a change in seasonal variation. Costard et al.(2002) have found that at high obliquities ~45°+, near-surface ground ice can be stable. Using a global climate model, they measured the surface and subsurface temperatures for different latitudes, obliquities, and slopes to determine where temperatures were above 0°C. Using studies of past martian obliquity cycles, they found that the regions above 0°C were in latitudes above 30° in both hemispheres. Temperatures were especially high on poleward facing slopes near the summer solstice. This is due to the fact that the model indicates that these slopes receive the most insolation. Costard et al. found that ice could have been melted down to 10-50 cm into the surface, depending on the thermal properties of the material. However, Mellon and Phillips (2001) modeled the same parameters in the southern hemisphere only, and found that ground ice melting could not occur even at high obliquities unless the water was a brine. This would depress the melting point, and allow for ice to melt below 0°C.

Obliquity changes will significantly affect the placement of water on and within the surface. If gullies require a source of water to form, then their locations should indicate where this water was present at the time of formation. Understanding where water has been present over the past obliquity cycle may help to constrain when gully formation occurred.

c. The effect of insolation and slope angle

Changes in obliquity affect the amount of insolation the surface receives seasonally. Insolation is the amount of incident solar radiation that reaches the surface. Insolation has a direct affect on the surface temperature; in general, the more insolation, the warmer the surface. Actual surface temperature is dependent upon the thermal properties of the surface material as well. Insolation is generally controlled by the solar declination angle, or the height of the Sun in the sky (Haberle et al., 1993). This is because the amount of insolation a slope receives is dependent on the angle of incidence of the incoming solar radiation. Insolation will have its maximum effect on temperature when the angle of incidence is perpendicular to the slope. A less direct angle of incidence will result in a reduction of the total insolation received by the slope.

Regional insolation is generally determined by the latitude and the season. Gullies have a specific latitude range (Edgett et al., 2003), occurring only in the midlatitudes of both hemispheres. This location preference suggests that regional insolation plays a role in gully formation. The slope angle on the surface will also contribute to the total insolation received locally, as well as the slope orientation. Costard et al. (2002)

found that the slopes with the highest insolation were pole-facing at high obliquities. Hecht (2002) modeled maximum insolation values for sun-facing slopes at the current obliquity, including in the model values for diffuse scattering, optical depth, slope value, and a solar constant reflecting a summertime perihelion. He found that relatively large insolation values could be achieved in high latitudes due to high zenith angles (Figure B10).

Changes in insolation can change where water is stable in surface and near-surface regions, as well as what phase it is in. The minimum requirement for liquid water on the surface is a temperature above 273 K, which can be achieved with solar heating. In Hecht and Costard et al's models, the slopes with maximum insolation have slopes that are the closest to perpendicular to the incident radiation. If gully formation is affected by insolation, one would expect gullies to have preferred orientations. In fact, this has been suggested by previous studies (Gilmore and Phillips 2002, Edgett et al. 2003, Heldmann and Mellon 2003, Gilmore and Goldenson 2004). For temperatures ~273 K to occur, specific insolations much be received by the slopes. Understanding the slope angles and orientations of gullied slopes would allow us to constrain the amount of insolation received there, and therefore to determine if liquid water could be stable at those locations.

III. Methods

To measure gully location, slope, depth, and orientation, I needed topographic data as well as images in order to identify the locations of the gullies in relation to topography. Two instruments exist that can provide these data: the Mars Orbiter Camera (MOC), a high resolution camera, provides gully images; and the Mars Orbiter Laser Altimeter (MOLA), an instrument for measuring topography, that works in tandem with MOC. Combining these datasets in ArcMap, a commercial GIS software, I could easily make the desired measurements.

1. Data sets

   a) Images from the Mars Orbiter Camera (MOC)

Gullies were first identified on Mars by Malin and Edgett (2000) with images from the Mars Orbiter Camera (MOC). This instrument is a high resolution camera onboard Mars Global Surveyor (MGS). Launched in 1996, MOC is still in operation. This instrument is comprised of one narrow angle and two wide angle cameras. The images from the narrow angle camera have obtained the highest resolution images of the surface to date, with resolutions as high as 1.5 m/pixel (Malin et al., 1998). MOC was therefore able to resolve gully features, which are generally ~1 km long and tens of meters wide. Using MOC images, information about their locations and morphologies could be obtained.

MGS is in a polar orbit, which allows frames of MOC data to be obtained primarily in the N-S direction.

b) Topography from the Mars Orbiter Laser Altimeter (MOLA)

The Mars Orbiter Laser Altimeter (MOLA) is an instrument also onboard MGS that measures the topography of the martian surface. MOLA emits a laser pulse that is reflected off of the surface; the time it takes to be returned indicates the height of the surface at that point. Each pulse is separated along its track by 300 m on the surface, and has a footprint of 160 m (Zuber et al., 1992). Until it ceased fully functioning in 2001, MOLA worked in tandem with MOC, so that each MOC image had an associated MOLA track. Just as with MOC, MOLA tracks are generally in the N-S direction. Each data point includes location coordinates and a height measurement.

c) Gully locations

Locations of gullies in the northern hemisphere were determined by lists compiled by Jennifer Heldmann and Martha Gilmore. These list were not comprehensive, but did include approximately 300 locations where gullies were found globally. Gilmore's list included location coordinates, a MOC image number, and a MOLA track number. Heldmann's list contained only location coordinates. Using the location as a guide, I used the online Planetary Interactive GIS-on-the-Web Analyzable Database (PIGWAD, accessed at http://webgis.wr.usgs.gov/mars.htm) to identify MOC image numbers in those regions. In many cases, additional gully images were found using this method.

2. Measurement technique

a) Creating digital elevation models from MOLA data

i. Interpolating with GMT

MOLA data were necessary to measure gully depth and slope. Since this data set consists of a series of points on a track moving in the N-S direction, with each point ~300 m away from the next one, many of the gullies did not have MOLA points directly on top of them. Thus, it was necessary to create a digital elevation model (DEM) of the region in order to make depth measurements. To do this, I followed the method developed by Okubo et al. (2004) to interpolate between MOLA points.

Okubo has compiled a searchable database of MOLA tracks. He has also written Perl scripts that can query this database. The Perl scripts could be accessed via a web interface until Fall 2005; this allowed the user to enter in lat/lon coordinates that bound a region of interest. The output is a text file that contains MOLA points in the region of interest.

The output also includes a batch file that allows the user to interpolate the MOLA points into a DEM using the Generic Mapping Tools (GMT), as well as a header file that includes information about the location and resolution of the DEM. Okubo et al.

(2004) tested several different interpolation methods in GMT, and determined that the *surface* routine gave the most accurate results. *Surface* is a routine that performs a spline-type interpolation. Okubo et al. (2004) determined that the optimal cell size for the least error should be set to 0.005, which is equivalent to a resolution of 200 pixels/degree. The vertical precision for this DEM was determined by Okubo et al. (2004) as ~1 m. Since GMT runs on a Unix machine here, I converted the commands in the batch file from DOS to Unix commands, and then ran each line individually through GMT. The output was an ascii file containing both the input data points and the interpolated points as a single column.

ii. Creating ArcMap compatible files using Perl

In order for ArcMap to display the interpolation correctly, it was necessary to append the header information to the data, and also to change the delimiter for the data to spaces. ArcMap requires the first lines of an ascii DEM file to have the following format:

NCOLS	Width (longitude) in pixels
NROWS	Length (latitude) in pixels
XLLCENTER	Center of uppermost left pixel (min. longitude in degrees)
YLLCENTER	Center of uppermost left pixel (min. latitude in degrees)
CELLSIZE	Degrees per pixel
NODATA_VALUE	Can be blank

These values were obtained from the header file output from the Okubo website. The resolution of the interpolated DEM is 200 pixels/degree. Thus, the CELLSIZE value was always 0.005. NCOLS and NROWS were obtained by determining the width and length of the DEM from the minimum and maximum values for lat/lon, and then converting that into degrees using the known resolution of 200 pixels/degree.

Once the header values were determined, they needed to be appended to the top of the ascii file and made into a text file, and all data in that file needed to be space delimited. This was accomplished by a perl script:

```
#!/usr/bin/perl

print "let the array building commence...\n\n";

$inputfile = "filename.asc";
$outputfile = "filename_hdr.txt";

open(infile, $inputfile);
@lines = <infile>;
close(infile);

open(outfile, ">$outputfile"); print outfile "NCOLS 800\nNROWS
800\nXLLCORNER 201\nYLLCENTER 43\nCELLSIZE
0.005\nNODATA_VALUE 9999\n";

for($i = 0; $i <= $#lines; ++$i) {@tokens = split(/\s/, $lines[$i]);
      print outfile "$tokens[0]\n";

}

close(outfile);
```

In this example, the input is filename.asc, and the values for the header information have been calculated separately and entered into the script. With the output from this, the data can be put into ArcMap and displayed correctly.

iii. Putting data into ArcMap

Once the DEM file has been created, it can be read by ArcMap. Before it can be displayed as an image in ArcMap, it must be converted into a raster. This can be achieved with the tool *Ascii to Raster*. In this process, ArcMap reads the information in the file header and then arranges the column of values into a rectangle with the correct length and width. In this way, the DEM can be displayed by ArcMap.

b) Processing MOC images with ISIS and Perl

Once the DEMs for the regions of interest were made, it was necessary to overlay the MOC images on them in order to determine the locations of individual gullies. To do this, the images needed to be converted from the PDS .img or .imq format to a geotiff, which can be read by ArcMap.

Using PIGWAD, MOC image numbers for gully locations were obtained. These images were then downloaded from the Malin Space Science Systems website (http://www.msss.com). These images were then processed using the USGS software ISIS for planetary datasets. Using the routine moclevall, the MOC images were converted into cube files. These files include information about the projection, as well as the coordinate system, which are set by the options for the routine.

[nlanza@envi]>moclevall from=file.imq mappars="SIMP:180,ocentric" lonsys=360 latsys=ocentric (creates file.lev2.cub)

For the R series of MOC images, moclevall always failed. The R series are images taken in the Relay mission, which ran from ~2003-2004 and was the third extended mission for the instrument. The failure of ISIS to process these images may have been due to the fact that we used ISIS 2.1, an older version of the software. In general, there were other images in the same location that could be used to determine gully location, and so the lack of the R series did not affect where gullies were measured. In addition, some other MOC images in both the M and E series also failed to be processes in ISIS, possibly due to errors in the image.

Once the MOC cube file was created, it could be converted to a geotiff with a worldfile compatible with ArcMap. This was achieved using the perl scripts dform.pl and isis2world.pl, both written by Trent Hare at the USGS and freely available at the ISIS support webpage (http://isis.astrogeology.usgs.gov/IsisSupport). Dform.pl converts the cube into a geotiff, and isis2world.pl creates the worldfile that contains header information for the tiff file. The syntax for both is as follows:

[nlanza@envi]>./dform.pl –t –gis=yes file.lev2.cub (creates file.tif)

[nlanza@envi]>./isis2world.pl –t file.lev2.cub (creates file.tfw)

These two files allow the MOC image to display in ArcMap with the proper georeferencing.

c) MOC and MOLA in ArcMap

To display both the DEM and the MOC images together in proper alignment, it is necessary to use the Mars2000 projection from the ISIS support website rather than the default Mars2000 in ArcMap. This is due to the fact that the DEM projection is defined in terms of degrees, while MOC images are projected in meters. To align the two data sets, the DEM must be reprojected into the ISIS projection. This is done by using the Project Raster tool, found in the ArcMap toolbox under Projections and Transformations → Raster → Project Raster. Once this done, the DEM is in the ISIS Mars2000 projection, and the MOC images can now be added, and will be overlayed correctly.

Even in the same coordinate system and projection, the MOC images and MOLA DEMs are not always perfectly aligned. When this occurs, it is necessary to georeference the MOC images by hand so that they lie correctly on top of the DEM. In most cases, it is clear that the MOC image is slightly offset from the DEM because crater walls do not line up as expected. To georeference by hand, the Georeferencing tool is used to slightly warp the MOC images so they fit correctly. The images generally only required a small translational adjustment to be aligned, and never needed rotational adjustment.

d) Digitizing features in ArcMap

Once the MOC images are properly aligned on the DEMs, it is possible to make measurements on the gullies. To do this, I digitized the gullies by defining them as straight lines, using the MOC image as a guide. This was done using the Editor tool. These lines were in the same coordinate system as the MOC and DEMs, and were defined as existing between two specific points. Once the gullies were digitized, I then used the 3D Analyst tool to convert the features to 3D. This procedure takes a digitized feature and uses it as a guide to extract data points from a raster. Thus, I extracted the DEM data at the points specified by the digitized gully features.

Using a set of free GIS tools called Easy Calculate, I then calculated the depths, slopes, and orientations of the digitized gullies.

IV. Results

1. Slope

The slope magnitudes of gullied and nongullied slopes were compared by latitude (Figure 2). The average slope for gullies is ~17° ± 6, and for nongullies is ~12° ± 6. In order to test if the difference between the two populations was significant, a t-test was performed. A P value of ~10^{-9} (<0.05) was returned, indicating that there is a meaningful difference between the gullied and nongullied slope magnitudes. Gullied slopes do not appear on the shallowest slopes at 5° and lower.

2. Depths

The average depths of the gully tops is 202 m ± 86 below the surface, but ranges from the top of the slope to over 1 km below the surface (Figure 3a). As latitude decreases, the gully depth generally increases. Figure 3b shows the absolute depth of the gully tops from the martian aeroid. The northern hemisphere is generally ~-4000 m below the aeroid (Smith et al., 1999). Our results show that the tops of the gullies follow the local topography of the northern hemisphere with an average depth of –4173 m ±86. Nongullies are on average slightly shallower, with an average depth of -3674 m ±86 from the aeroid.

3. Orientations

Figure 1a shows the orientations of gullies and nongullies in relation to latitude. Orientation was measured as the direction parallel to the gully from the top to the bottom of the slope. Slopes were defined as either pole facing or equator facing, with ~0° and 360° considered poleward and ~180° considered equator facing. Both gullied and nongullied slopes may have all orientations. However, while nongullied slopes have no preferred orientation with latitude, gullied slopes are pole facing from ~30°-45° latitude and equator facing from ~45°-55° latitude. There are slightly more equator facing gullies than other directions, with 29% of the total population (Table 1).

Table 1. Orientation of gullied slopes binned by orientation (0° = pole facing, 180° = equator facing).

Orientation bin (°)	Facing direction	Total number	Population percent
0-45, 316-359	Poleward (north)	35	23%
46-135	East	35	23%
136-225	Equatorward (south)	44	29%
225-315	West	39	25%

MOC images may exclude E-W slopes due to the fact that the N-S trending MOC footprints are often centered on craters. However, both populations are fairly evenly distributed across all orientations, which implies that the orientation preference of the gullied slopes is not an artifact of the data set.

In order to determine if our gullied orientations were meaningful, we performed a t-test on the data. We divided the orientations for both gullies and nongullies into low and high latitude groups. Over the entire latitude range, gullies have all orientations, and so a significant difference between gullies and nongullies would not be expected. For the low latitude group, we found P = 0.09, while for the high latitude group P = 0.6. These values are not suggestive of these groups being different. This does not detract from the observation that the certain orientations for gullies are not observed in specific latitudes. Since all orientations are represented in both the gullied and nongullied populations, there is no measured difference between the two groups. However, the gully orientations are not distributed evenly by latitude, which makes gullies different from nongullies.

We next grouped the orientation data by facing direction. The values from 0-90° were added to 360 in order to place all poleward gullies together (Figure 1b). A best-fit line was found for the gullies with an R value = 0.6. Binned in this way, the data show a better correlation between orientation and latitude. The nongullied values show a low R value = 0.2, which is expected if their distribution is random.

4. Insolation

a) Present obliquity 25.2°

The angle of incidence of incoming solar radiation will determine how much of the total insolation will be received by the slope. Angle of incidence is determined by the slope magnitude and orientation, as well as the height of the sun in the sky. Once all factors are taken into consideration and the angle is determined, the intensity of insolation received by the slope can be expressed in terms of percent of the potential maximum value:

Intensity = sin (θ) where θ = angle of incidence (90° is normal to surface)

With this in mind, a relationship between the angle of incidence on flat ground and angle of incidence on a slope at the same latitude was determined. In this way, the insolation on the slope could be characterized as a percentage of the maximum insolation received. Angle of incidence is dependent on the latitude, season, and time of day; this relationship is slightly different for poleward and equatorward slopes. For poleward slopes, the intensity is described as

$c = a - b$ where c = gully angle of incidence

b = slope angle

a = regional angle of incidence due to latitude

For equatorward slopes, the direction of measurement can affect the value of the angle. No angle of incidence can be higher that 90°, since that is when the ray is perpendicular to the slope. If an angle is measured as larger than 90°, no sunlight reaches the slope and the intensity value is 0. Thus,

$c = a + b$ if $(a + b) < 90°$

if $(a + b) < 90°$, then intensity = 0

In order to find the insolation amount on the gullied slopes, it was necessary to determine the angle at which insolation hits the unsloped surface in the same regions. This is called the solar zenith angle, and it is given by

$$\cos(z) = \sin(d)\sin(L) + \cos(d)\cos(L)\cos(2\pi t/24.6)$$ (Haberle et al., 1993)

where z = zenith angle

d = solar declination angle

L = latitude (deg)

t = time of day (hours, noon = 0)

24.6 = number of hours in martian diurnal day

At t = 0, or local noon, this equation can be simplified to

$z = |L - d|$ where L = latitude (deg)

d = solar declination angle

Solar declination angle, d, is given by

$\sin(d) = \sin(e)\sin(L_s)$ where e = obliquity = 25.2° today (Haberle et a., 1993)

L_s = Mars orbital position (deg)

To solve for d, a value for L_s must be chosen. L_s corresponds to different times of the martian year. In order to compare insolation values over the entire year, four L_s values were chosen in each season: the solstices and the equinoxes. The L_s values for these times are as follows:

Spring $L_s = 0°$

Summer $L_s = 90°$

Fall $L_s = 180°$

Winter $L_s = 270°$

With these values, the equation for solar declination angle (d) and solar zenith angle (z) was solved for every gully location at noon. The angle of incidence can then be determined:

Incidence = 90 - z

The next step is to determine the actual solar irradiance at the locations of interest, and then use the calculated angle of incidence to determine the irradiance values on the slopes. Irradiance describes the amount of insolation received by a given area, and it is expressed in units of power per area. The solar irradiance is given as

$S = S_0 \cos(z)(r_{bar}/r)^2$ where S_0 = solar irradiance at Mars' mean distance from Sun = 590 W/m^2 (Haberle et al., 1993)

z = solar zenith angle

(r_{bar}/r) = average Sun-Mars distance / actual distance

(r_{bar}/r) is given by

$(r_{bar}/r) = [1 + (e)\cos(L_s - L_s^p)/1 - (e)^2]$ (Haberle et al., 1993)

where e = orbital eccentricity = 0.0934

Ls = orbital position

L_s^p = areocentric longitude at perihelion = 248° today

Using these two equations, the maximum (noontime) solar irradiance on gullied and nongullied slopes was determined for each season.

For the nongullied population at present day obliquity, the slope irradiance changes depending on season and latitude. In all seasons, the noontime irradiance is highest near the equator and lowest near the pole (Figure 5a). This trend holds for flat surfaces as well, since the global noontime irradiance is dependent on latitude and season. Nongullied slopes have their highest noontime irradiance values in summer, with an average of 446 W/m^2, and have their lowest values in winter, with an average of 115 W/m^2 (Figure 5b). Additionally, nongullied slopes that face poleward tend to have lower noontime irradiances in all seasons than do equator facing slopes in each season.

If the winter and summer occurred at aphelion and perihelion, then we would expect that the fall and spring insolation values would be identical. However, this is not the case; at the present day orbital configuration, perihelion occurs in mid fall. This causes Mars to be closer to the Sun in fall than in spring, which in turn makes insolation values slightly higher in fall than in spring. This is true for all slopes, and is reflected in our calculated irradiance values for both gullies and nongullies.

Figure 5c shows maximum noontime irradiance on gullied slopes by latitude. In contrast to the nongullied slopes, the gullied slopes receive either the same or more irradiance at higher latitudes. Slopes show the greatest change in noontime irradiance with latitude in the winter, with a range of 0-400 W/m^2. Figure 5d shows the maximum irradiance by orientation. In every season, the gullied slopes receive on average between 200-400 W/m^2. As a result, wintertime equator facing gullies slopes receive more insolation than their nongullied counterparts. Equator facing nongullied slopes in the winter range from 0-200 W/m^2, while equator facing gulled slopes in the same season receive 200-600 W/m^2, the same range as they receive in all other seasons.

In order to compare the irradiance of gullied and nongullied populations, the data were binned for both gullies and nongullies by latitude and by orientation and then the differences compared. For latitude, the data were grouped in 5° bins from 30°-55°. Next, the values in the bin were averaged for each season. The nongullied bin values were then subtracted from the gully bin values. A similar method was used for the orientation data. The data were grouped in 45° bins from 0°-360°. The values in each bin were then averaged for each season, and the nongullied values were subtracted from the gullied values.

Figure 9c show the results by latitude. Negative values indicate that nongullied slopes have a higher value, while positive slopes indicate that gullies have a higher value. The gullied slopes have lower insolation values at lower latitudes and higher insolation values at higher latitudes than do nongullied slopes. At 25.2° obliquity, gullies receive ~100 W/m^2 more irradiance than do nongullies.

The difference in wintertime insolation is even more pronounced by orientation (Figure 9d). As with latitude, positive values indicate that gully values are higher, while negative values indicate that nongully values are higher. The equator facing gullies receive more insolation in winter than do equator facing nongullies. In every other season, gullies receive up to 50 W/m^2 less insolation than do nongullies. These results are summarized in Table 2.

Table 2. Averages and ranges of irradiance on gullied and nongullied slopes at 25.2° obliquity.

Slope type	Spring	Summer	Fall	Winter
	Average insolation (W/m^2)			
Gully	294.8	441.5	338.9	200.5
Nongully	306.4	445.9	352.2	115.1
	Range (W/m^2)			
Gully	181-468, diff = 287	372-484, diff = 112	208-538, diff = 330	0-395, diff = 395
Nongully	126-474, diff = 348	326-497, diff = 171	145-545, diff = 400	0-328, diff = 328

The next step was to determine the daily average irradiance at gullied and nongullied slopes. The daily average includes irradiance values from sunrise to sunset. This can be found using the following relationship:

$$S = (S_0/\pi)(r_{bar}/r)^2[\cos(d)\cos(\theta)\sin(H) + H\sin(d)\sin(\theta)]$$ (Haberle et al., 1993)

where S_0 = solar irradiance at Mars' mean distance from Sun = 590 W/m^2

(r_{bar}/r) = average Sun-Mars distance / actual distance d = solar declination angle

θ = latitude

H = half day (radians), given by $\cos(H) = -\tan(\theta)\tan(d)$

Figures 6a and 6b show the daily average irradiance for nongullied slopes on the solstices and equinoxes. As with the noontime irradiance results, the nongullied slopes receive less irradiance at higher latitudes. Similarly, pole facing slopes receive slightly less daily average insolation than equator facing slopes in all seasons.

Figures 6c and 6d show the daily average irradiance on the solstices and equinoxes for gullied slopes. The gullied slopes also follow the trend seen for noontime irradiance, with slopes receiving on average either the same amount or more insolation as the latitude increases. Slopes in the summer show the greatest difference with latitude, with a range of 48-125 W/m^2. The orientation results for gullies are within the same range as nongullies, but have less spread within each season. The summer-to-winter difference for gullied slopes is ~152 W/m^2, while for nongullies is ~146 W/m^2.

b) Other obliquities (5° and 60°)

Thus far, all examination of insolation has been at the current obliquity of 25.2°. Since the obliquity of Mars has changed significantly over time (Ward, 1992), we decided to examine how different obliquities would affect insolation on these same slopes. We chose 5° and 60° because these values are approximately the lowest and highest values expected throughout the obliquity cycle (Laskar and Robutel, 1993). Testing the temperatures at the extreme ends of all possible obliquity values will allow us to examine how much the insolation environment on Mars has changed over time. This may help us constrain the time of gully formation if there are significant differences in insolation over the obliquity cycle.

Mars' orbital eccentricity and season of perihelion also changes over time (Mellon and Phillips (2001). These will affect how much total insolation is received in any given season. When the eccentricity is high, Mars will receive more insolation at perihelion than it would at lower eccentricities. If perihelion coincides with summer, then that season will be far warmer than usual. By the same token, winter will then coincide with aphelion, and will therefore be much colder than usual. If a period of high eccentricity coincides with high obliquity, water may be quite stable in the equatorial regions. While eccentricity is less important for solar heating than obliquity, it is important to recognize that it has changed significantly in the recent history of the planet. Given the complexity of martian orbital models, it is difficult to determine the past eccentricity and perihelion at a given obliquity. For the purposes of these calculations, eccentricity and time of perihelion was set to today's values, and only obliquity was changed.

Figures 7a and 7b show noontime irradiance on gullied slopes for an obliquity of 5°. At this lower obliquity, the range of irradiances is again smaller for gullies than for nongullies (Figures 7c and 7d). The majority of gullied slopes fall between 200-550 W/m^2, while nongullies range from 0-550 W/m^2. As at the current obliquity, the nongullied slopes receive less insolation at higher latitudes, while the gullied slopes receive about the same amount or more. The exception to this are the poleward gullies in the lower latitudes, which show a lower insolation range of 0-200 W/m^2. The narrow range of the gullied slopes is apparent when insolation is examined by orientation (Figure 7b). Here, summertime values are often below fall and even winter values. This small range is not evident in the nongullied slopes (Figure 7d), which show the coldest slopes in winter and warmest slopes in summer.

Next, we examined the insolation on the same slopes at an obliquity of 60°. There was a large difference in the amount of insolation received in the winter for both gullied and nongullied slopes. In winter, neither gullied nor nogullied slopes receive any insolation (Figure 8a, b, c, d). The half day = 1 when Sun never rises, and the solar declination = -60 at 60° obliquity in the winter. Using these values in the equation for half day returns a minimum latitude of 30°. All measured slopes are at 30° latitude or higher, so they are not expected to receive any insolation at this time.

At 60° obliquity in all other seasons, gullied slopes receive 200-500 W/m^2 (Figure 8c, d). Compared to nongullied slopes, gullied slopes still have a smaller range of insolation values at 60° obliquity. Nongullied slopes range from 120-500 W/m^2 (Figure 8a, b). The effect of orientation on slope insolation disappears for nongullied slopes at 60° obliquity, with seasonal values remaining consistent for all orientations (Figure 8b). Gullies slopes show a similar trend, although there is still an ~50 W/m^2 difference between pole facing and equator facing slopes, with equator facing slopes receiving slightly more insolation (Figure 8d).

As for the insolation results at 25.2°, the insolation data for 5° and 60° were binned in order to compare the gully and nongully results. For 5°, the results mimic those at 25.2°, with gullied slopes receiving less insolation at low latitudes than nongullies and more in the high latitudes (Figure 5a). Similarly, by orientation equator facing gullied slopes are always cooler than nongullied slopes except for in the winter (Figure 5b). For 60°, the relationship between gullied and nongullied slopes was the same as for lower obliquities, but the differences were less pronounced. There was rarely more that 100 K difference between gullies and nongullies by latitude (Figure 9e). By orientation, equator facing gullied slopes were warmer than equator facing nongullied slopes in both the winter and the summer (Figure 9f). This is different than observations at 5° and 25.2°, where equator facing gullies receive more insolation than their nongullied counterparts in winter only.

In order to compare the seasonal differences between gullies and nongullies, the binned data were plotted in terms of season and obliquity. For fall and spring, there was no difference in the gully-nongully difference; this is due to the fact that the season of perihelion remained constant for all three obliquities (Figures X1, X2, X5, X6). By latitude, the summer and winter gully-nongully difference is most pronounced for 60° obliquity (Figures X1, X3, X5, X7). In the winter at 60°, there is no difference between the populations because no slopes receive insolation at this time. At the same obliquity in the summer, the gullies receive more insolation than nongullies in the upper latitudes only. By orientation (X2, X4, X6, X8), the gullies almost always receive more insolation than nongullies in the winter at 60° obliquity. At 60° in the summer, the pole facing gullies receive ~100 W/m^2 more insolation than nongullies, which is different than the results at 5° and 25.2° obliquity (Figure X4).

5. Slope temperatures

Insolation is not equivalent to temperature. However, it is the main factor affecting surface temperature. The temperature of a surface is dependent on the difference between the incoming and outgoing thermal energy. Incoming thermal energy includes insolation and heating from the geothermal gradient. The thermal inertia and emissivity will affect how much incoming radiation is reflected or absorbed. A blackbody is a surface that will reemit all incoming thermal energy, so that the incoming irradiance is equivalent to the output irradiance. The geothermal gradient on Mars is ~30 mW/m^2 (Heldmann and Mellon, 2004), which is orders of magnitude smaller that the insolation received from the Sun. Thus, the contribution from insolation to the total heat input is more important that that from the geothermal gradient. For simplicity, we only change emissivity to get a sense of how different materials will affect the slopes' temperatures. Understanding the temperatures on the gullied and nongullied slopes would help to determine if the slopes are at the correct temperatures for liquid water, and thus would help constrain models of their formation. Here, we determine slope temperatures varying material and obliquity.

a) Blackbody

If the slope material is assumed to behave as a blackbody, the Stefan-Boltzmann Law can be modified as follows:

$\Phi = \sigma T^4$ where Φ = Solar irradiance (W/m^2)

σ = Stefan-Boltzmann constant = 5.67×10^{-8} J K^{-4} m^{-2} s^{-1}

T = temperature (K)

The temperature could then be calculated for gullied and nongullied slopes at 5°, 25.2°, and 60° obliquities.

It is important to note that these temperatures only take into account insolation. If there is no insolation on the slope, the temperature is calculated as 0 K. This is clearly not an accurate temperature, since the ambient surface and air temperatures will be affected by insolation. However, for slopes that do receive insolation, these temperatures represent the maximum value possible for that slope and insolation. By our model, the temperature range will always mimic insolation.

The gullied slopes at 5° reach maximum temperatures that are ~15 K lower than at 25.2° obliquity (Figure 10a, b). The range for spring, summer, and fall is within 225-325 K for all obliquities, but the wintertime temperatures show a larger range from 0-300 K over all obliquities. At 60° obliquity, the gullied slopes receive no insolation and thus return a temperature value of 0 K (Figure 10c).

The wintertime nongullied slopes are always cooler than in other seasons (Figures 11a, b, c, d, e, f). At 5° and 25.2°, nongullied slope temperatures range between 100-300 K in the winter, with more 0 K values and slightly lower winter temperatures at 25.2°. At 60°, nongullied slopes receive no insolation. At this high obliquity, the difference between summer and winter temperatures are dramatic. Like the gullies, at all three obliquities the nongully temperatures for spring, summer, and fall are all in the same range ~200-300 K, which is a slightly larger range than the gullies. The changes in seasonal temperature with obliquity can be more easily understood when viewed one season at a time. Figures Z1, Z2, Z3, and Z4 show the gullied slopes in each season for all three obliquities, while Z5, Z6, Z7, and Z8 show the nongullies for each season. Fall and spring for both populations are the same, due to the choice of perihelion.

Looking at the temperature results by orientation, similar observations as for latitude can be made. At all three obliquities, gullied slopes show a temperature range of ~250-300 K for spring, summer, and winter at all orientations except for pole facing gullies in the winter (Figure 10c, d, e). At 5° and 25.2°, winter pole facing gullies range between ~125-250 K.

At all three obliquities, nongullied slopes that are pole facing are always cooler than equator facing slopes by at least 25 K (Figure 11 d, e, f). In all cases, there are nongullies that receive no insolation in winter; at lower obliquities, these are always pole facing slopes. The range for spring, summer, and fall is similar at all obliquities, falling between 225-320 K for all orientations.

b) Basalt

We next examined the effect of changing the slope material to basalt on its temperature. Because the insolation trends determine the temperature trends at all obliquities, and because the effect of emissivity will be of the same magnitude for all obliquities, we only examined slopes at the current obliquity of 25.2°. Emissivity can be incorporated into the Stefan-Boltzmann equation in the following way:

$$\Phi\varepsilon = \sigma T^4$$

where Φ = Solar irradiance (W/m^2)

σ = Stefan-Boltzmann constant = $5.67 \times 10^{-8}\ J\ K^{-4}\ m^{-2}\ s^{-1}$

T = temperature (K)

ε = emissivity constant of material

From Kirchoff's Law, we know that emissivity is usually equivalent to absorption. Thus, we can use the emissivity constant to modify the amount of insolation that is returned. The total insolation goes in; radiation less than the input is returned due to absorptions in the material. The remaining radiation is reflected, which is the effect of albedo. The emissivity coefficient is a ratio of the actual emitted radiation to the expected emitted radiation of a black body. The emissivity is dependent on both the wavelength being examined as well as the material's temperature. In general, the emissivity of basalt is around 0.72.

Our results show that slopes made of basalt will have temperatures ~20 K lower than the values returned for a blackbody. This is true for both gullies and nongullies (Figure 12a, b, c, d). These lower temperatures mean that the gullied slopes generally do not reach 273 K except for in the summer and fall. The same is true for nongullied slopes.

We next applied our basalt results to the temperatures at 5° and 60° obliquities. For 5°, we find that the reduction in temperature of 20 K is enough to remove all but a few gullies from the 273 K range. For gullied slopes at 60°, the summer and fall temperatures are still within range, but the spring and winter temperatures are well below the melting point of water. If gullied slopes are made of basalt, then gullies are less likely to form at high obliquities. However, it seems unlikely that the gullied slopes could be solid basalt, given their appearance in MOC images.

c) Sand

We also tested the temperatures of the slopes when the material is sand. Sand generally has a higher emissivity than basalt, although how much higher is dependent on its composition and grain size. Smaller grain sizes lead to larger emissivities, and so we chose a sand emissivity value of 0.9. We used the same Stefan-Boltzmann relationship to calculate sand values as we did for basalt, changing only the emissivity value.

Our results show that for slopes made of sand, the slope temperatures are reduced by ~7 K for gullies and nongullies (Figure 13a, b, c, d). The majority of the gullied slopes are between 250-300 K in all seasons if the slopes are sand, which is almost centered on 273 K.

For a 5° obliquity, sand slopes will be just around 273 K in almost every season. As our blackbody temperatures indicated, gullied slopes at 5° obliquity are in a very narrow temperature range. When the slope material is sand, the gullied slopes achieve an excellent temperature range for water. For a 60° obliquity, sand slopes will often be ~15 K above the melting point of water in the summer, making liquid unstable there. Sand will allow for temperatures closer to melting in the spring and fall, but the wintertime temperatures are still ~50 K lower than what is required for liquid.

Our sand results allow for a temperature more conducive to liquid water than basalt. Sand is also a more reasonable material for the gullied slopes, since MOC images indicate that gullies form on unconsolidated material.

6. Summary of results

We find that gullied slopes occur at specific latitudes, slopes, and orientations that are distinct from nongullied slopes. These geometries lead to the gullies' achieving a narrower range of insolation values than nongullies. We examined how obliquity changes affected the insolation amount, and found that the difference between summer and winter insolation was largest for 60° obliquity, and smallest for 5° obliquity.

The magnitude of the slope angle affects the amount of insolation a slope receives. Hecht (2002) finds that at today's obliquity, equator facing slopes receive more insolation, slopes must be shallower at lower latitudes for maximum insolation. Our results show that gully-bearing slopes are steeper at lower latitudes. Thus, maximum insolation at current obliquity is not desirable for gully formation. This may be due to the fact that maximum insolation can give slope temperatures well above the melting point of water. Our temperature results show that gullied slopes can reach temperatures ~273 K at a variety of obliquities; however, the majority of gullied slopes will fall within the stability field for liquid water at obliquities at 25.2° and lower. Gullies are in general within the same temperature range in all latitudes and seasons. In contrast, nongullied slopes have a larger range of temperatures throughout the seasons, and are cooler at higher latitudes.

The idea of a specific gully temperature range is further supported by the results for maximum irradiance by latitude. For a flat surface at current obliquity, one would expect to see lower noontime irradiances at higher latitudes in all seasons. This is in fact the result found for nongullied slopes. Gullied slopes, on the other hand, show either no change or a slight increase in maximum irradiance at higher latitudes. The daily average irradiance shows a similar trend to the maximum irradiance. This again points to a need for a specific insolation—and therefore temperature—range that allows gullies to form.

Edgett et al. (2003) also point out that all documented gullies occur poleward of 30° in both hemispheres. Since location and orientation preference is mirrored in both hemispheres, it implies that a global phenomenon is responsible for gully formation. At today's obliquity, the lower latitudes receive more insolation in general than the higher latitudes. Even though gullies are concentrated in the midlatitudes, one would expect lower latitude gullies to receive more insolation than higher latitude gullies. However, both slope magnitude and orientation will affect how much insolation a slope receives. As the results show, the gullies have preferred orientations. Higher latitude gullies are equator facing, while lower latitude gullies are pole facing. At current obliquity, the orientation preference of the gullies means that gullies in warmer low latitudes have cooler, pole facing slopes, while gullies in colder high latitudes have warmer, equator facing slopes. It is important to recognize that irradiance is not equivalent to temperature; however, the insolation received by a slope will directly affect its temperature, as our results show. At the current obliquity of 25.2°, the gullied slope maximum temperatures range between 250-300 K at all latitudes, orientations, and emissivities except for low latitude, pole facing gullies in the winter. Since the melting point of water is ~273 K, the gullied slopes are generally around the stability range of liquid water. This is not the case for nongullied slopes, which show a maximum temperature range of 100-300 K. Some nongullied slopes are above 273 K at some points during the year, but not for as many of the days tested as the gullied slopes. Thus, our results suggest that not only is a specific temperature range required for gully formation, but also that the temperatures should be sustained over the course of the year. For gullied slopes, this can only be achieved at mid to low obliquities.

Our results show that obliquity tends to exaggerate seasonal temperature differences. The largest difference was between summer and winter at 60°. This affect also reduces the measured days of the year that have maximum temperatures close to 273 K. The gullied slopes were always closer to the 273 K range than nongullied slopes at all seasons and obliquities, but only in mid to low obliquities were gullied slopes able to maintain this range in all seasons.

V. Discussion

1. Gully Slopes

The magnitudes of the gully slopes strongly suggest that mass wasting is not the primary mechanism of formation for the gullies. Our results show that gullied slopes below the alcove have an average slope of ~17° ±6°. These results are in agreement with Heldmann and Mellon (2003), who found that gullied slopes in the southern hemisphere have an average slope of ~18°. Since the angle of repose on Mars is ~35°, it is clear that many gullies are not solely the product of dry flow from mass wasting, as Treiman (2003) has proposed. Treiman (2003, 2006 personal communication), however, suggests that the magnitude of the gullied slope below the alcove is not relevant to gully formation, and he points to the gully alcoves as evidence that gullies form as a result of mass wasting. He suggests that gullies form in regions with specific geologies, in which there is layering of resistant rock with more friable material. As the less resistant material erodes, the more resistant material will remain and form cliff faces. Material is removed from the alcove region and is transported to lower on the slope via gravity, resulting in a cliff face with a streak of debris moving downslope from it. In this scenario, the magnitude of the slope below the alcove only affects the length of the gully and not its placement, since the mass movement is initiated above the slope. This explains the observation that many gullies appear to be associated with cliff layers (Malin and Edgett, 2000; Gilmore and Phillips, 2002). However, past observations have shown that gullies have steep, levied walls and sinuous channels as are often seen in terrestrial gullies that are formed by water

(Malin and Edgett, 2000). While Treiman (2003) claims that dry flow can form levies, he acknowledges that it does not generally form sinuous channels. Thus, the model cannot fully explain the observed gully morphologies. Mass wasting may play a role in gully formation; however, not all gullies can have formed by this mechanism alone.

Our results also show that gullies do not form on slopes with magnitudes of less than ~5°. This suggests that the material forming the gully requires that the slope be higher than this value in order to create a gully with a noticeable length. Heldmann and Mellon (2004) measured the lengths of gully channels in the southern hemisphere and found that there was a slight correlation between length and latitude, with the length increasing as latitude decreased. They interpret this as indicative of the amount of time that the water has on the surface before freezing or sublimating. Gullies in the lower latitudes have more time to form because these regions are generally warmer than higher latitudes. However, too-warm temperatures will lead to immediate sublimation of any water, thus limiting the equatorward extent of gullies by Heldmann and Mellon's (2004) interpretation. If this is the case, then it follows that gullies must form on slopes that are also steep enough for liquid to flow down them before the water either sublimates or freezes.

2. Gully Depths

We found that gully channels have an average starting depth of ~202 m from the surface, with a range of 0-1000 m. This is consistent with Heldmann and Mellon (2003) and Gilmore and Phillips (2002) in the southern hemisphere, as well as northern hemisphere measurements by Gilmore and Goldenson (2004). Our results show that at lower latitudes, gullies appear to form deeper from the surface (Figure 3a). The R value = 0.32, which does not show a strong correlation between depth and latitude. Heldmann and Mellon (2003) found that southern hemisphere gullies tended to start deeper from the surface in lower latitudes. Their deepest measured gully depth from the surface was ~1000 m, although the majority began between 0-400 m from the surface. This is nearly identical to our depth results. Gilmore and Phillips (2004) also measured the depths of gullies in the southern hemisphere, and found that the average depths ranged from 200-400 m below the local surface. They did not observe deepening of gully tops closer to the equator; however, they measured a narrow range of latitudes between 26°-38°N, and thus did not cover the same range as Heldmann and Mellon's (2003) or this study. Gilmore and Goldenson (2004) found that gullies in the northern hemisphere show a range of depths between 0-500 m from the surface, with an average of ~240 m. Again, this is in good agreement with our results.

The fact that the gully depths are observed to have the same limited range in both hemispheres is consistent with a thermal control on where they will form. Water ice is currently not stable on the surface at midlatitudes; however, ice or even liquid water may be stable in the near-surface due to the increased lithostatic pressure. Heldmann and Mellon (2004) modeled the temperature at depths of the gully alcoves, taking into account the soil density, heat capacity, thermal conductivity, thermal inertia, gravity, and geothermal heat flux. They found that the majority of gully alcoves were well within the stability field of liquid water. Heldmann and Mellon (2004) note that they assumed that the above listed factors such as thermal conductivity remained constant for all gullied regions. They point out that changing the thermal conductivity for the anomalous gullies would place all gullies within the stability field of water. Thus, the depths of the gullies may be controlled by where the material that forms them is most stable.

Gilmore and Phillips (2002) suggest an alternative scenario in which the gully depths are controlled by permeability changes within the subsurface. They hypothesize that the relatively highly permeable near-surface may be underlain by impermeable layers. Seasonal melting of near-surface ice would percolate into the regolith and collect on the impermeable layers. Thus in this model, the gully depths also represent the location of the source material. However, the source location is controlled by local geology rather than thermally, as in Heldmann and Mellon's (2004) model.

Fanale et al. (1986) modeled the effect of large-scale obliquity driven temperature changes in the subsurface to determine where ice will be emplaced. Their model included factors such as albedo changes, thermal conductivity, internal heat flow of the regolith, orbital eccentricity, and emissivity. They found that over time, changes in obliquity will cause ice to be emplaced at depths of ~80 m close to 30° latitude and almost at the surface at 50° latitude. This is shallower than our average gully depths of ~200 m. In this context the depth results suggest that the locations of gully tops are controlled by a source material that may be at greater depths closer to the equator due to temperature requirements. Our depth results do not speak directly to insolation as a driving mechanism; however, they may be indicative of the type and location of source material that may be affected by insolation changes.

3. Gully orientation

Our orientation results agree with previous orientation measurements for both hemispheres. Heldmann and Mellon (2003) find that within the midlatitudes of the southern hemisphere (30°S-58°S), gullies occur at all orientations. However, in the lower latitudes (30°S-44°S), the gullies face poleward, while in the higher latitudes (44°S-58°S), gullies face equatorward. Edgett et al. (2003) studied ~10,000 individual gullies in both hemispheres and determined that gullies are found at all orientations. Like Heldmann and Mellon (2003), they found that gullies in both hemispheres occurred at all orientations, although they did not examine orientation specifically in terms of latitude.

At the current obliquity, pole facing slopes receive less sunlight than equator facing slopes (Hecht, 2002). Gullies occur at all orientations, but not all orientations are represented equally by latitude. In general, gullied slopes at higher latitudes (> ~ 40°) receive more insolation than lower latitudes. Our measurements show that at low latitudes where angle of incidence is more direct regionally, gullies are polefacing, while high latitude gullies are equator facing. This suggests that gullies require a specific range of insolation values to form, where the gullies will not form on the hottest or coolest slopes. An explanation for this may be that slopes that are too far from 273 K do not allow for liquid water to exist. On slopes that are too warm, liquid water will quickly sublimate, while on slopes that are too cold, water will freeze and cease to flow. The locations of the gullies may therefore be indicative of the locations at which liquid water may exist for at least short periods of time. Heldmann et al. (2005) modeled the flow rates and flow velocities required to form gullies with the observed lengths. They used terrestrial gullies in the Arctic as an analog, noting that gully formation there occurs as water is simultaneously freezing in and evaporating from the channel. They found that for a standard martian gully length of ~500 m, a flow rate of 30 m^3/s is required to counteract the effects of freezing and sublimation. Using an average channel slope value of 18°, roughness values ~1 m, and estimated channel depths from 0.15-1 m, they determined a flow velocity of ~10 m/s. Given this flow rate and flow velocity, water will reach the end of the channel in 50 seconds. Thus, liquid water need not be present for extended episodes for gullies to form.

4. Insolation modeling

In order for liquid water to exist on the surface Mars today, the correct temperature-pressure environment must be present. The current atmospheric pressure is ~6 mbar, which means that liquid water requires a temperature of ~273 K to exist. Insolation is the most important factor determining the surface temperature, and so these slopes must receive the correct amount of insolation in order to reach the necessary temperatures for liquid water. The surface insolation may or may not directly cause the release of liquid, but it must at least be sufficient to allow for liquid water to exist long enough to form a gully.

Our insolation results show that gullied slopes do receive a different amount of insolation than nongullied slopes. This is the case for a wide range of obliquities (5°, 25.2°, and 60°). At every obliquity tested, gullies receive a more constant amount of insolation throughout the year than do nongullies. At today's obliquity, the average gullied irradiance is 319 W/m^2 ± 116, with this value representing the averaged values of the solstices and equinoxes. Nongullies have a lower average irradiance of 304 W/m^2 ± 144, showing a wider spread of values than gullies. A more constant range of insolation values throughout the year means that gullied slopes have similar temperature environments most of the time. The fact that the gullies' temperature range is so close to the temperature at which liquid water is stable suggest that the amount of insolation received by gullied slopes allows for liquid water to be present in all seasons.

More insolation leads to higher slope temperatures, as our results indicate. For an emissivity = 1, all slopes were generally warmer in summer, when insolation values were highest. At today's obliquity, we found that gullied slopes have maximum temperatures that range from ~250-300 K in all seasons except for pole facing gullies in the winter. Nongullies, in contrast, have a much wider range of maximum temperatures. Even if we exclude the coldest wintertime polefacing slopes, the nongullies still have a range of ~150-300 K throughout all seasons. The maximum temperatures for gullied slopes are above 273 K in at least one season, and are usually in the same range for two or more seasons. This temperature range suggests that gully formation occurs in all seasons as long as the surface conditions are correct.

The emissivity of the slope material also affects the temperature, causing it to be lower than if the material were a blackbody. Basalt slopes will have lower temperatures than sand slopes; however, it is unlikely that either the gullied or nongullied slopes are made of solid basalt. MOC images suggest that the slope material is unconsolidated, although the grain size cannot be resolved. Slopes made of sand have emissivities of ~0.9, which translates into a 6-7 K lowering of slope temperatures from the blackbody calculations. This slight lowering of temperature places the gullied slopes closer to the 273 K range than for blackbody slopes. Our generalizations for the blackbody plots will therefore hold true when the emissivity of sand is included in the temperature calculation.

Our results suggest that average seasonal temperatures are less important than daily maximums. The daily average irradiance values (Figure 6a, b, c, d) are generally below 180 W/m^2, and as a result are never above 273 K even in the summer. If the average temperatures controlled gully formation, we would not expect gullies to form, since liquid water cannot exist on the surface with insolations much lower than ~315 W/m^2, which is the lowest irradiance that will return a temperature of 273 K in the Stefan-Boltzmann equation for blackbody emissivity. The maximum insolation values, on the other hand, are often above 315 W/m^2. The daily average values show little variation between gullies and nongullies, whereas the maximum values are very different for these two populations over the course of a year. This suggests that gullies may form in any season as long as the proper temperature is reached.

Our results show that the maximum temperatures on the surface are never much above ~300 K, even at different obliquities. This is due to the fact that total insolation on the surface is limited by Mars' distance from the Sun. The solar constant is a measure of how much radiation is received at the top of the atmosphere from the Sun. The solar constant for the Earth is 1368 W/m^2; Mars is 1.5 times as distant from the Sun as Earth, and the solar constant varies as 1/distance. Thus, the solar constant for Mars is ~600 W/m^2. The solar constant can then be used to determine the average incident radiation:

$S_{avg} = S / 4$ where S_{avg} = average insolation (W/m^2)

S = solar constant (W/m^2)

Using this equation gives an average martian insolation value ~150 W/m^2. Using this value in the Stefan-Boltzmann equation, this returns an average temperature value of ~226 K. This temperature is likely to be lower in reality due to factors such as albedo. In any case, this demonstrates that the average temperatures on the surface never surpass the melting temperature of water at any obliquity. This indicates that the average temperatures are likely to be less important for gully formation that the maximum temperatures, which often exceed 273 K.

It is important to recognize that our temperature calculations are approximate, and do not include several factors. In order to calculate the surface (and subsurface) temperatures accurately, it is necessary to determine the total thermal energy entering the surface versus the total thermal energy exiting. In Fanale et al.'s (1986) model of the heat budget of the regolith, they include factors such as the thermal conductivity, geothermal heating, thermal diffusivity, emissivity, albedo, and soil density and specific heat. These quantities determine rates of heating and cooling, which will greatly affect the ultimate temperature of the material for a given insolation. For simplicity, we have chosen to include only emissivity in our temperature calculations. Schorghofer and Aharonson (2005) point out that differences in thermal inertia cause variations in longitudinal ice distribution. This is due to the fact that some materials require more time to become warm, and warm up less than other materials do given the same input, allowing for ice to develop on these surfaces. Clearly, this and other material properties are important for determining the temperature of the gullied slopes. We assume the only input to our heat budget is the received insolation on the slope. The only modifier for this input is emissivity; we assume that our slopes behave as blackbodies in every other way. Consequently, our calculation will give slightly higher temperatures for slopes that receive insolation, and temperatures of 0 K for slopes that receive no insolation. Nevertheless, our temperature values allow us to examine how insolation alone relates to gully formation.

Regardless of the absolute magnitude of slope temperatures, the relationship between seasons and between gullies and nongullies is likely to hold even when more factors for the heat budget are taken into consideration. Received insolation dictates the general surface temperature, and so we can use our calculated insolations and temperatures to highlight the differences between populations. The difference between gullied and nongullied slopes hinges on the wintertime temperatures. In the gullied population, equator facing slopes are at around the same temperatures in the winter as in the other seasons. However, pole facing gullied slopes receive significantly less insolation in the winter than in all other seasons. This is difficult to explain in terms of water stability; if gullies require a specific temperature range to form, then one would expect that all gullies, regardless of orientation, would fall within that range. This difference may be explained by a material difference between the gullied slopes. It is important to recall that pole facing gullies are generally in the lower latitudes. Results from the Thermal Emission Spectrometer (TES) instrument indicate that the regions from 30°-40° have thermal inertias ~30 $Jm^{-2}s^{-1/2}K^{-1}$ lower than the regions between 40°-50° (Mellon et al., 2002). Lower thermal inertias cause these regions to change more quickly in response to thermal change, which in turn gives these regions higher temperatures. While we do not attempt here to quantify the increase in temperature for these slopes when thermal inertia is included in the temperature calculation, it is reasonable to assume that these temperatures are in reality closer to the temperatures of wintertime equator facing slopes.

5. Constraints on gully formation

    a) Water emplacement at high obliquity

In order for insolation to create gullies, it must be affecting a source that can supply liquid water. This source must exist in the midlatitudes where gullies are found. Currently, water ice is not stable near the surface in the lower midlatitudes. However, both Head et al. (2003) and Milliken et al. (2003) found landforms associated with ground ice in the lower latitudes. They suggest that ground ice could have been emplaced during a period of high obliquity. This is supported by Jakosky and Haberle (1992), who modeled the water cycle at several obliquities by examining the change in atmospheric water content. They found that at high obliquities, water vapor would be removed from the poles and emplaced at the equator regions. Mellon and Jakosky (1995) have modeled the condensation of water vapor into the regolith. Their model shows that as the obliquity increases, atmospheric water vapor also increases, even as surface temperatures fall. They point out that this allows water ice to be stable both closer to the surface and to the equator. Mellon and Jakosky (1993) previously determined that the amount of ice condensation is dependent on the density of atmospheric water vapor, which itself is limited by the atmospheric saturation temperature. Mellon and Jakosky (1995) found that at higher obliquities, the amount of water vapor released from the polar caps into the atmosphere increases. In addition, the saturation temperature also increases, leading to a larger vapor column at higher obliquities. This vapor can travel to lower latitudes, which at higher obliquities will be cooler than the poles. When the surface temperature is below the frost point, the water vapor will begin to condense. Mellon and Jakosky (1993) determined that within 10^5 years, as much as 30-40% of the available pore space could be filled. The depth of the atmospheric condensation is controlled by the depth of the frost point isotherm.

b) Insolation differences at varying obliquities

i. Thermal heating and water stability

Once there is a source material in place, a specific temperature range is needed in order to sustain liquid water on the surface. Our results show that gullies form on slopes that reach 273 K or above in at least one season for mid to low obliquities, and for all seasons except for winter at high obliquity (Figures Z1, Z2, Z3, Z4). This is not the case for nongullied slopes, which can only achieve 273 K in the lower latitudes in the spring and fall at all obliquities. From this one might expect gullies to form at all seasons and obliquities except for high obliquity winter. It is important to recognize that seasonal thermal changes can only allow for liquid water to exist on the surface; seasonal surface temperatures will not significantly affect ice—or water—at depth. If the source of gully forming material is below the top few meters of the surface, then seasonal insolation alone does not drive gully formation due to the inability of the thermal wave to penetrate below this depth. A subsurface source is strongly suggested by the gullies' depths, along with their latitudinal placement. The gullies' temperature range therefore represents the effect of insolation on already-liquid water. Our seasonal insolation ranges at different obliquities cannot constrain the behavior of the subsurface material while it is at depth, only when it is exposed to the surface.

While the subsurface gully material may not be affected by seasonal insolation, it may be affected by long-term temperature changes over the obliquity cycle. Mellon and Phillips (2001) modeled changes in the stability of aquifers at depth, and found that the surface temperatures will affect the subsurface temperature on the order of magnitude of ~100-200 m. They found that these changes would be sufficient to freeze or melt water at these depths over the period of the obliquity cycle. Interestingly, they also found that aquifers tended to freeze at lower obliquities and melt at higher obliquities. This is due to the fact that temperatures tend to oscillate less at lower obliquities, allowing the aquifer more time to reach the average temperatures of the surface, which are always below the freezing point of water. If the gully material is not affected by insolation, then it must already be liquid at the time it reaches the surface. Subsurface aquifers meet this requirement. However, this implies that gullies must form between high and low obliquities. This will insure that the aquifers are still liquid, while the maximum surface temperatures are the closest to 273 K in all seasons, allowing for the liquid to form gullies.

ii. Development of gullies by release of subsurface water

Mellon and Phillips (2001) examined how previously emplaced near-surface ice could begin to melt. They take into account the lithostatic pressure, thermal conductivity, geothermal gradient, and density and porosity of the regolith. Using this model, they note that seasonal variation in insolation is not sufficient to change the temperature of the near-surface below ~4 m because the thermal wave cannot penetrate the material. Thus, seasonal changes in insolation cannot be driving the release of liquid water from a subsurface ice source. However, our results show that gullied slopes receive more constant seasonal insolation than do nongullied slopes. This may speak to the fact that liquid water can only exist on the surface at temperatures ~273 K. The seasonal temperature ranges of the gullied slopes imply that they can support liquid water flow throughout the year for limited episodes. However, seasonal insolation changes cannot be responsible for the release of water if the source is at depths ~100 m.

Insolation changes can also occur over longer time periods. The model of Mellon and Phillips (2001) also indicates that obliquity changes will affect the amount of insolation received by a region over a longer period of time, and can cause temperature changes at depth. With the same model, they determined that the location of the 273 K isotherm changes with obliquity. Liquid water may be present at depths of 100-150 m at obliquities between 20°-40°; and at depths of 100-120 m at higher obliquities of 40°-60°. The isotherm is at shallower depths at lower latitudes. The change in the isotherm's depth is the result of the propagation of a long-period thermal wave, and is not affected by annual seasonal temperature changes. Mellon and Jakosky (1993) also examined the role of the geothermal gradient in the 273 K isotherm location, and found that a low conductivity, unconsolidated regolith can raise the depth of the melting isotherm to within a few hundred meters of the surface. Like Mellon and Phillips (2001), they found that at current obliquities, melting would initiate closer to the surface near the equator. This is not consistent with the observation that gullies appear to form deeper from the surface in low latitude regions. Heldmann and Mellon (2004) point out that if global ice distribution were the only parameter controlling gully formation, gullies should then be found globally as well, which is not the case. This may be explained if the gullies represent a transitional period in which ground ice has been removed from the near surface, but still remains at depth in the lower latitudes. At high obliquities, ground ice is either being emplaced or is relatively stable. If the gullies formed after a significant amount of ice has been removed, this suggests that gullies began forming well within the time of ice removal, which would occur when obliquities are lower. Gullies therefore do not form at high obliquities, but rather at lower obliquities that follow higher periods.

Our insolation measurements do not directly suggest a specific mechanism for water release. However, the range of insolation values suggests that the gully material is not melt from solid ice. Ice melting requires temperatures at or above 273 K, which from the daily average insolation values we know are not achieved at the gully sites. The maximum noontime temperatures for gullied slopes are such that if liquid water were released on the slope, it would likely persist long enough to move down the slope before subliming or freezing. Heldmann et al. (2005) modeled flow rates in the gullies at the current temperatures and pressures, and found that they have a flow rate ~30 m^3/s. With this flow rate as a constraint, they examined how long water would flow on the surface, and measured this in terms of channel length. They found that the gullies' measured channel lengths were similar to the lengths returned by their model, suggesting that liquid water can exist long enough to form gullies on the surface today. We suggest that once lower obliquities are achieved, the release of water from subsurface sources may commence through a process not specified by our measurements. This release may occur anywhere there is source material; however, gullies will only form in regions that allow for liquid water to be stable for a short amount of time. In addition, the slope must be above ~5° in order for the liquid to flow down the slope fast enough to form a visible gully.

6. Model constraints

   a) Subsurface ice, aquicludes, and shallow aquifers

As previously discussed, subsurface ice cannot be melted at depth via insolation alone. Obliquity changes may change the depth at which liquid water is stable, and subsurface ice may be melted by this process, but simply changing obliquity will not cause this liquid water to be released on the surface. One potential way around these issues can be found when one notes that in general, gullies form on crater walls. These slopes cut through the surface strata, exposing layers that are usually covered. Ice that occupies a specific layer may be exposed to the near-surface by crater walls. Mellon and Phillips' (2001) model suggests that this ice could be melted seasonally where it is within ~4 m of the surface. Gullies would form wherever subsurface ice coincided with the surface. However, our depth results suggest that gully formation began after some subsurface ice had already been removed. If ice layers were melted wherever they coincided with the surface and when they reached 273 K, then gullies should have begun forming at high obliquities, and no relationship between depth and latitude would be observed. Heldmann and Mellon (2004) also point out that this ice would not be stable for much time in regions that routinely reach above 273 K. The ice would most likely be removed by sublimation first, since in order to melt ice and release liquid at the same time, the temperatures must be just at 273 K and not above. Our results show that the gullied slopes can seasonally be much warmer than 273 K at high obliquities. The subsurface ice melt model also cannot explain why warmer wintertime temperatures would assist in gully formation.

If the subsurface gully forming material is already liquid, it does not require insolation to both melt and release it, which requires a specific temperature. As previously mentioned, Mellon and Phillips (2001) calculated the depth of the 273 K isotherm and found it to be ~146 m. This is near our result of ~200 m for average gully depths, which allows for the gully source material to be subsurface liquid water. Gilmore and Phillips (2002) suggest that these aquifers can be formed through thermal heating. Insolation on the surface can melt shallow seasonal surface ice and allow it to percolate deeper into the surface, and that this liquid can collect on impermeable layers called aquicludes. They point out that this can explain the resistant layers often seen at the tops of the gullies. In this model, the water may be discharged on the surface if the impermeable layer has the correct tilt, and if the layer is exposed on the surface. Impact craters cut through near surface strata, and thus many gullies can be seen on their walls. The gully morphology can also be explained by this model; water will flow over the resistant layer and begin to form a channel below the layer.

Mellon and Phillips (2001) have proposed a similar model, in which water is trapped between impermeable layers. In this model, an ice plug will form when the aquifer becomes closer to the exterior, such as by a slope face that exposes these layers. Mellon and Phillips (2001) modeled the effects of changing obliquity and surface temperatures on the aquifer, and found that at lower obliquities, more of the aquifer would freeze. At lower obliquities, the mean annual surface temperature does not vary as much over time as it does in high obliquities. At high obliquities, the mean annual temperature can vary significantly, preventing the buildup of ice in the aquifer with high temperature excursions. Mellon and Phillips (2001) suggest that the buildup of ice in the aquifers would increase the pressure, which in turn could cause the ice plug to rupture. This would cause a sudden release of water onto the surface. Heldmann et al.'s (2005) water stability model indicates that if the slope temperatures were within the range of liquid water, that this released liquid could persist long enough on the slope to form a gully. Mellon and Phillip's (2001) model works well with our observations, since it does not invoke seasonal insolation to release liquid. The ice plugs could burst at any season or time of day; however, if the surface temperatures were not correct, a gully would not form. The observation that gullied slopes receive a smaller range of insolation than nongullied slopes may speak to the fact that while ice plug bursting may occur in many locations, gullies will only form as a result if the surface temperatures are correct.

b) Snowmelt

Thus far, the discussion has focused on subsurface ice as the material that forms the gullies. However, several other possibilities exist. As previously discussed, Jakosky and Haberle (1992) found that at high obliquities, water will move from the poles to lower latitudes. Water vapor may remain in the atmosphere, or it may condense into the regolith or on the surface as snow. Christensen (2003) suggests that obliquity changes have led to snow deposits in the midlatitudes. He points to the presence of curvilinear features on pole facing slopes, and suggests they are analogous to similar terrestrial features formed by snow. In his model, melt from this snow is the source of water forming the gullies. Lee et al. (2006) studied snow gullies in the Arctic, and found that their morphologies closely match those of the martian gullies. Although they did not observe these snow gullies cutting into the underlying material, they suggest that over time the snow gullies could incise channels into the slope. Like Christensen (2003), Lee et al. (2006) suggest that snow was emplaced during high obliquity, and would easily remain in regions that were somewhat shielded from receiving too much insolation. Like Treiman (2003), they suggest that the cliff forming layer that occurs above some gullies is the result of erosion instead of a source. In their model, snow can accumulate on and around these cliff layers. When the correct amount of insolation is received, the snow melts and forms gullies within the snow pack itself. Lee et al. (2006) suggest that given time, these snow gullies can carve similar looking features into the loose materials below the cliff layer. They acknowledge, however, that this has not been observed in terrestrial field sites.

Our results suggest that snowmelt is not the primary mechanism for gully formation. Heldmann and Mellon (2004) point out that for gullies to be formed by snowmelt, the gullies should be found on the coolest slopes, since this is where snow can be somewhat stable. Hecht (2001) shows that at current obliquity, pole facing slopes are the coolest. Thus, gullies should show a poleward orientation preference in all latitudes if they are formed by snow. Our results show that all orientations are represented in the gully population, with more gullies facing N-S than E-W.

The gully depths also do not support formation by snowmelt. Our measurements show that gullies appear to start deeper from the surface at lower latitudes. This agrees with the depth results of Heldmann and Mellon (2004). It is difficult to explain why snowmelt would initiate gully formation lower on the slope face at lower latitudes, since snow is a near-surface phenomenon. In addition, Heldmann and Mellon (2004) point out that snow is expected to form regionally, rather than in small patches. Gullies should therefore form on every appropriate slope in a given region. This is not the case; gullies are often seen on one crater, but not the adjacent one. Given these difficulties, it seems unlikely that gully formation is driven primarily by snowmelt.

7. Summary of discussion

The martian obliquity cycle has allowed for a large range of surface temperatures over the last few million years. At high obliquities, water ice will be emplaced at lower latitudes, including the midlatitudes where gullies are found. As the obliquity decreases, ice becomes unstable in those regions and begins to be removed via sublimation. The fact that gully depths change with latitude suggests that ice removal had already begun at the time of the gullies' formation. At all obliquities, liquid water is seasonally stable on the surface for short periods of time. However, our obliquity results suggest that mid to low obliquities provide more opportunities for liquid water to be present due to varying insolation amounts. The gullies may thus represent a transitional obliquity period in which the release of water from the subsurface may form gullies in all seasons at or around noon. It is important to recognize that our results allow for either subsurface ice or subsurface aquifers to form the gullies. Both mechanisms require insolation to occur, and are dependent on a specific temperature range. Gullies are geologically recent features, but it is not clear whether they are still forming today. Mellon and Phillips (2001) find that the obliquity was much higher as recently as 1 m.y. ago, so it is reasonable to suggest that gullies were forming in between the maximum and minimum obliquities.

VI. Conclusions and recommendations

The gullies are only found in the midlatitudes in both hemispheres, suggesting that a global phenomenon like insolation is responsible for their formation. The amount of insolation a region receives is dependent on latitude, season, and obliquity, all of which affect change on a global scale. Insolation generally determines the surface temperature, and so the gullies' latitude restriction also implies a temperature restriction. Our orientation and slope results demonstrate that gullies preferentially form on slopes that receive an optimal amount of insolation to achieve the needed temperature range of ~273 at lower obliquities. Gullies in the low, warm latitudes are on cooler slopes, while gullies in the high, cool latitudes are on warmer slopes. Their slope magnitudes also help to control the amount of insolation the slopes receive by moderating the angle of incidence of solar irradiance. The geometries of the gullied slopes are different from nongullied slopes, which do not show a slope or orientation preference.

The range of temperatures on gullied slopes varies with obliquity, but is generally centered ~273 K. The martian atmospheric pressure currently resides at ~0.006 bar; for liquid water to exist, either the temperature must be ~273 K or the atmospheric pressure must increase slightly. Our thermal modeling results indicate that the requisite temperatures can occur at gully sites, and thus gullies may have formed as the result of the release of water.

The martian obliquity has changed significantly over time, and has ranged from 0°-60° (Laskar and Robutel, 1993). Past studies on the martian water cycle have shown that at high obliquities, water ice could have been emplaced in the lower latitudes, where it is not currently stable at today (Haberle and Jakosky, 1990; Mellon and Jakosky, 1995; Head et al., 2003). However, it may remain at depth, where it is stable (Fanale et al., 1986). Additionally, models of the subsurface indicate that liquid water is also stable at depths of ~100 m (Mellon and Phillips, 2001; Heldmann and Mellon, 2004). Gilmore and Phillips (2002) suggest that seasonal near-surface ice can melt and percolate into the regolith, where it will collect on impermeable layers. If these layers are at the depth of liquid water stability, an aquifer can develop. A source for gully-forming water may be thus be found in the subsurface today.

We find that the gullies' geometries provide optimal insolation for liquid water only at specific obliquities. When the obliquity is high, then the gullied slopes do not receive a constant amount of insolation throughout the year, which allows for fewer opportunities for liquid water to exist on the surface. Gullied slopes are well above 273 K in the winter, and well below this temperature in winter at 60°. Fall and spring temperatures are still within the liquid water range. At obliquities equal to or less than today's value of 25.2°, the insolation on the gullies remains consistent in all seasons, irrespective of latitude, and the temperatures are centered around 273 K. An exception to this are pole facing gullies, which are cooler in the winter than equator facing gullies. However, these slopes can achieve the same temperature range as equator facing gullies in all other seasons.

The material of the slope face will modify the heating effect of insolation. We tested the effect of different material emissivities on our slope temperatures, and found that the slope material will often determine whether a slope is within range of 273 K. We chose basalt and sand as likely candidates for slope material. In all cases, changing the emissivity from a blackbody value = 1 will depress the temperatures somewhat. We found that slopes made of sand will keep the slope temperatures within the range of liquid water. MOC images indicate that gullied slopes are made of unconsolidated material, and so sand is also a good fit for the observed morphologies. However, the grain size of the slope material is unknown. The actual emissivity may deviate from our chosen value of 0.9 depending on both grain size and composition.

The temperatures on gullied slopes allow for liquid water to be present on the surface for short periods of time. However, seasonal insolation values will not have an effect on the temperatures at depth (Fanale et al., 1986). We suggest that the water source for the gullies must be in the liquid phase independent of the seasonal insolation. Thus, the seasonal insolation does not act to release the water.

We propose that gully formation is the result of the release of subsurface liquid water in regions where liquid may persist on the surface long enough to form a gully. The mechanism of the water's release is not clear from our measurements. However, once the water is released, we find that the best surface conditions for gully formation exist during mid to low obliquities. Subsurface water, on the other hand, is emplaced during high obliquities. We therefore suggest that gully formation occurs as a result of the transition between high and low obliquities. The geologic youth of the gullies works well with the fact that Mars is presently moving from a period of high obliquity to one of lower obliquity (Mellon and Jakosky, 1995). Therefore, gullies may be forming today.

Our results work well with the gully formation model of Mellon and Phillips (2001), who propose that aquifers at depth provide liquid water for gullies. As in Gilmore and Phillips' (2002) model, these aquifers are located on impermeable strata at depths ~150 m, and are only exposed to surface at slope faces. The aquifer will develop an icy plug where it is near the surface, which effectively close the pore space and keep the aquifer confined behind it. This plug will also serve to protect against sublimation.

Mellon and Phillips (2001) modeled the behavior of the aquifers over the obliquity cycle, and found that long-term changes in insolation as a result of obliquity differences will determine how deeply the icy plug will freeze into the aquifer. Interestingly, their model showed an increase in aquifer ice at lower obliquities. This is interpreted as the result of surface temperatures becoming more constant. The average surface temperature of Mars will never exceed ~225 K at any obliquity, and so water at depth will freeze as surface temperatures approach this value over time. Mellon and Phillips (2001) point out that increasing the amount of ice in a confined aquifer will increase the pressure within it. If the pressure is sufficient, the icy plug may break, thereby releasing liquid water onto the surface. According to the model of Mellon and Phillips (2001), the ice plugs are most likely to burst at lower obliquities. We find that liquid water is also stable on gullied slopes at lower obliquities; thus, gullies are formed when an aquifer plug bursts on a slope that is at ~273 K.

The stability of water on the surface is dependent upon the magnitude of maximum temperatures, rather than average temperatures. As previously mentioned, the daily average temperature on Mars will never exceed ~225 K. Average temperatures cannot be responsible for gully formation because it is far below the melting point of water. Maximum temperatures, on the other hand, often exceed the melting point by 30 K. This suggests that ice plug bursting will only form gullies if it occurs in the day near noontime. This is plausible because ice plugs that burst at night (or during colder parts of the day) will quickly freeze and stop the flow of water. However, Mellon and Phillips (2001) point out that this will weaken the ice plug. The plug may go through a break-freeze cycle several times before it coincidentally bursts around local noon, at which point a gully will form.

In order to test our model further, a better understanding of the global distribution of water is needed. At the time of writing, the Shallow Subsurface Radar (SHARAD) instrument has just arrived at Mars on the Mars Reconnaissance Orbiter (MRO). This is a ground penetrating radar instrument that has been designed to map subsurface structures. Its primary objective is to determine whether there is subsurface ice or water, and if so to map its extent (Phillips et al., 2005). The data from this mission may be able to confirm the presence of water at the locations suggested by the gullies.

Currently, gullies are just barely resolved in images of the surface; higher resolution images of these features would allow us to understand the details of their morphologies. From MOC images, it is not clear what the grain size of the slope material is, and this will have a significant affect on the thermal inertia of that surface. In addition, the nature of the gullies' levied walls is not currently resolvable. Another instrument onboard MRO is the High Resolution Imaging Science Experiment (HiRISE), the next generation of high resolution camera. This camera will be able to resolve the gullies in finer detail than MOC, with a resolution as high as 25-50 cm/pixel (McEwen et al., 2002). This will provide insight on both the slope materials and the gully morphologies.

Additional thermal modeling of the surface and near-surface will also help to constrain the temperatures on the slopes. Our model of slope temperature does not include important factors such as thermal inertia, density, thermal conductivity, geothermal gradient, and the atmospheric opacity. All of these factors will serve to modify the final temperatures experienced by the slope. Future work should include detailed modeling of gullied slope temperatures to confirm that they do reach the necessary temperatures for liquid water.

VII. References

Christensen, P.R. (2003). Formation of recent martian gullies through melting of extensive water-rich deposits. *Nature* 422, 46-48.

Costard, F. et al. (2002). Formation of recent martian debris flows by melting of near-surface ground ice at high obliquity. *Science* 295, 110-113.

Edgett, K. S. et al. (2003). Polar- and middle-latitude martian gullies: A view from MGS MOC after 2 Mars years in the mapping orbit. *Lunar and Planetary Science Conference XXXIV*, Houston, TX, abstract no.1038.

Fanale, F.P. et al. (1986). Global distribution and migration of subsurface ice on Mars. *Icarus* 67, 1-18.

Fanale, F.P. et al. (1992). Mars: Epochal climate change and volatile history. In *Mars*, edited by H.H. Kieffer et al., pp. 686-729. University of Arizona Press: Tucson.

Felix, G. and Thomas, N. (2004). Relation between dry and granular flow regimes and morphology of deposits: formation of levees in pyroclastic deposits. *Earth and Planetary Science Letters* 221, 197-213.

Gilmore, M.S. and Goldenson, N. (2004). Depths and geologic settings of northern hemisphere gullies (and comparison to their southern counterparts). *Lunar and Planetary Science Conference XXXV*, Houston, TX, abstract no.1884.

Gilmore, M.S. and Phillips, E.L. (2002). Role of aquicludes in formation of Martian gullies. *Geology* 30; 12, 1107-1110.

Greeley, R. et al. (1992). Martian aeolian processes, sediments, and features. In *Mars*, edited by H.H. Kieffer et al., pp. 686-729. University of Arizona Press: Tucson.

Haberle, R.M. and Jakosky, B.M. (1990). Sublimation and transport of water from the northern residual polar caps on Mars. *Journal of Geophysical Research*, v.95, no.B2, 1423-1437.

Haberle, R.M. et al. (1993). Atmospheric effects on the utility of solar power on Mars. In *Resources of Near-Earth*, eds. Lewis, J., Matthews, M.S., and Guerrieri, M.L. The University of Arizona Press: Tucson.

Hartmann, W.K., Thorsteinsson, T., and Sigurdsson, F. (2003). Martian hillside gullies and Icelandic analogs. *Icarus* 162, 259-277.

Head, J.W. et al, (2003). Recent ice ages on Mars. *Nature* 426, 797-802.

Hecht, M.H. (2002). Metastability of liquid water on Mars. *Icarus* 156, 373-386.

Heldmann, J.L. and Mellon, M.T. (2004). Observations of martian gullies and constraints on potential formation mechanisms. *Icarus* 168, 285-304.

Heldmann, J.L. et al. (2005). Formation of Martian gullies by the action of liquid water flowing under current Martian environmental conditions. *Journal of Geophysical Research,* v.110, E05004, doi:10.1029/2004JE002261.

Higgins, C.G., Hill, B.R., and Lehre, A.K. (1990). Gully development. *Geological Society of America*, Special Paper 252, 139-155.

Hoffman et al, 2000. Ideas about the surface runoff features on Mars. *Science* 290; 5492, 711-714.

Hoffman, N., 2002. Active polar gullies on Mars and the role of carbon dioxide. *Astrobiology* 2; 3, 313-323.

Jakosky, B.M. and Haberle, R.M. (1992). The seasonal behavior of water on Mars. In *Mars,* eds. Kieffer, H.H. et al. The University of Arizona Press: Tucson.

Kieffer, H.H. et al. (1992). The planet Mars: From antiquity to the present. In *Mars*, eds. Kieffer, H.H. et al. The University of Arizona Press: Tucson.

Laskar, J. and Robutel, P. (1993). The chaotic obliquity of the planets. *Nature* 361, 608-612.

Laskar, J., Levrard, B., and Mustard, J.F. (2002). Orbital forcing of the martian polar deposits. *Nature* 419, 375-377.

Lee, P. et al. (2006). Gullies on Mars: Fresh gullies in dirty snow, Devon Island, High Arctic, as end-member analogs. *Lunar and Planetary Science Conference XXXVII,* Houston, TX, abstract no. 1818.

Malin et al. (1998). Early views of the martian surface from the Mars Orbiter Camera of Mars Global Surveyor. *Science* 279, no.5357, 1681-1685.

Malin, M.C. and Edgett, K.S. (2000). Evidence for recent groundwater seepage and surface runoff on Mars. *Science* 288, 2330-2335.

Malin, M. et al, 2004. Mars Global Surveyor Mars Orbiter Camera in the extended mission: the MOC toolkit. *Lunar and Planetary Science Conference XXXV*, Houston, TX, abstract no. 1189.

McEwen, A.S. et al. (2002). HiRISE: The High Resolution Imaging Science Experiment for Mars Reconnaissance Oribiter. *Lunar and Planetary Science Conference XXXIII*, Houston, TX, abstract no.1163.

Mellon, M.T. and Jakosky, B.M. (1993). Geographic variations in the thermal diffusive stability of ground ice on Mars. *Journal of Geophysical Research*, v.98, no.E2, 3345-3364.

Mellon, M.T. and Jakosky, B.M. (1995). The distribution and behavior of Martian ground ice during past and present epochs. *Journal of Geophysical Research*, v.100, no.E6, 11,781-11,799.

Mellon, M.T., and Phillips, R.J. (2001). Recent gullies on Mars and the source of liquid water. *Journal of Geophysical Research* 106; E10, p.23, 165 (2000JE001424).

Mellon, M.T. et al. (2002). A global map of thermal inertia from Mars Global Surveyor mapping-mission data. *Lunar and Planetary Science Conference XXXIII*, Houston, TX, abstract no. 1416.

Milliken, R.E., Mustard, J.F., and Goldsby, D.L. (2003). Viscous flow features on the surface of Mars: Observations from high-resolution Mars Orbiter Camera (MOC) images. *Journal of Geophysical Research*, v.108, no.E6, 5057, doi:10.1029/2002JE002005.

Musselwhite, D.S., Swindle, T.D., and Lunine, J.I., 2001. Liquid CO_2 breakout and the formation of recent small gullies on Mars. *Geophysical Research Letters* 28; 7, 1283-1285.

Okubo, C.H., Schultz, R.A., and Stefanelli, G.S. (2004). Gridding Mars Orbiter Laser Altimeter data with GMT: effects of pixel size and interpolation methods on DEM integrity. *Computers & Geosciences* 30, 59-72.

Paige, D.A. (1992). The thermal stability of near-surface ground ice on Mars. *Nature* 356, 43-45.

Phillips, R.J. et al. (2005). SHARAD: Radar sounder on the 2005 Mars Reconnaissance Orbiter. *Workshop on Radar Investigations*, Lunar and Planetary Institute, Houston, TX, abstract no.6013.

Smith, D.E. et al. (1999). The global topography of Mars and implications for surface evolution. *Science* 284, no.5419, 1495-1503.

Stewart, S.T. and Nimmo, F. (2002). Surface runoff features on Mars: Testing the carbon dioxide formation hypothesis. *Journal of Geophysical Research*, v.107, no.E9, 5069, doi:10.1029/2000JE001465.

Sullivan et al. (2001). Mass movement slope streaks images by the Mars Orbiter Camera. *Journal of Geophysical Research*, v.106, no.E10, 23,607-23,633.

Thomas, P. et al. (1992). Polar deposits of Mars. In *Mars*, edited by H.H. Kieffer et al., pp. 686-729. University of Arizona Press: Tucson.

Treiman, A.H. (2003). Geologic settings of Martian gullies: Implications for their origins. *Journal of Geophysical Research*, v.108, no.E4, 8031, doi:10.1029/2002JE001900.

Ward, W.R. (1992). Long-term orbital and spin dynamics of Mars. In *Mars*, eds. Kieffer, H.H. et al. The University of Arizona Press: Tucson.

Zuber, M.T. et al. (1992). The Mars Observer Laser Altimeter investigation. *Journal of Geophysical Research*, v.97, no.E5, 7781-7797.

Zurek, R.W. (1992). Comparative aspects of the climate on Mars: an introduction to the current atmosphere. In *Mars*, eds. Kieffer, H.H. et al. The University of Arizona Press: Tucson.

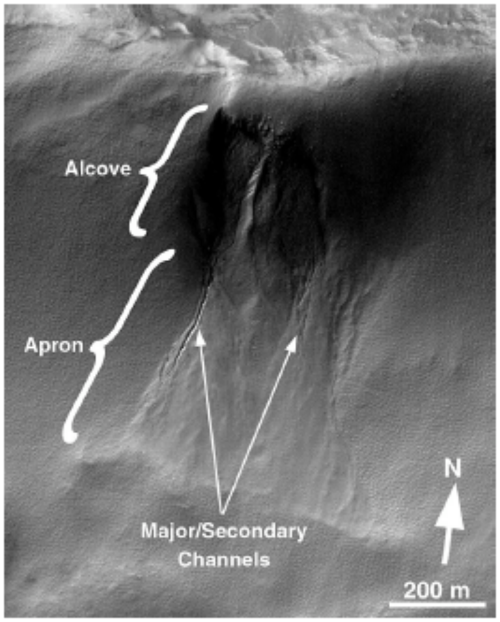

Figure B1

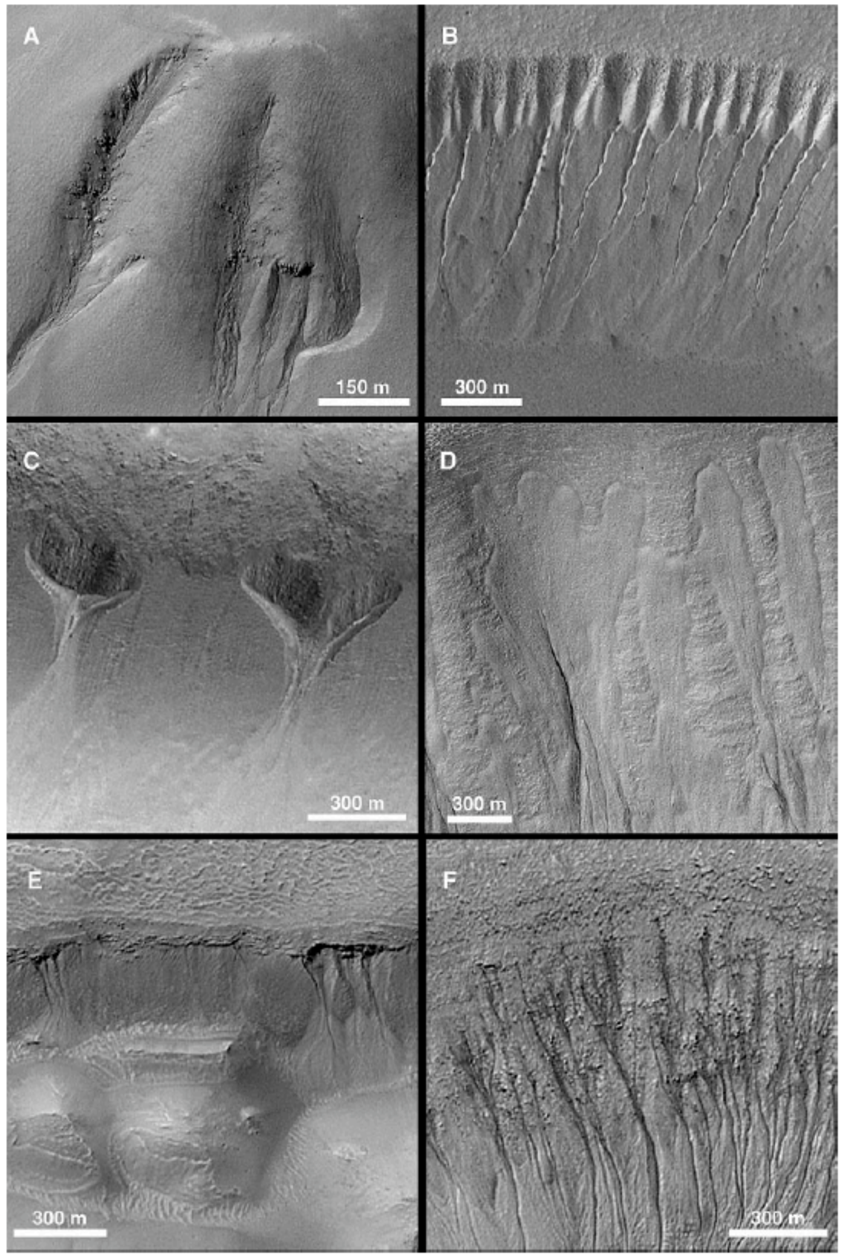

Examples of alcoves. Lengthened alcoves (**A**) are longer (downslope) than they are wide; where they occur in close proximity, they form characteristic badlands (**B**). Widened alcoves (**C**) are broad in transverse dimension and may include more than one smaller alcove. Occupied alcoves (**D**) are those that appear to be filled with material. Abbreviated alcoves (**E** and **F**) show strong topographic or stratigraphic control of landform location, which limits the extent of the alcove. Each picture is a subframe of a MOC image illuminated from the upper left, except for (C), which is illuminated from the upper right, and (F), which is illuminated from the left: (A) image M07-05535 (54.8°S, 342.5°W); (B) image M03-02709 (70.8°S, 355.8°W); (C) image M03-02214 (58.9°S, 336.0°W); (D) image M11-01601 (33.1°S, 266.8°W); (E) image M07-02909 (38.5°S, 171.3°W); and (F) image M11-00944 (41.1°S, 159.8°W).

Figure B2

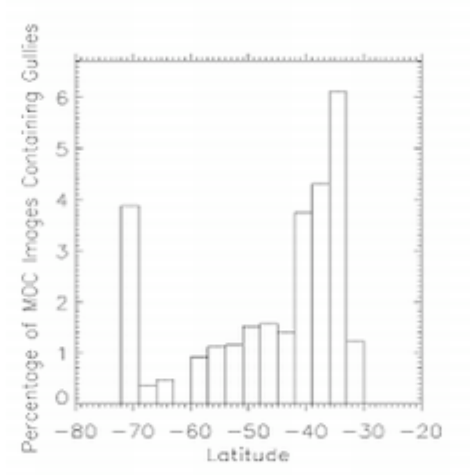

Figure B3

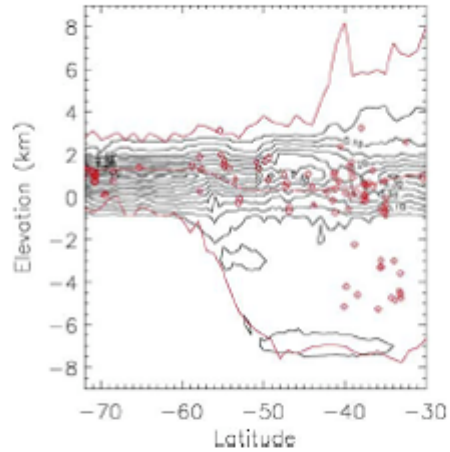

Figure B4

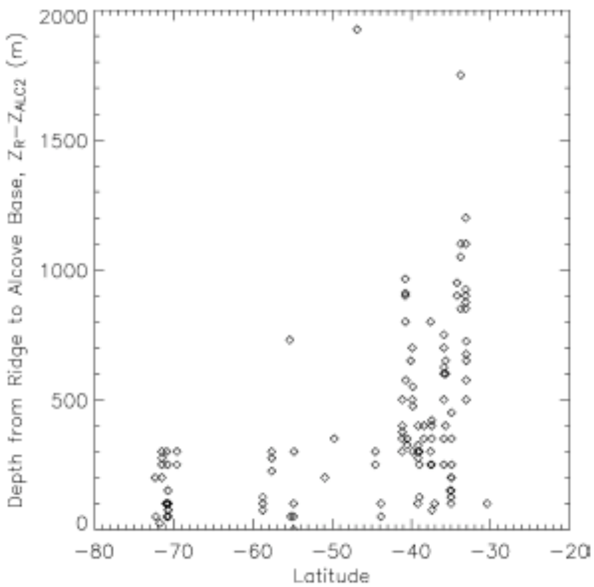

Figure B5

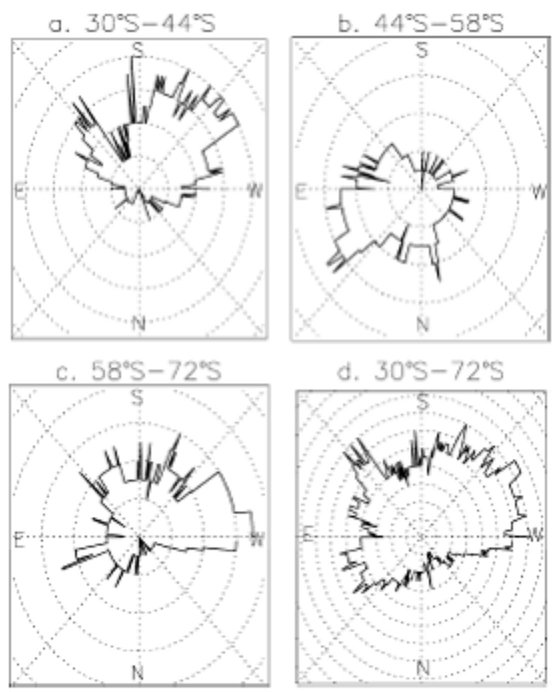

Figure B6

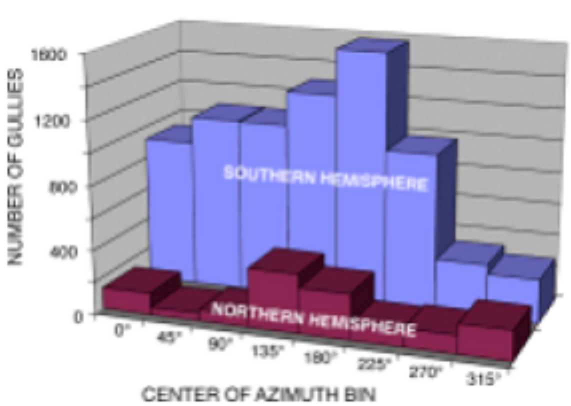

Figure B7

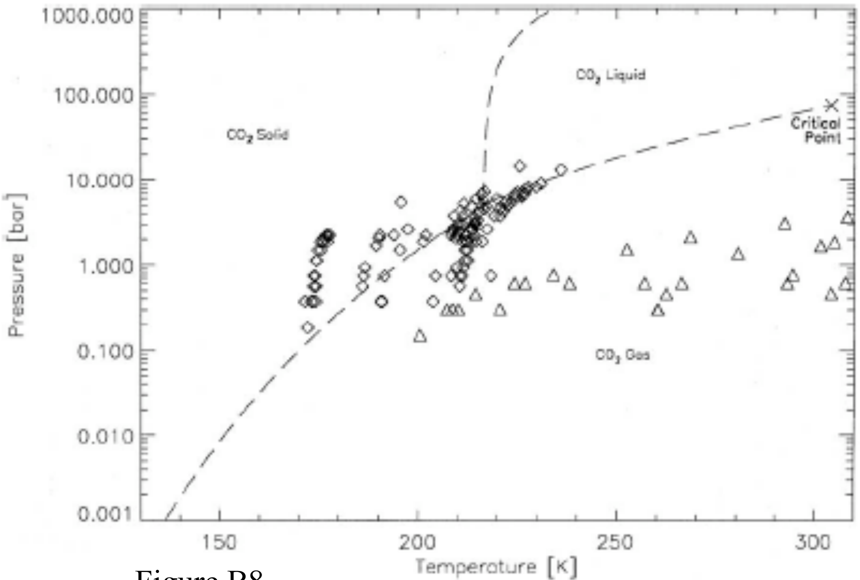

Figure B8

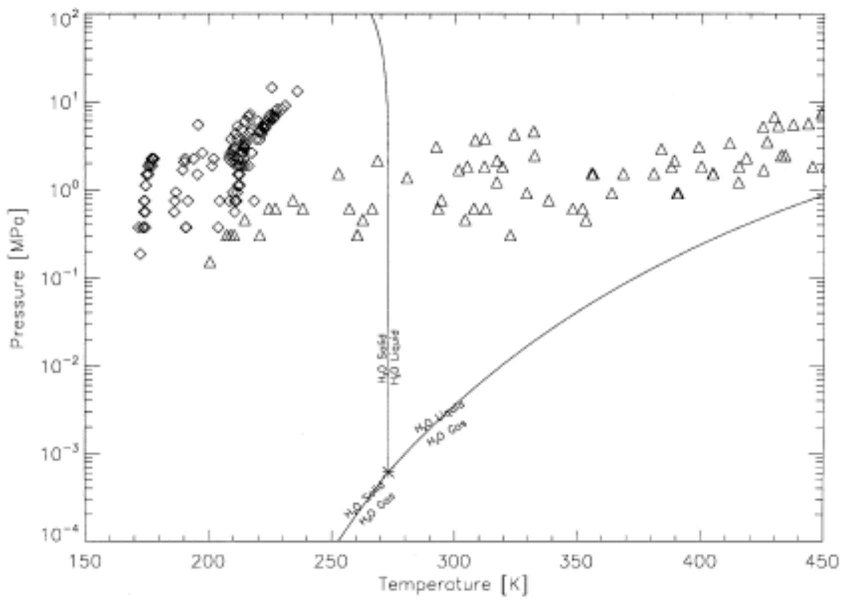

Figure B9

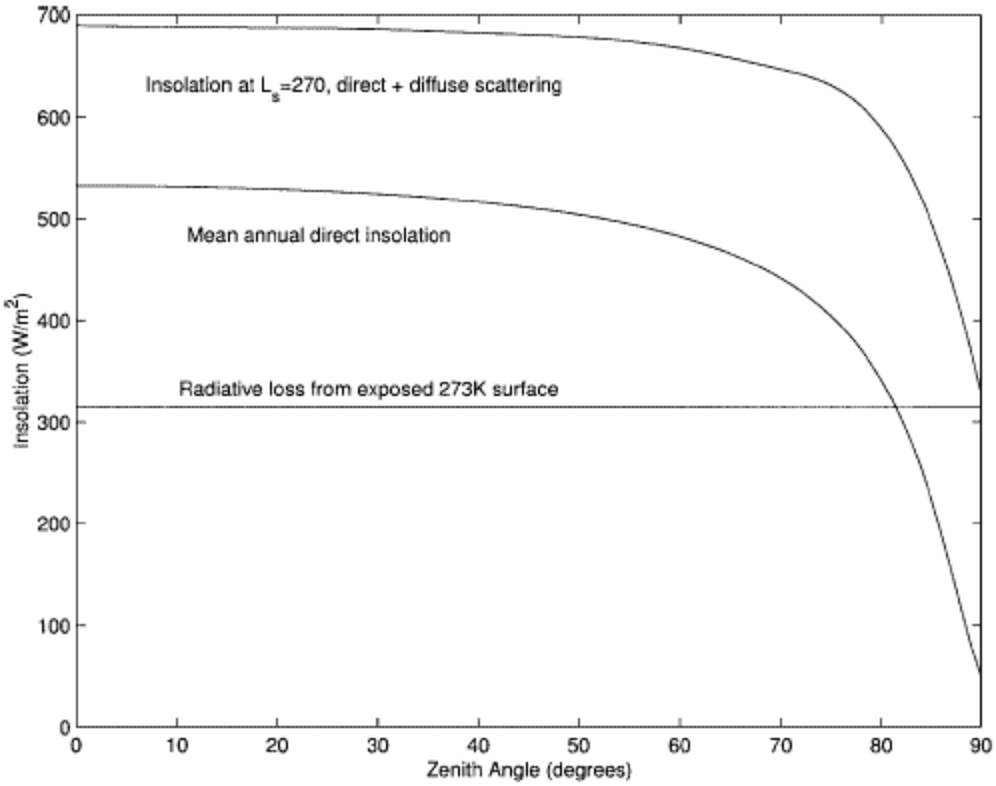
Insolation at L_s=270, direct + diffuse scattering
Mean annual direct insolation
Radiative loss from exposed 273K surface
Insolation (W/m^2)
Zenith Angle (degrees)
0
100
200
300
400
500
600
700
10
20
30
40
50
60
70
80
90

Figure B10

Figure 1a.

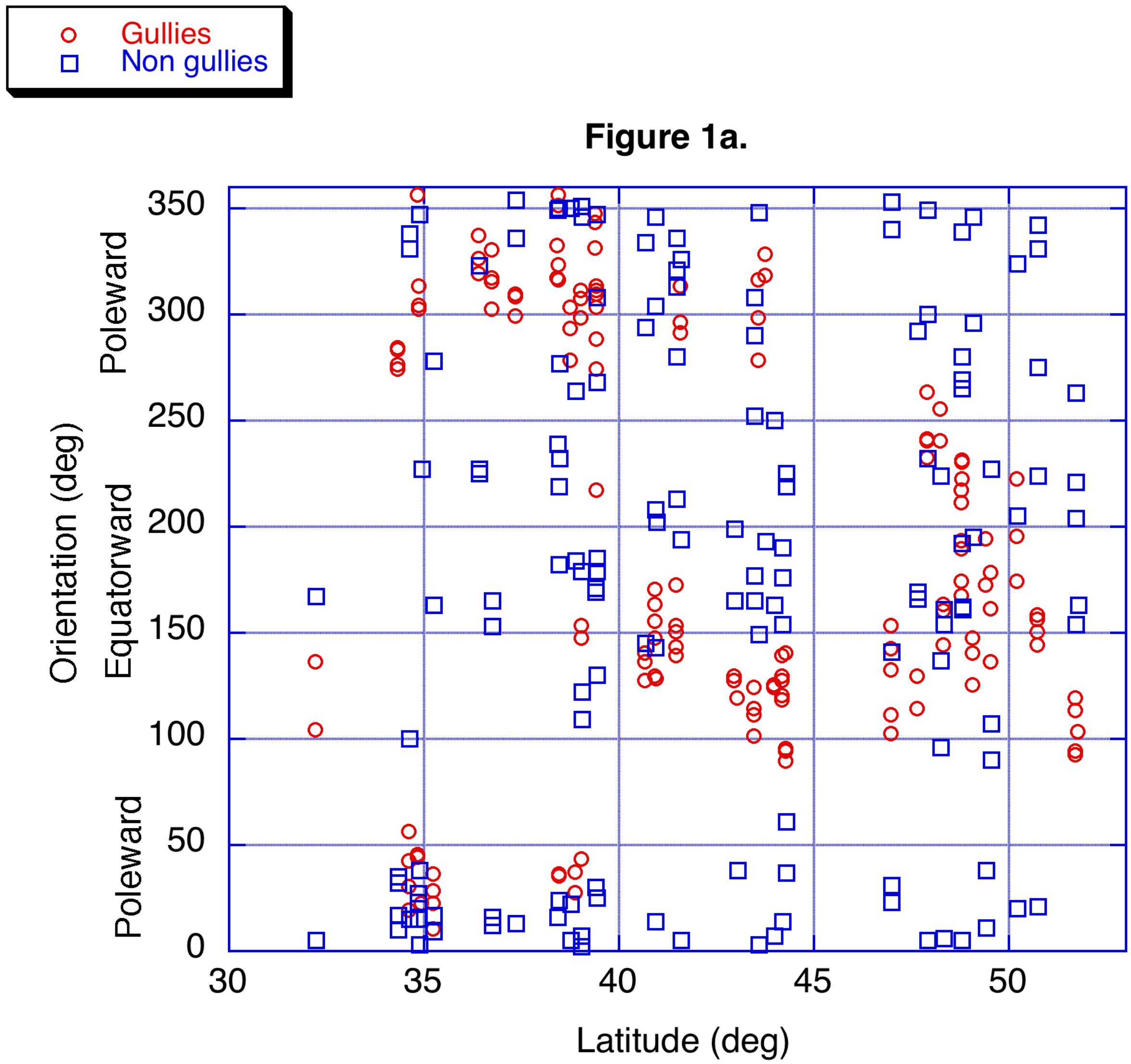

Gullies
Non gullies
Poleward
Equatorward
Poleward
Orientation (deg)
350
300
250
200
150
100
50
0
30
35
40
45
50
Latitude (deg)

Figure 1b.

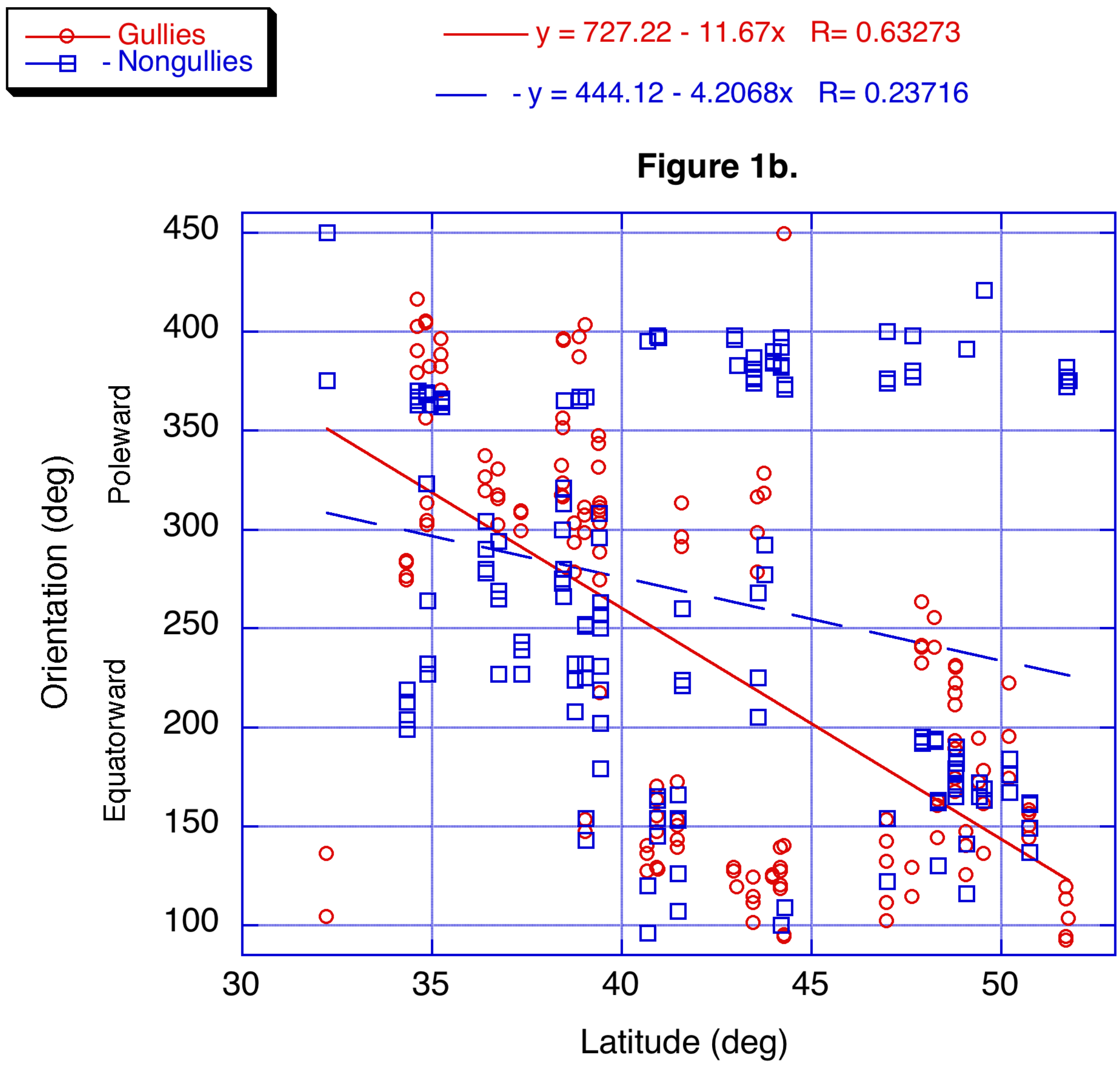

Gullies
- Nongullies
y = 727.22 - 11.67x R= 0.63273
- y = 444.12 - 4.2068x R= 0.23716
Orientation (deg)
Poleward
Equatorward
450
400
350
300
250
200
150
100
30
35
40
45
50
Latitude (deg)

Figure 2.

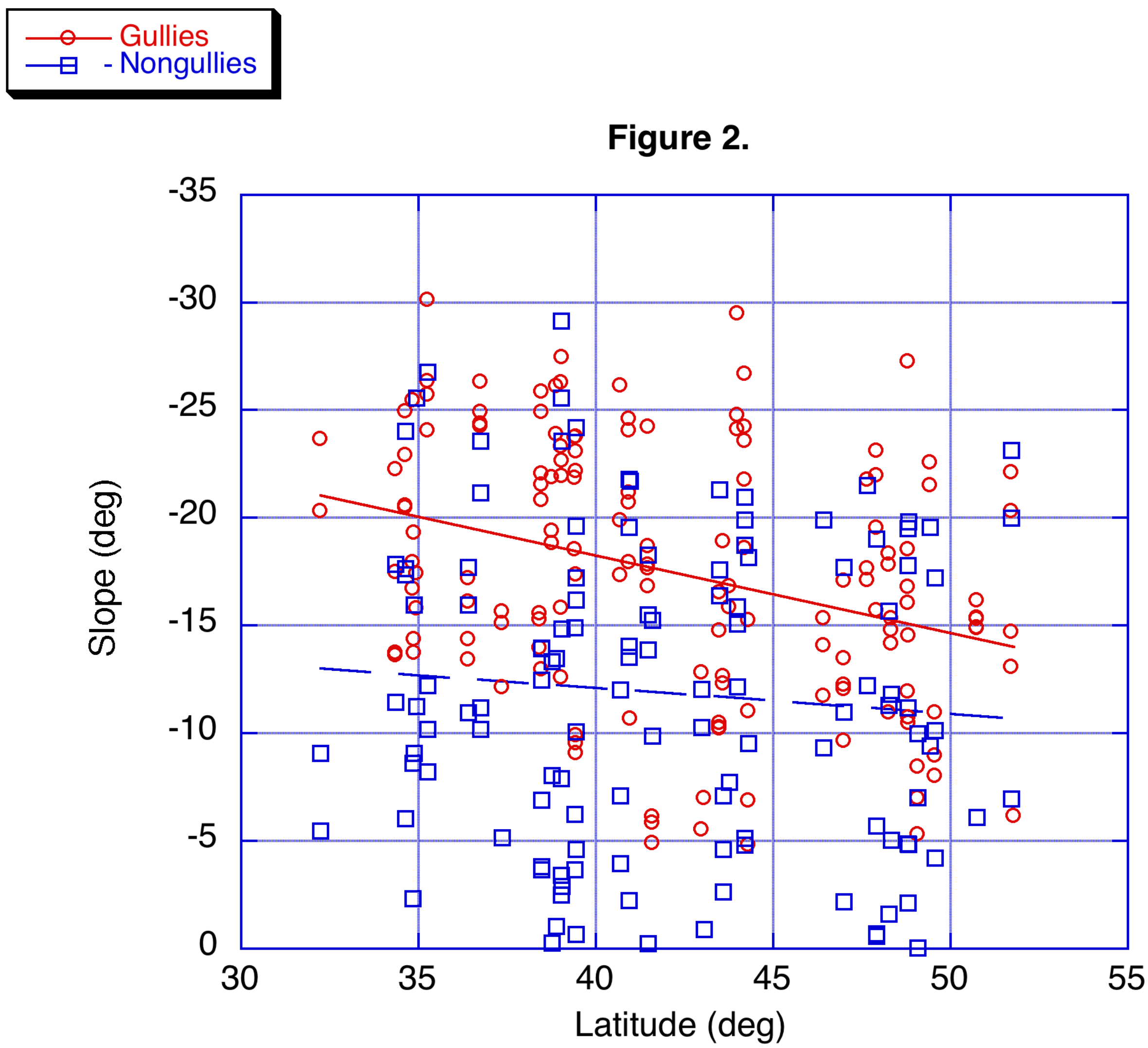
Gullies
- Nongullies
-35
-30
-25
-20
-15
-10
-5
0
30
35
40
45
50
55
Slope (deg)
Latitude (deg)

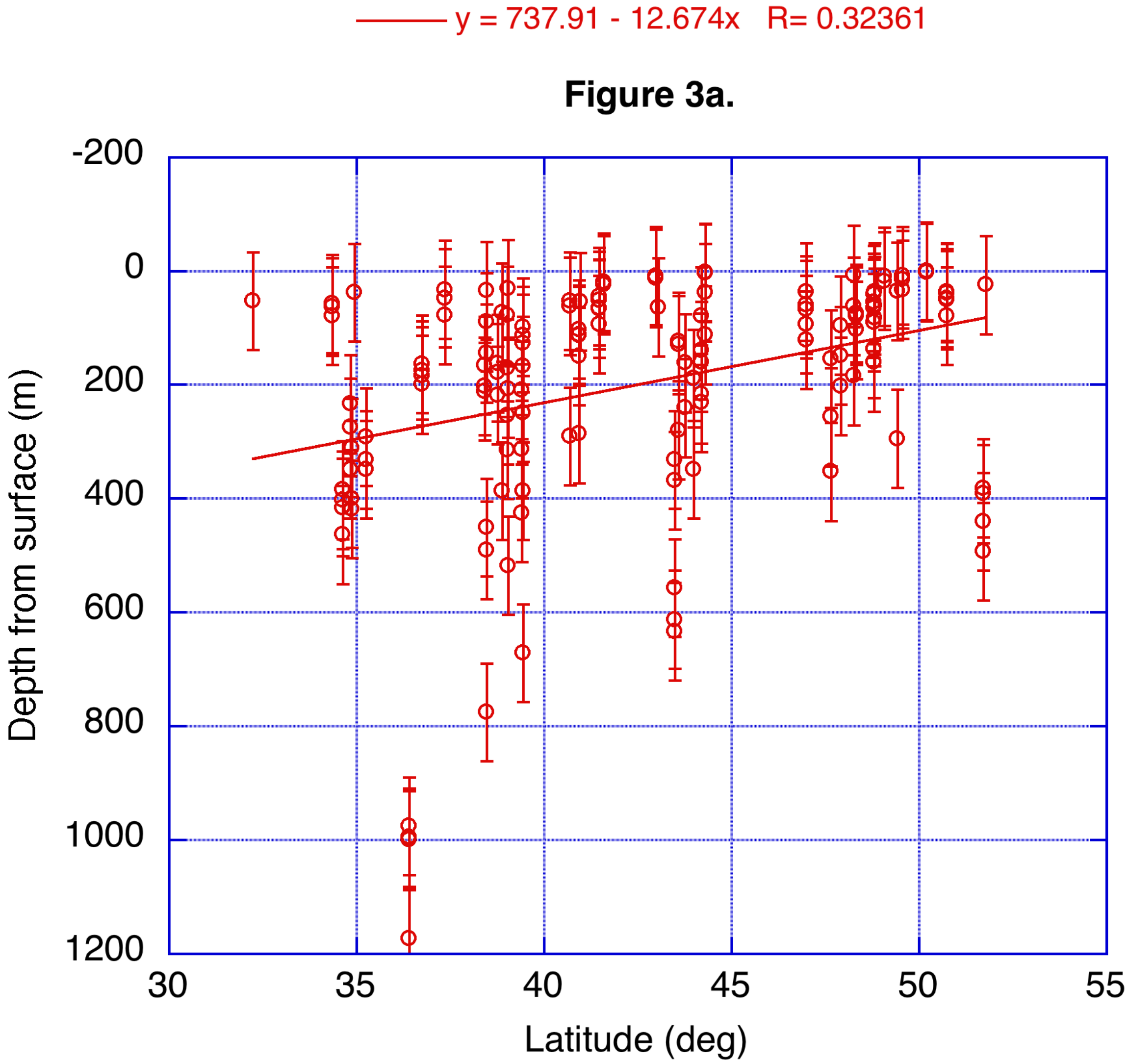

y = 737.91 - 12.674x R= 0.32361
-200
0
200
400
600
800
1000
1200
Depth from surface (m)
30
35
40
45
50
55
Latitude (deg)

Figure 3a.

Figure 3b.

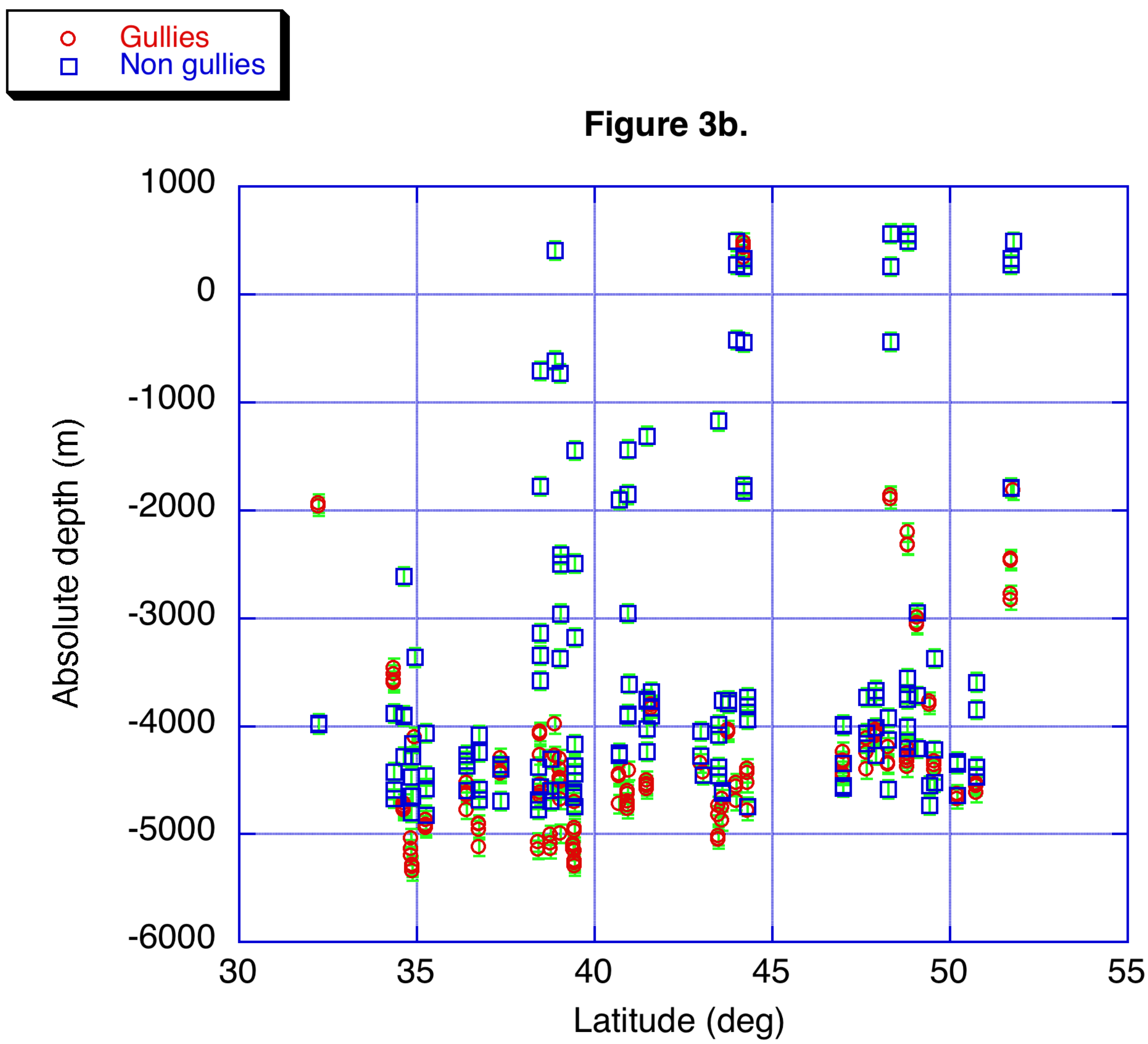
Gullies
Non gullies
1000
0
-1000
-2000
-3000
-4000
-5000
-6000
Absolute depth (m)
30
35
40
45
50
55
Latitude (deg)

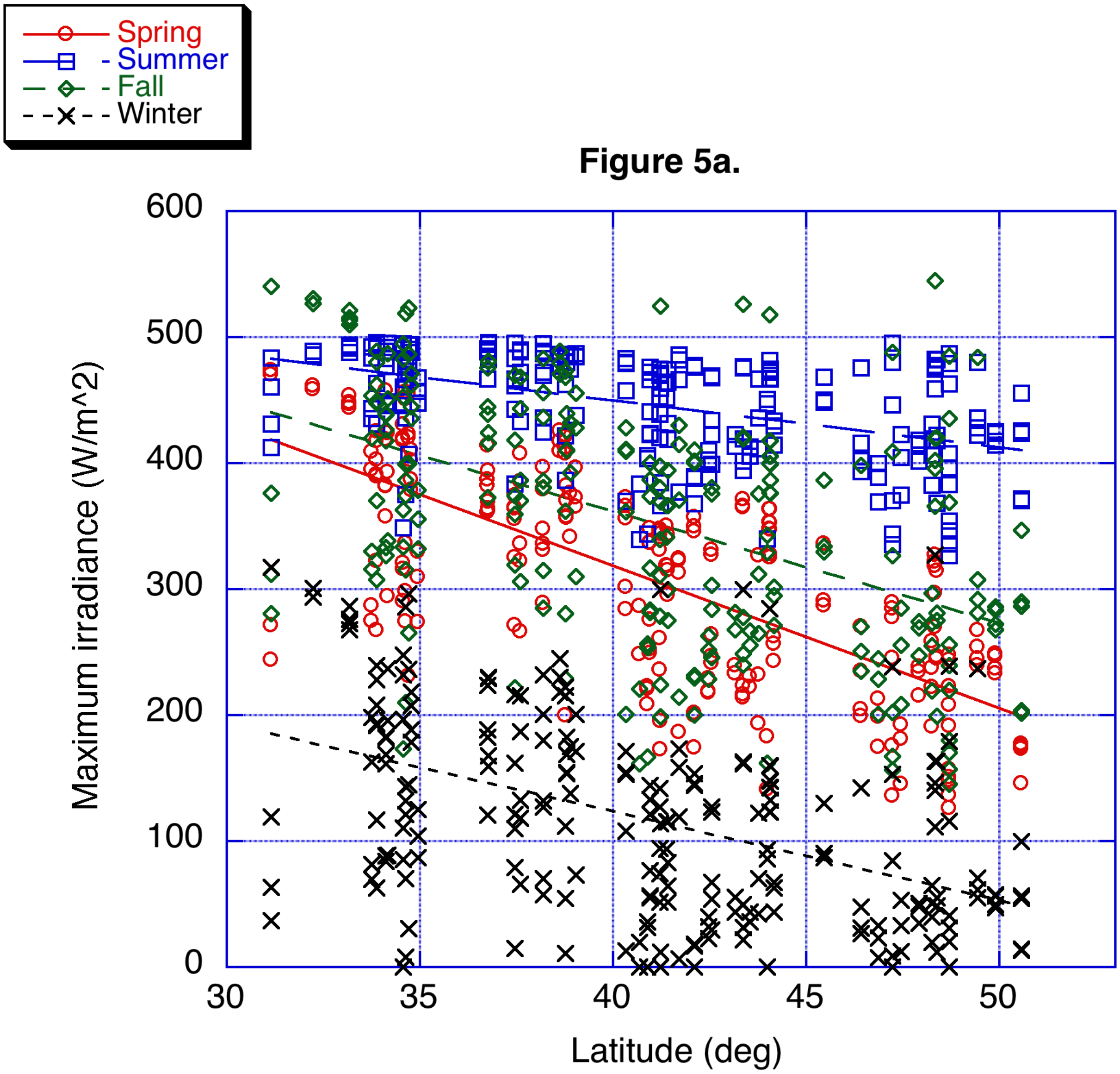
Spring
- Summer
- Fall
Winter
600
500
400
300
200
100
0
Maximum irradiance (W/m^2)
30
35
40
45
50
Latitude (deg)

Figure 5a.

Figure 5b.

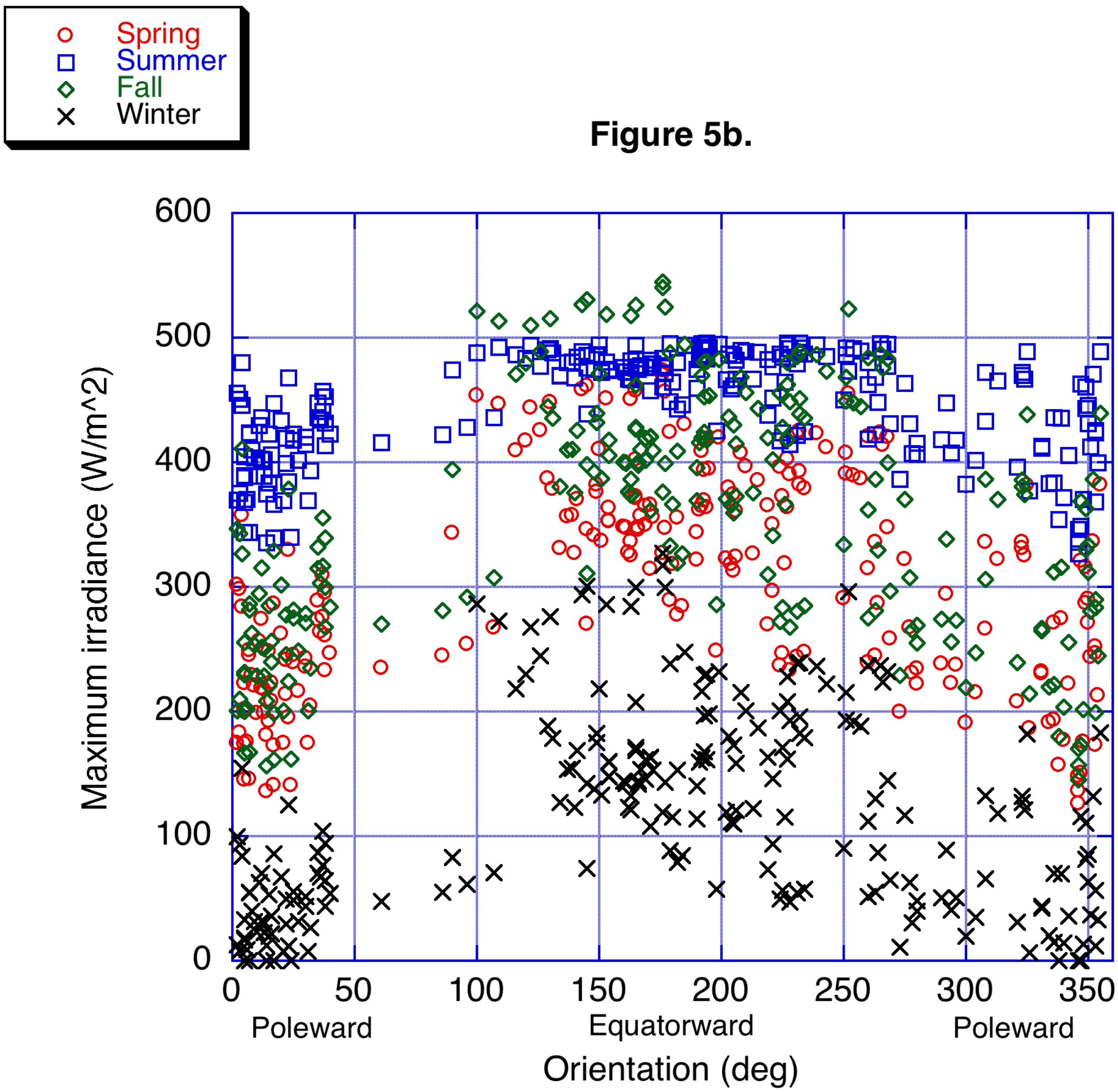

Spring
Summer
Fall
Winter
600
500
400
300
200
100
0
Maximum irradiance (W/m^2)
0
50
100
150
200
250
300
350
Poleward
Equatorward
Poleward
Orientation (deg)

Figure 5c.

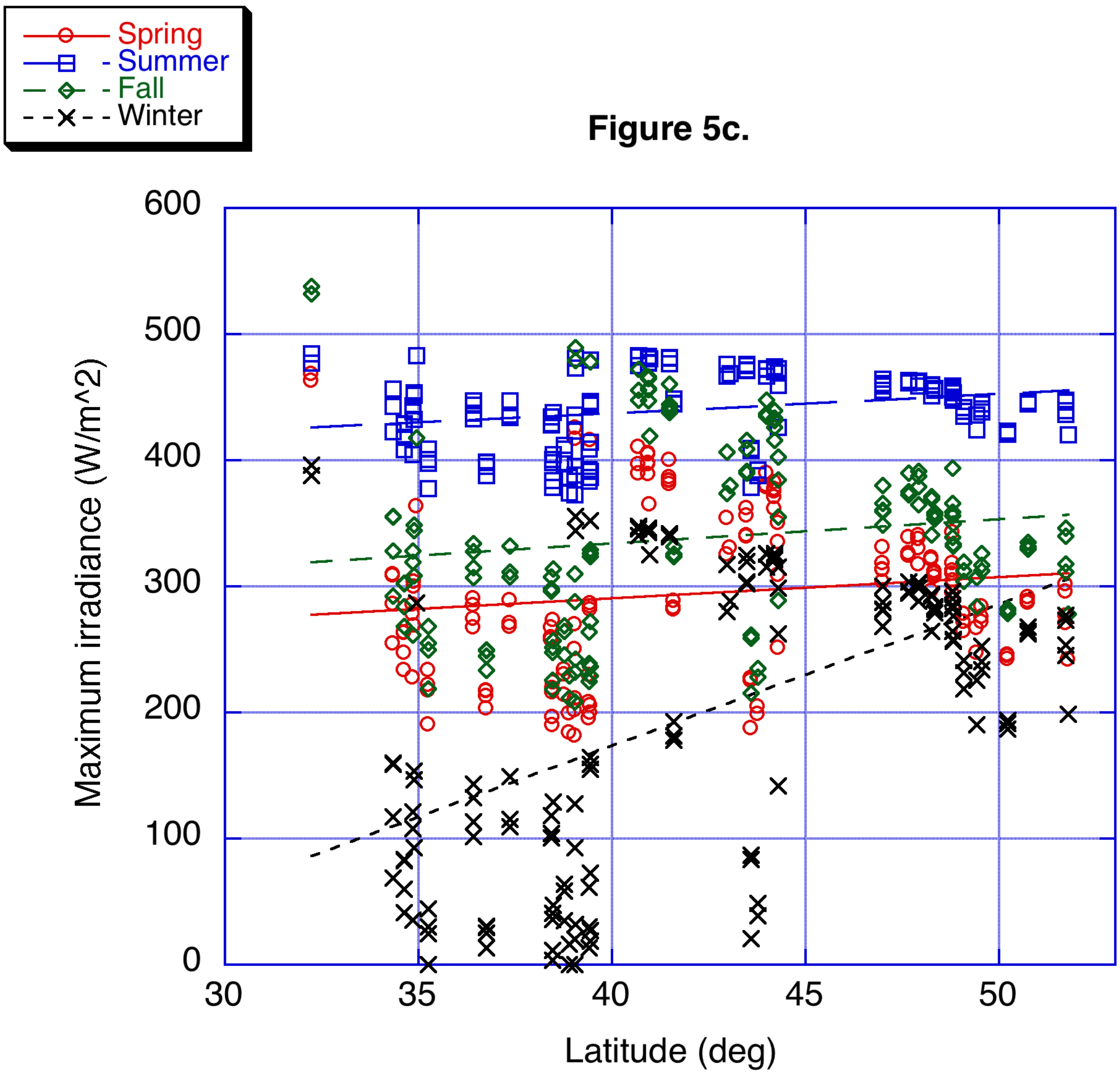

Spring
Summer
Fall
Winter
600
500
400
300
200
100
0
30
35
40
45
50
Maximum irradiance (W/m^2)
Latitude (deg)

Figure 5d.

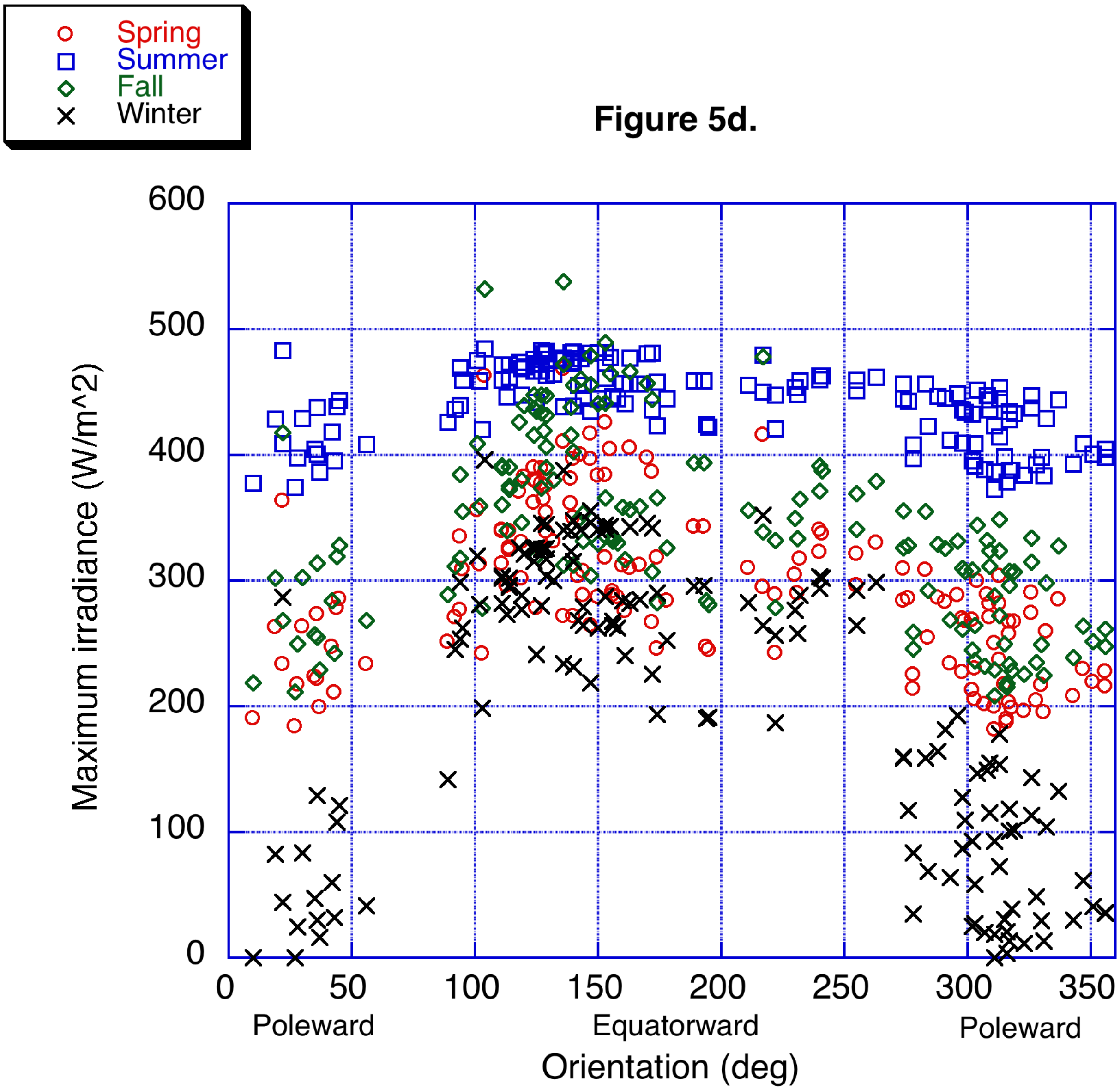

Spring
Summer
Fall
Winter
600
500
400
300
200
100
0
0
50
100
150
200
250
300
350
Maximum irradiance (W/m^2)
Poleward
Equatorward
Poleward
Orientation (deg)

Figure 6a.

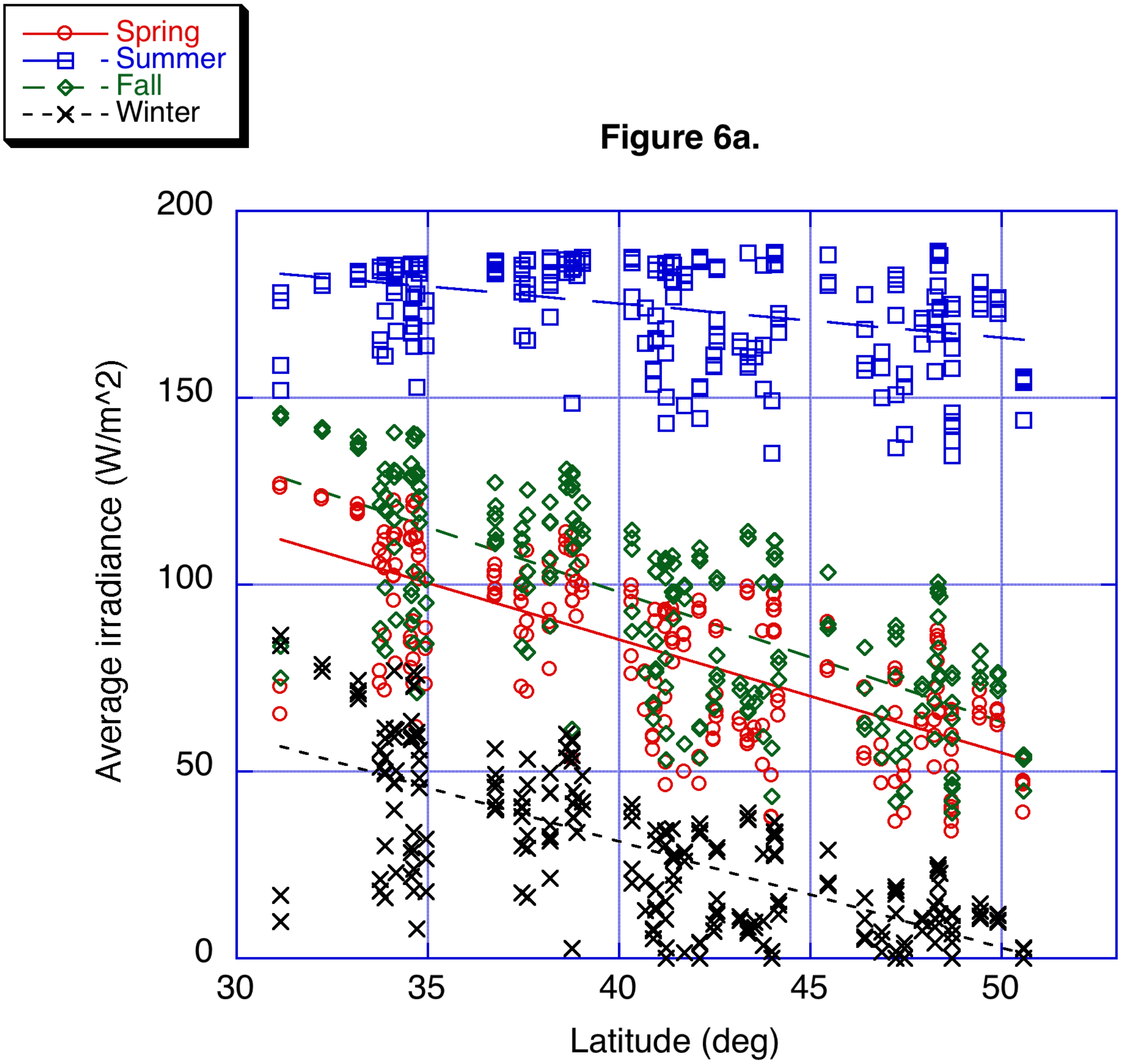

Spring
- Summer
- Fall
- - Winter
200
150
100
50
0
Average irradiance (W/m^2)
30
35
40
45
50
Latitude (deg)

Figure 6b.

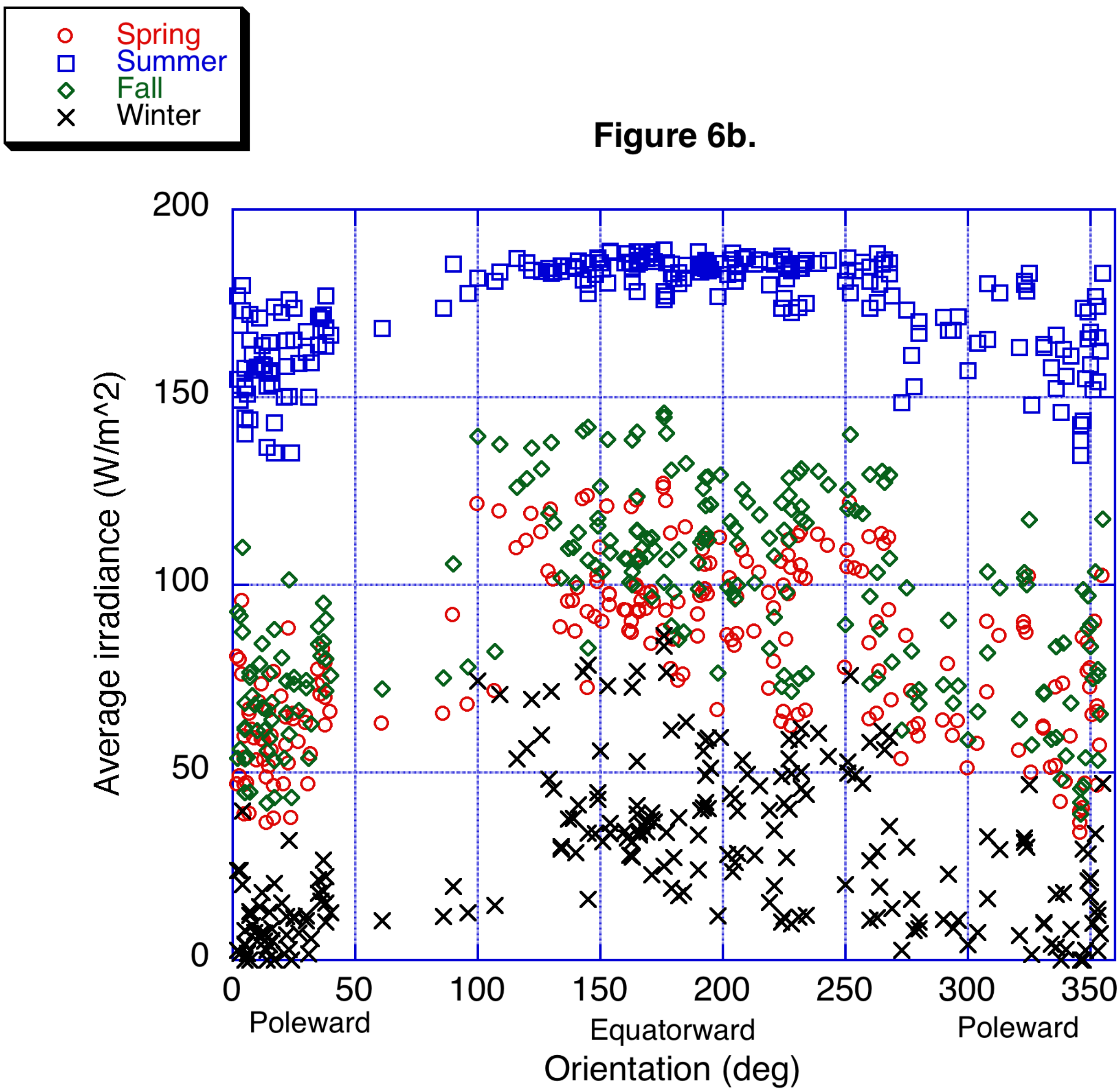

Spring
Summer
Fall
Winter
200
150
100
50
0
Average irradiance (W/m^2)
0
50
100
150
200
250
300
350
Poleward
Equatorward
Poleward
Orientation (deg)

Figure 6c.

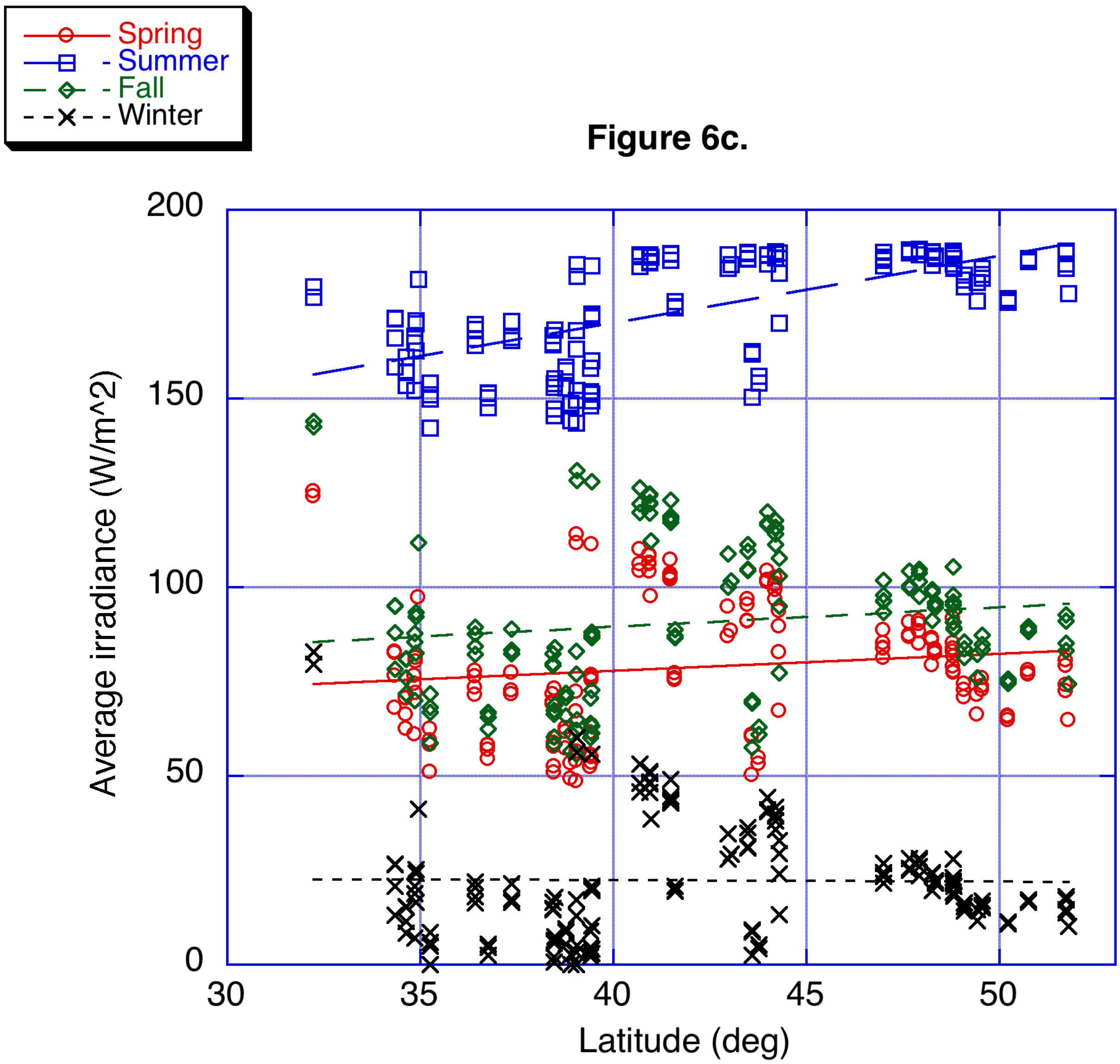

Spring
- Summer
- Fall
- - Winter
200
150
100
50
0
Average irradiance (W/m^2)
30
35
40
45
50
Latitude (deg)

Figure 6d.

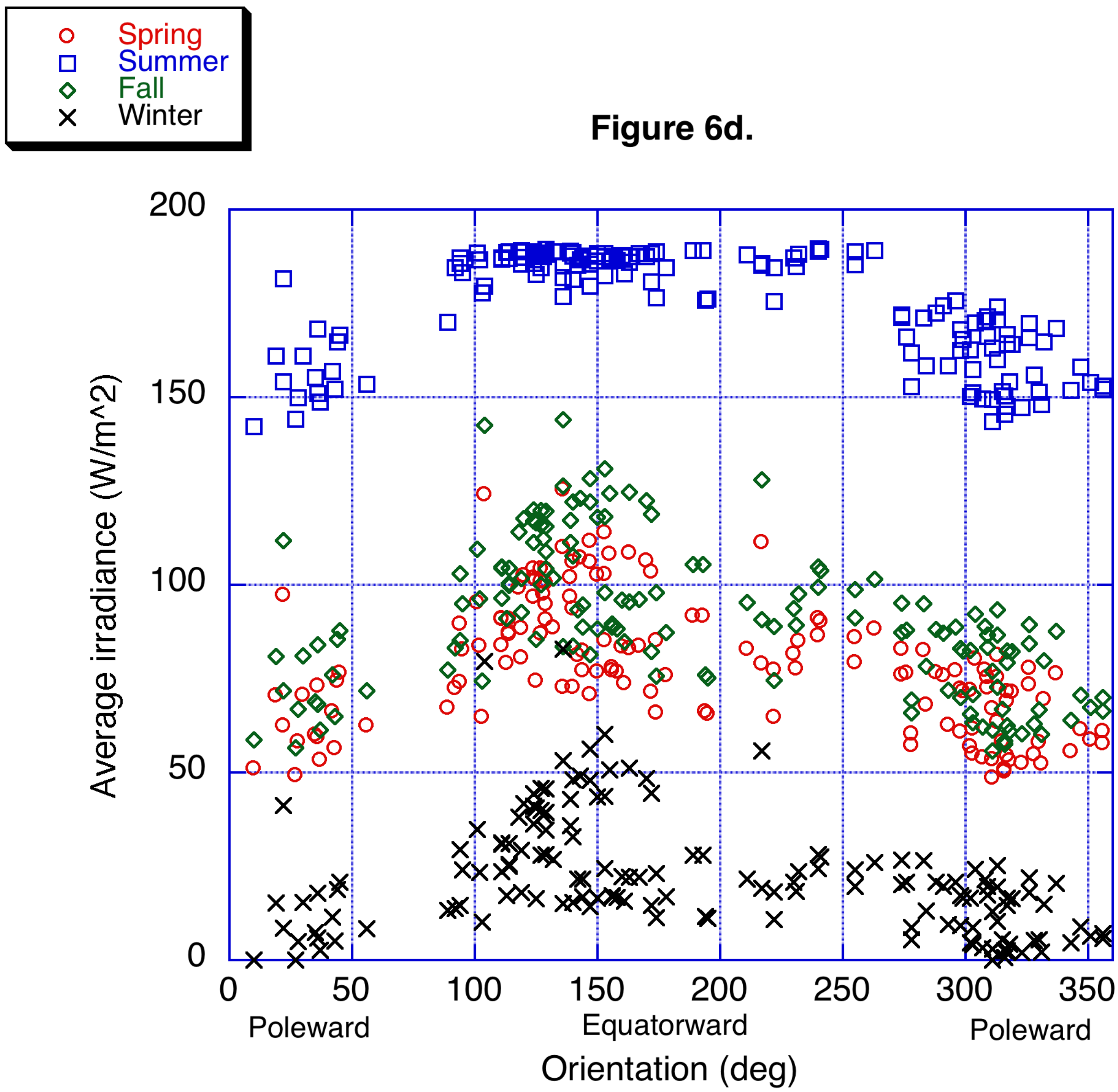

Spring
Summer
Fall
Winter
Average irradiance (W/m^2)
200
150
100
50
0
0
50
100
150
200
250
300
350
Poleward
Equatorward
Poleward
Orientation (deg)

Figure 7a.

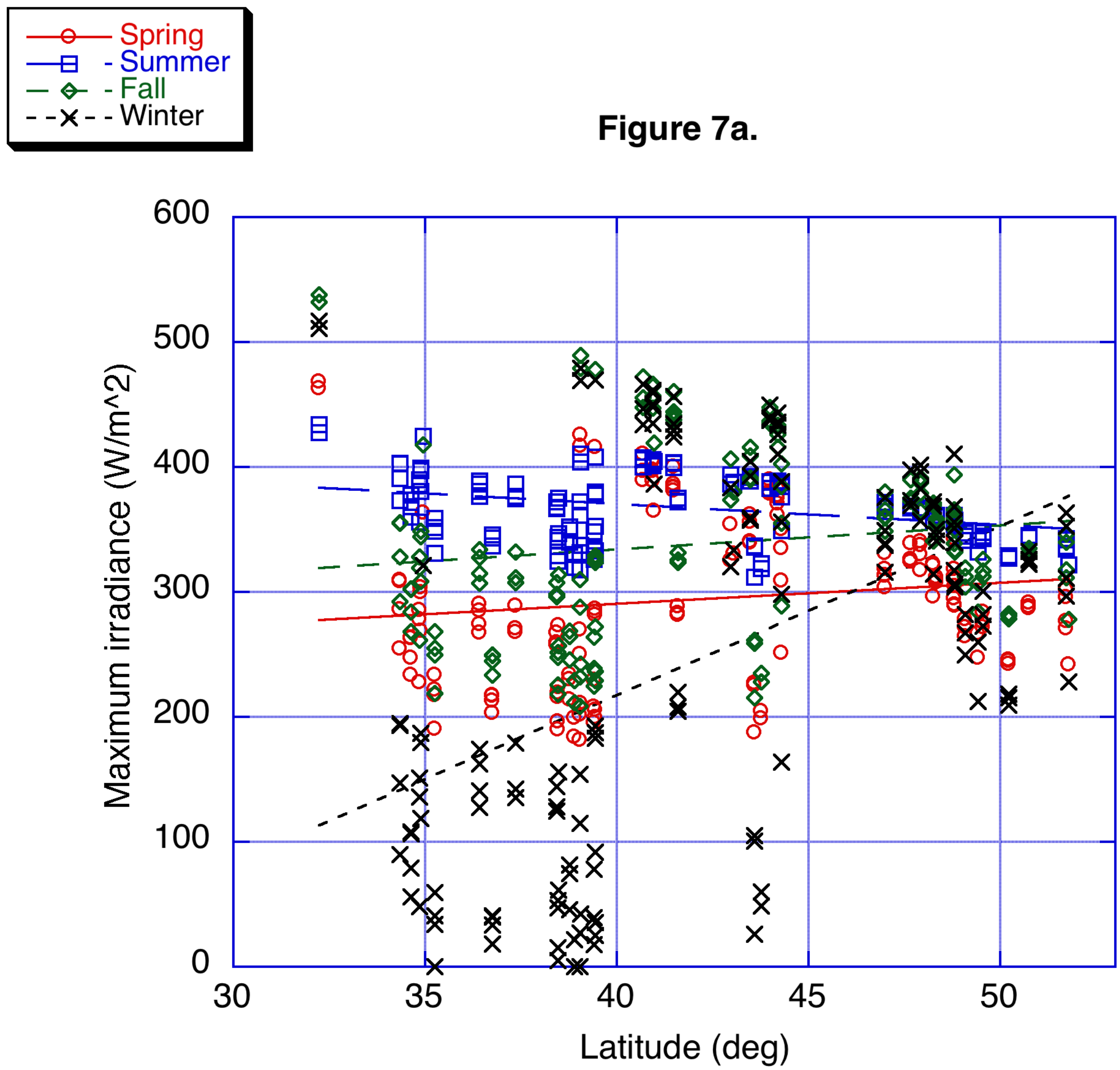

Spring
Summer
Fall
Winter
600
500
400
300
200
100
0
Maximum irradiance (W/m^2)
30
35
40
45
50
Latitude (deg)

Figure 7b.

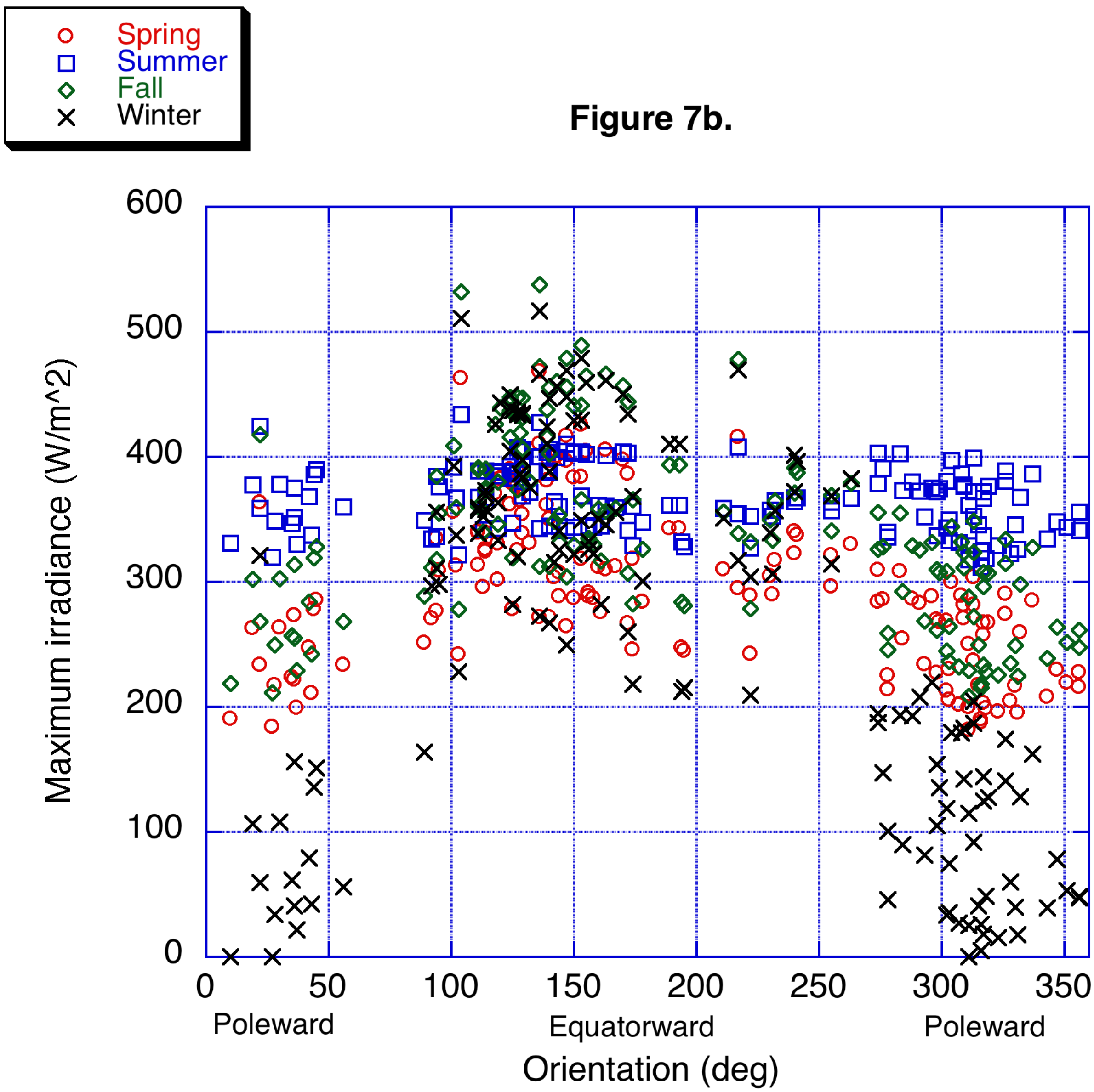

Spring
Summer
Fall
Winter
600
500
400
300
200
100
0
Maximum irradiance (W/m^2)
0
50
100
150
200
250
300
350
Poleward
Equatorward
Poleward
Orientation (deg)

Figure 7c.

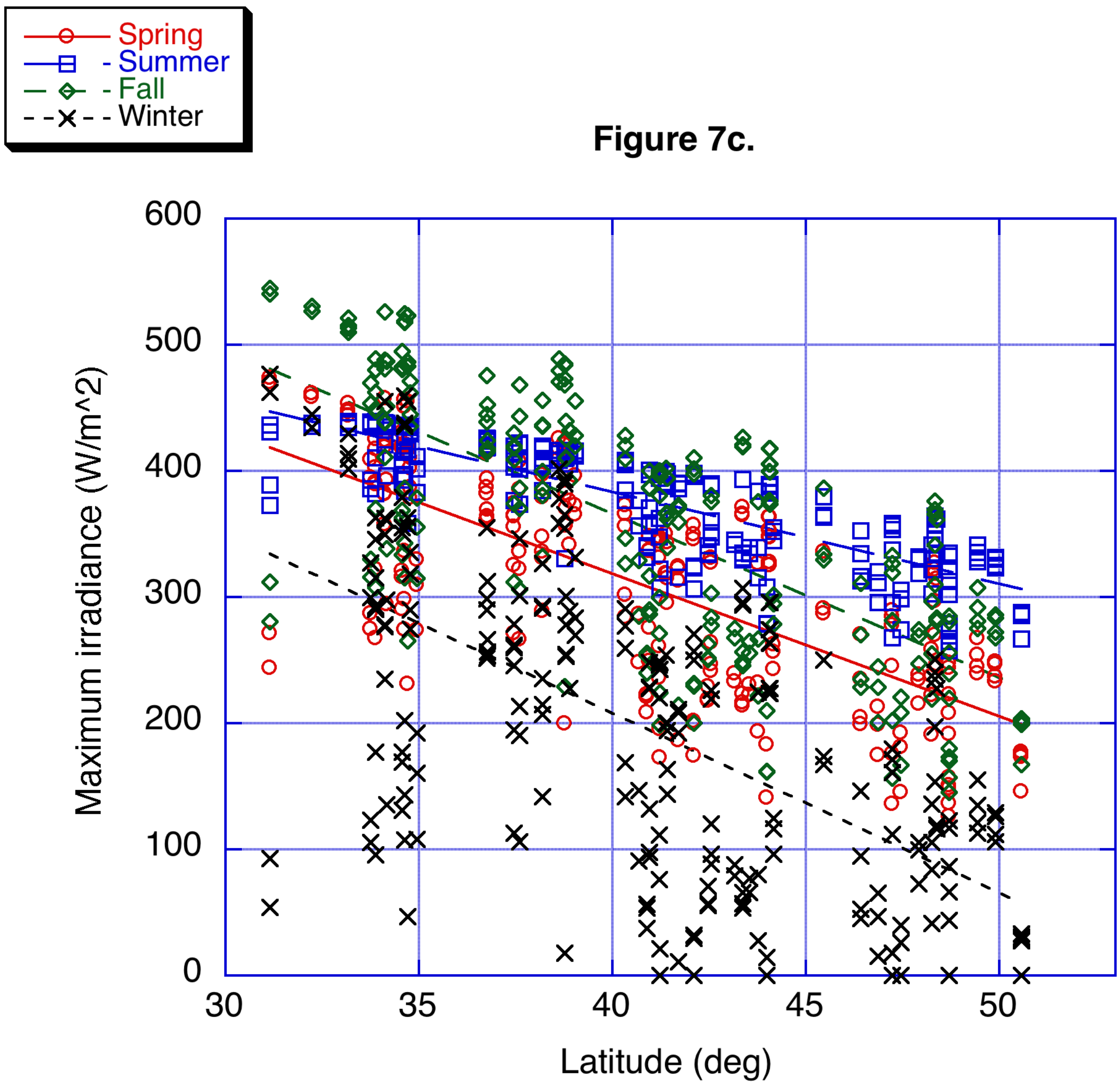

Spring
Summer
Fall
Winter
600
500
400
300
200
100
0
30
35
40
45
50
Maximum irradiance (W/m^2)
Latitude (deg)

Figure 7d.

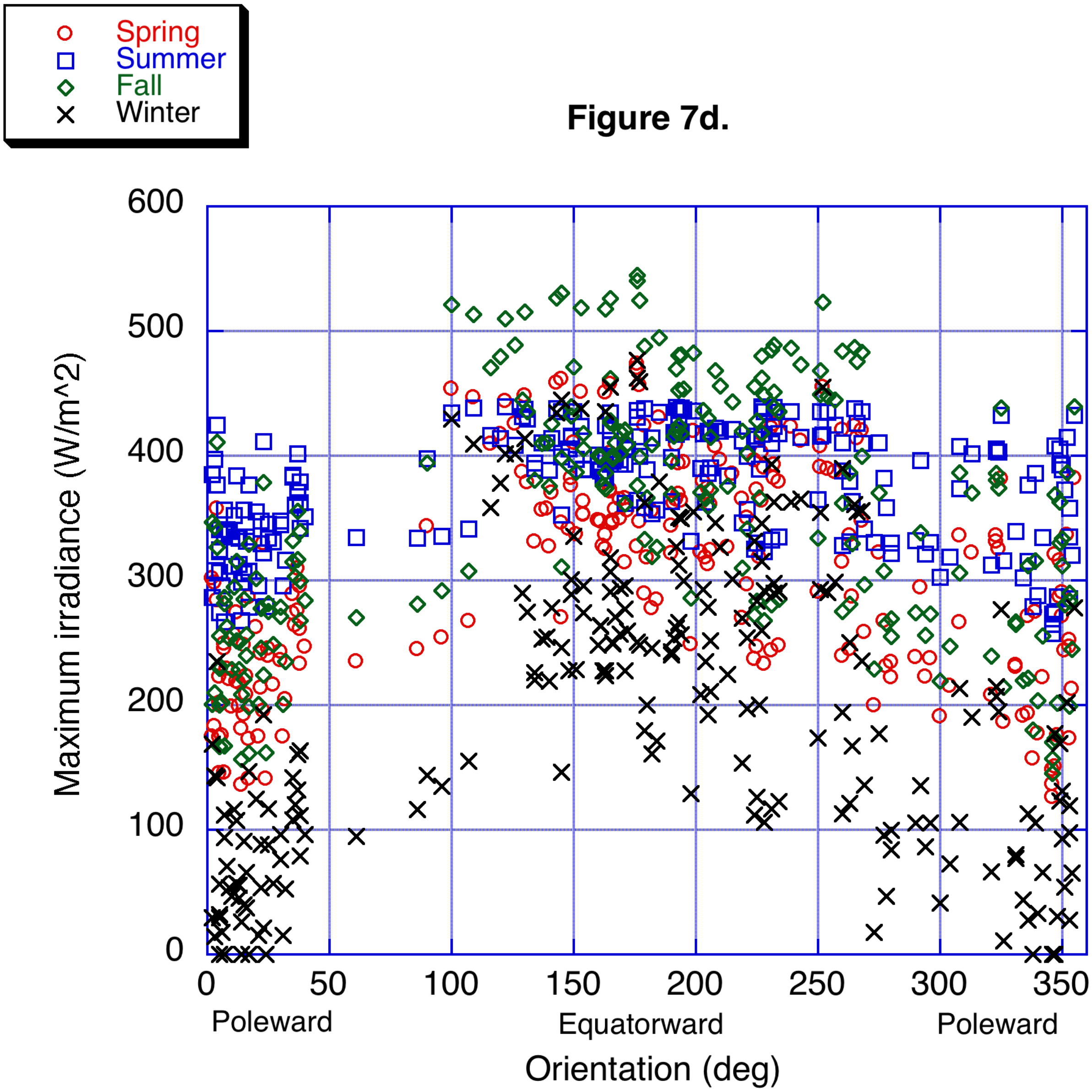
Spring
Summer
Fall
Winter
Maximum irradiance (W/m^2)
600
500
400
300
200
100
0
0
50
100
150
200
250
300
350
Poleward
Equatorward
Poleward
Orientation (deg)

Figure 8a.

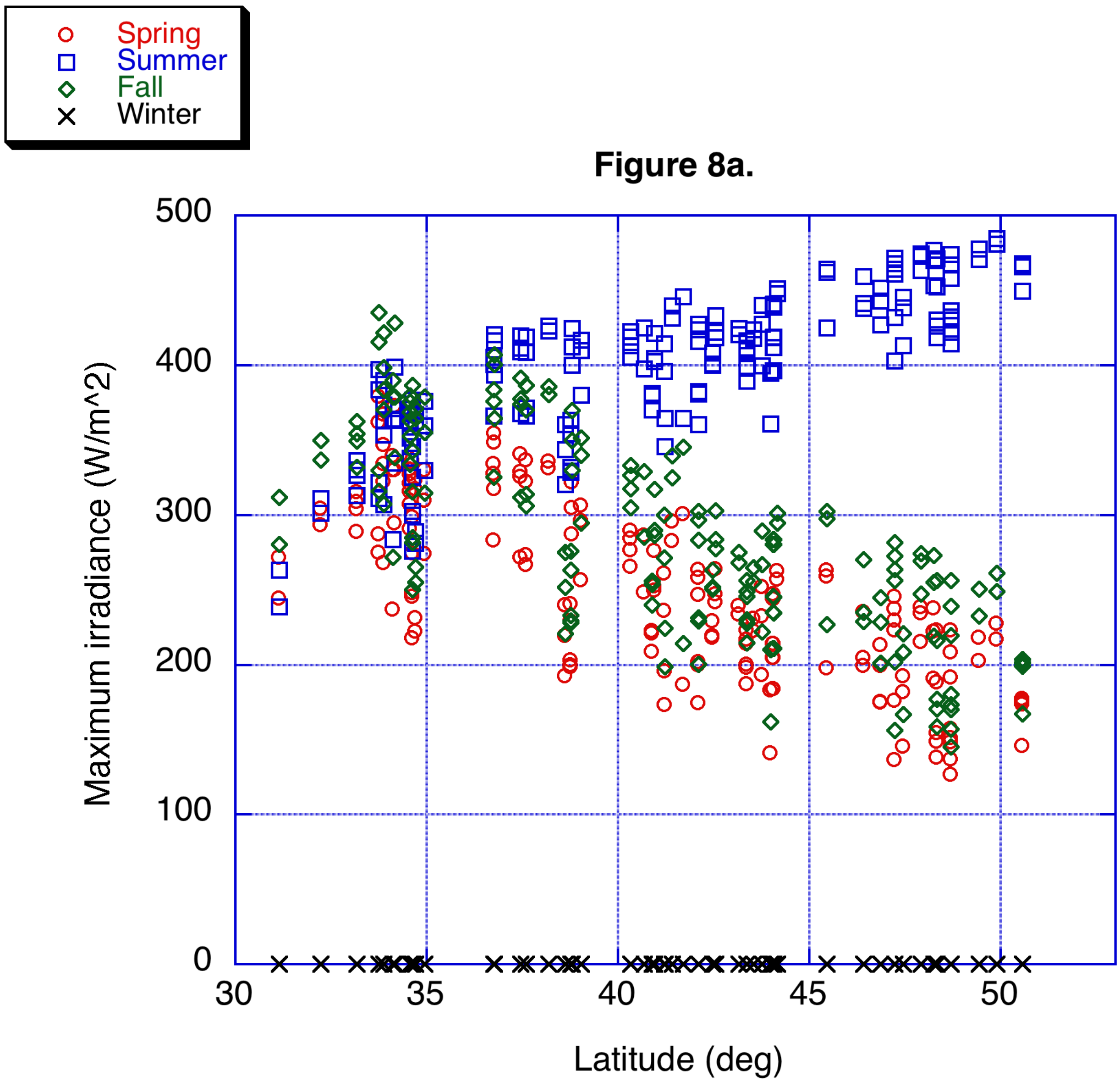
Spring
Summer
Fall
Winter
Maximum irradiance (W/m^2)
500
400
300
200
100
0
30
35
40
45
50
Latitude (deg)

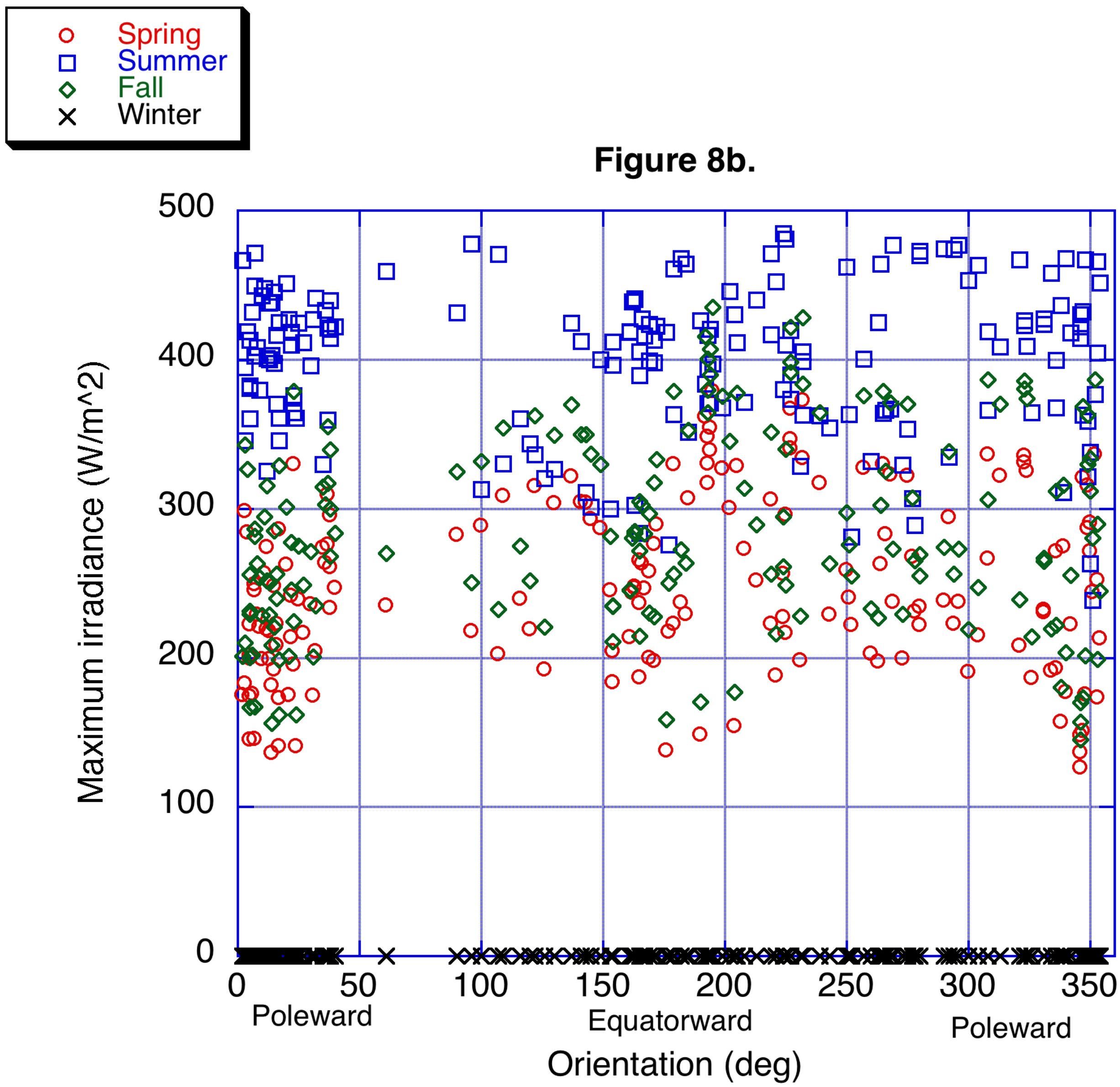

Spring
Summer
Fall
Winter
Figure 8b.
500
400
300
200
100
0
Maximum irradiance (W/m^2)
0
50
100
150
200
250
300
350
Poleward
Equatorward
Poleward
Orientation (deg)

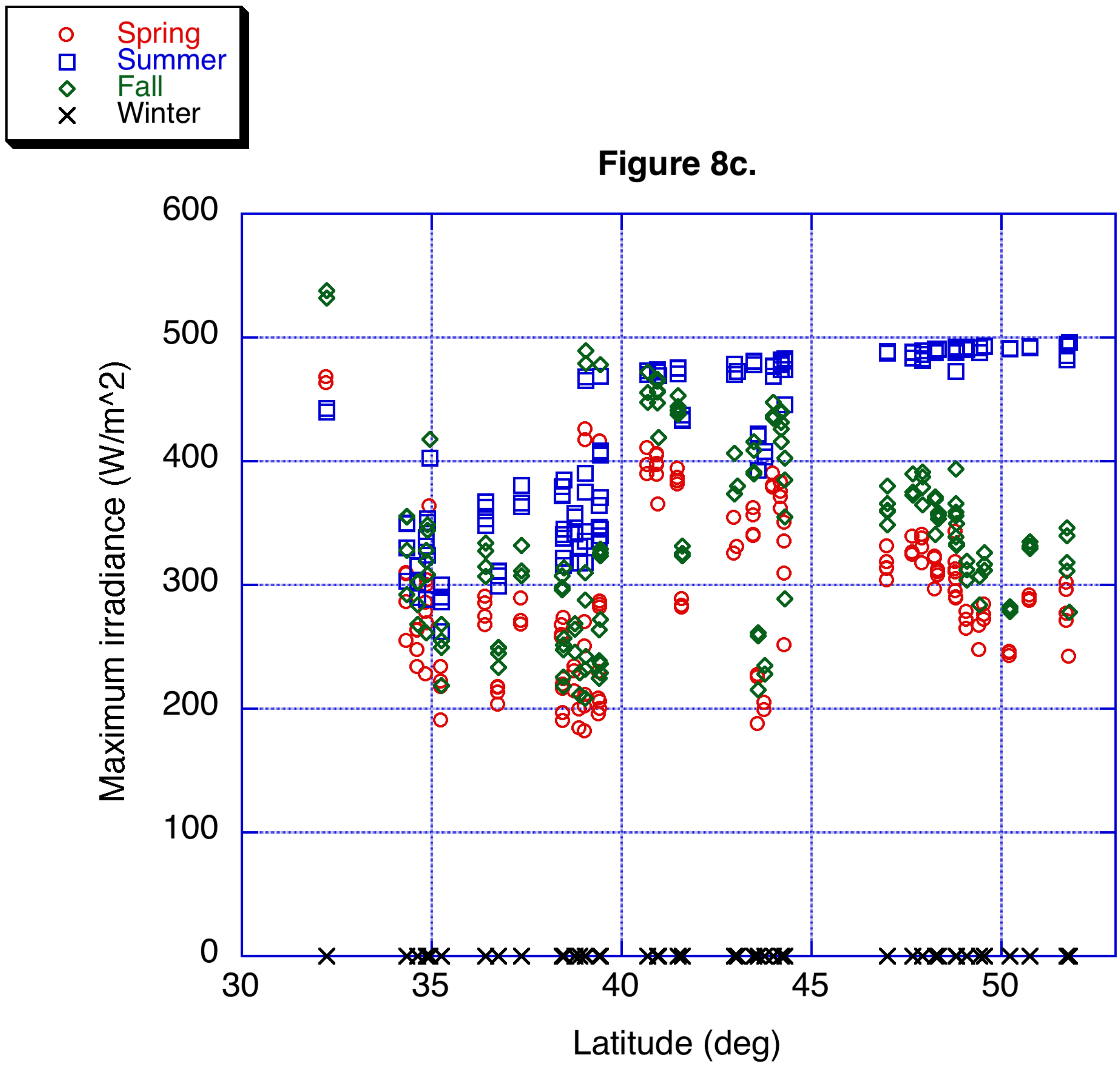

Spring
Summer
Fall
Winter
Figure 8c.
Maximum irradiance (W/m^2)
600
500
400
300
200
100
0
30
35
40
45
50
Latitude (deg)

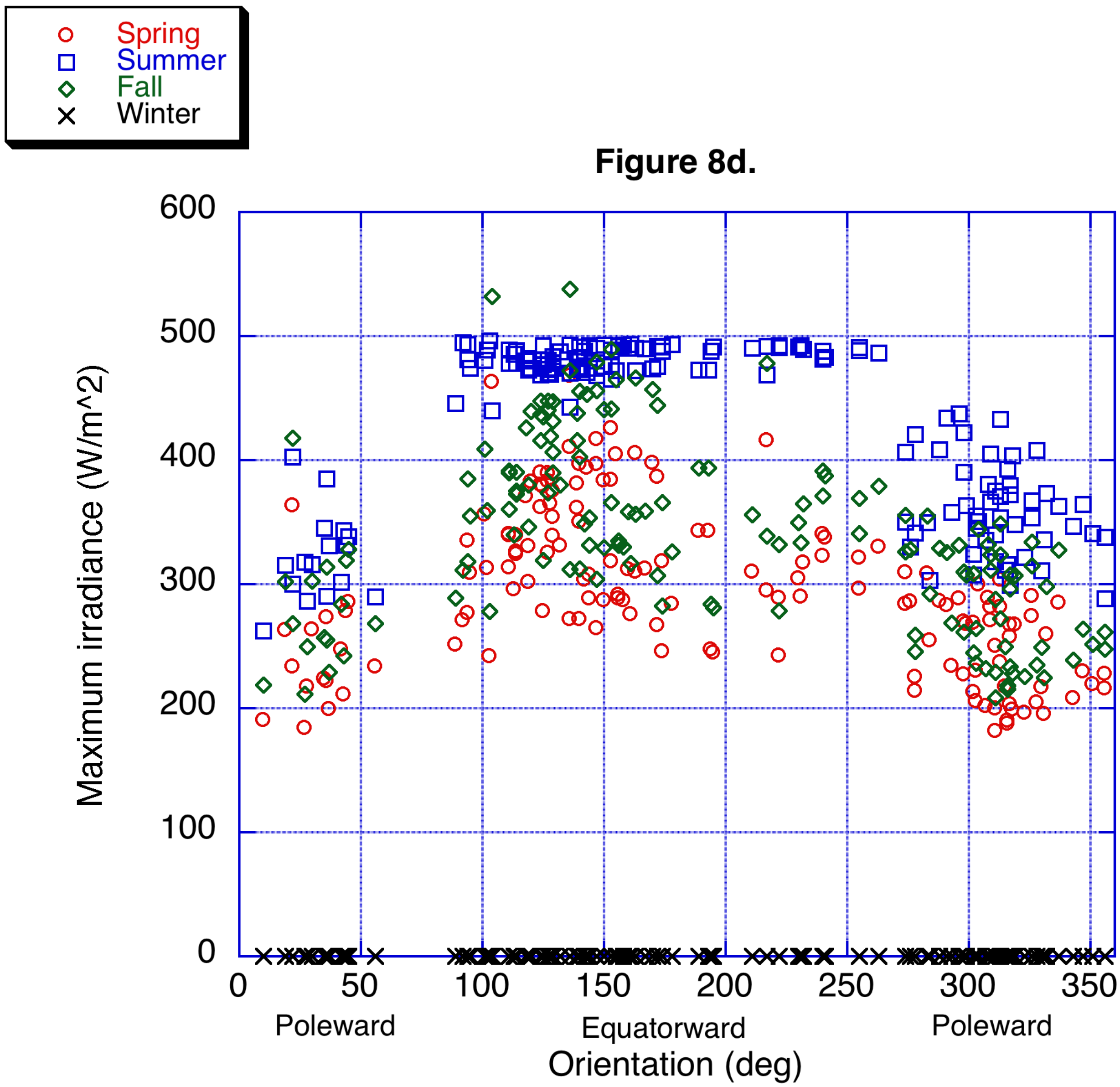

Spring
Summer
Fall
Winter
Figure 8d.
600
500
400
300
200
100
0
Maximum irradiance (W/m^2)
0
50
100
150
200
250
300
350
Poleward
Equatorward
Poleward
Orientation (deg)

Figure 9a.

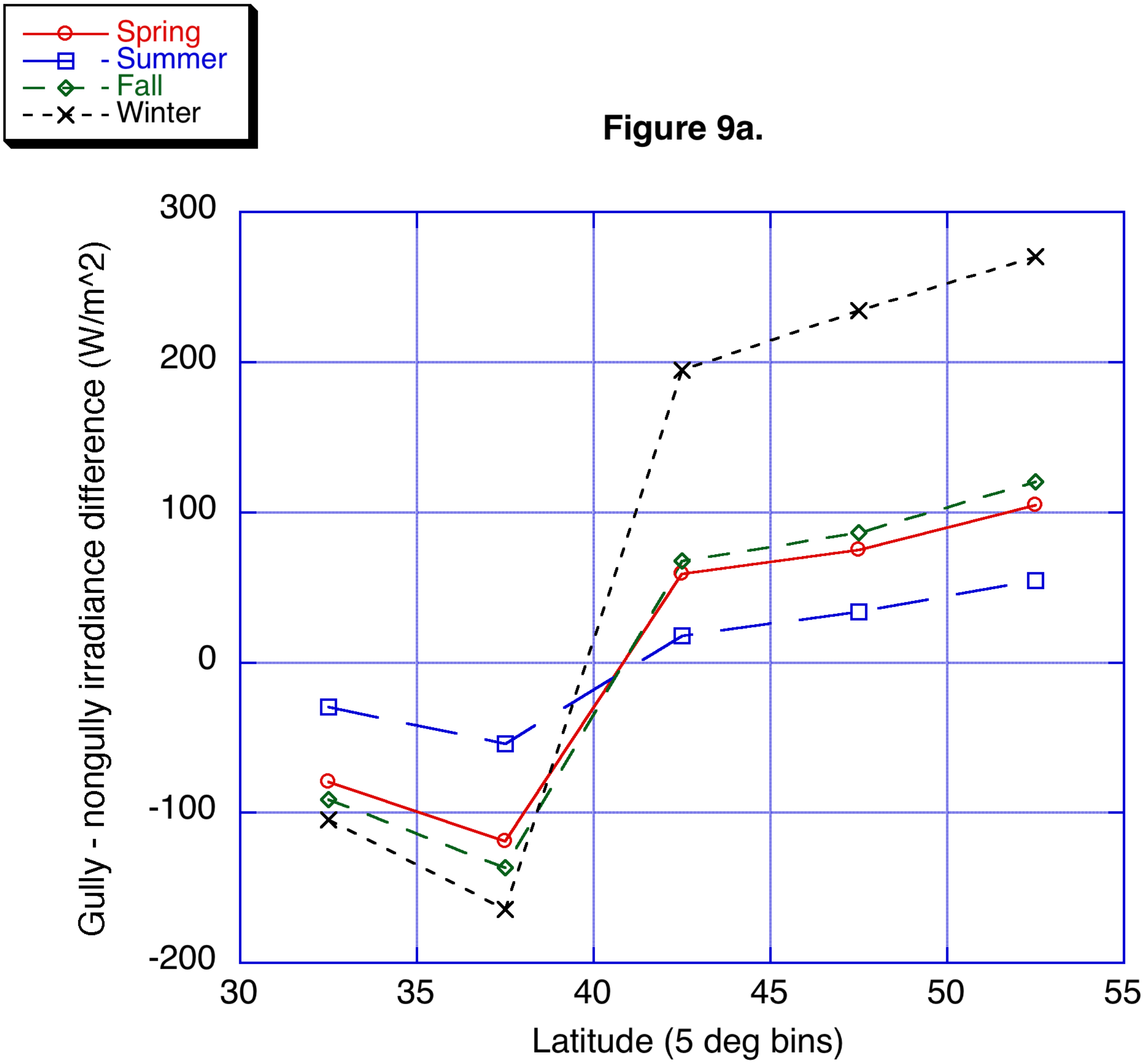

Spring
Summer
Fall
Winter
300
200
100
0
-100
-200
30
35
40
45
50
55
Gully - nongully irradiance difference (W/m^2)
Latitude (5 deg bins)

Figure 9b.

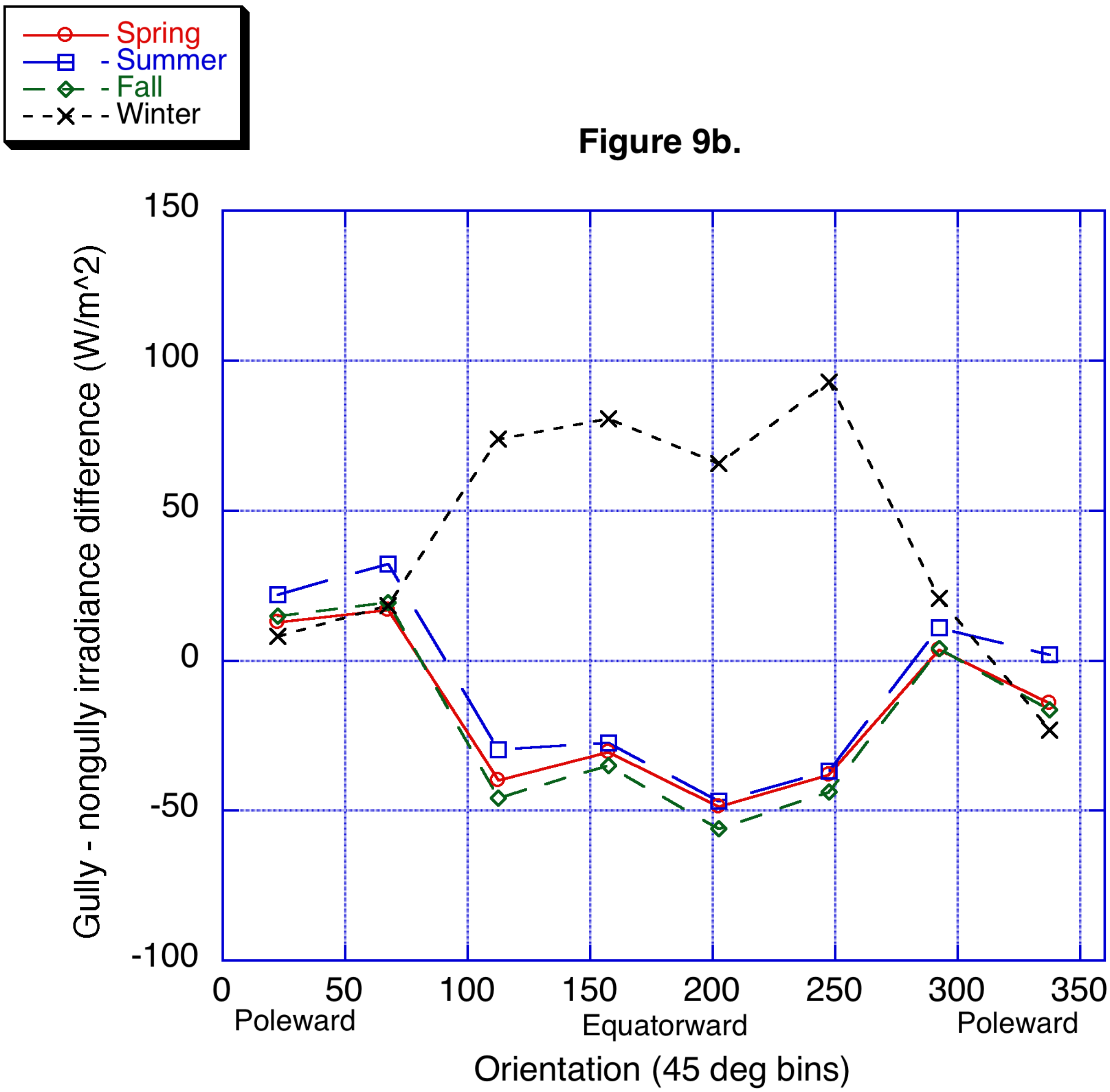
Spring
Summer
Fall
Winter
150
100
50
0
-50
-100
Gully - nongully irradiance difference (W/m^2)
0
50
100
150
200
250
300
350
Poleward
Equatorward
Poleward
Orientation (45 deg bins)

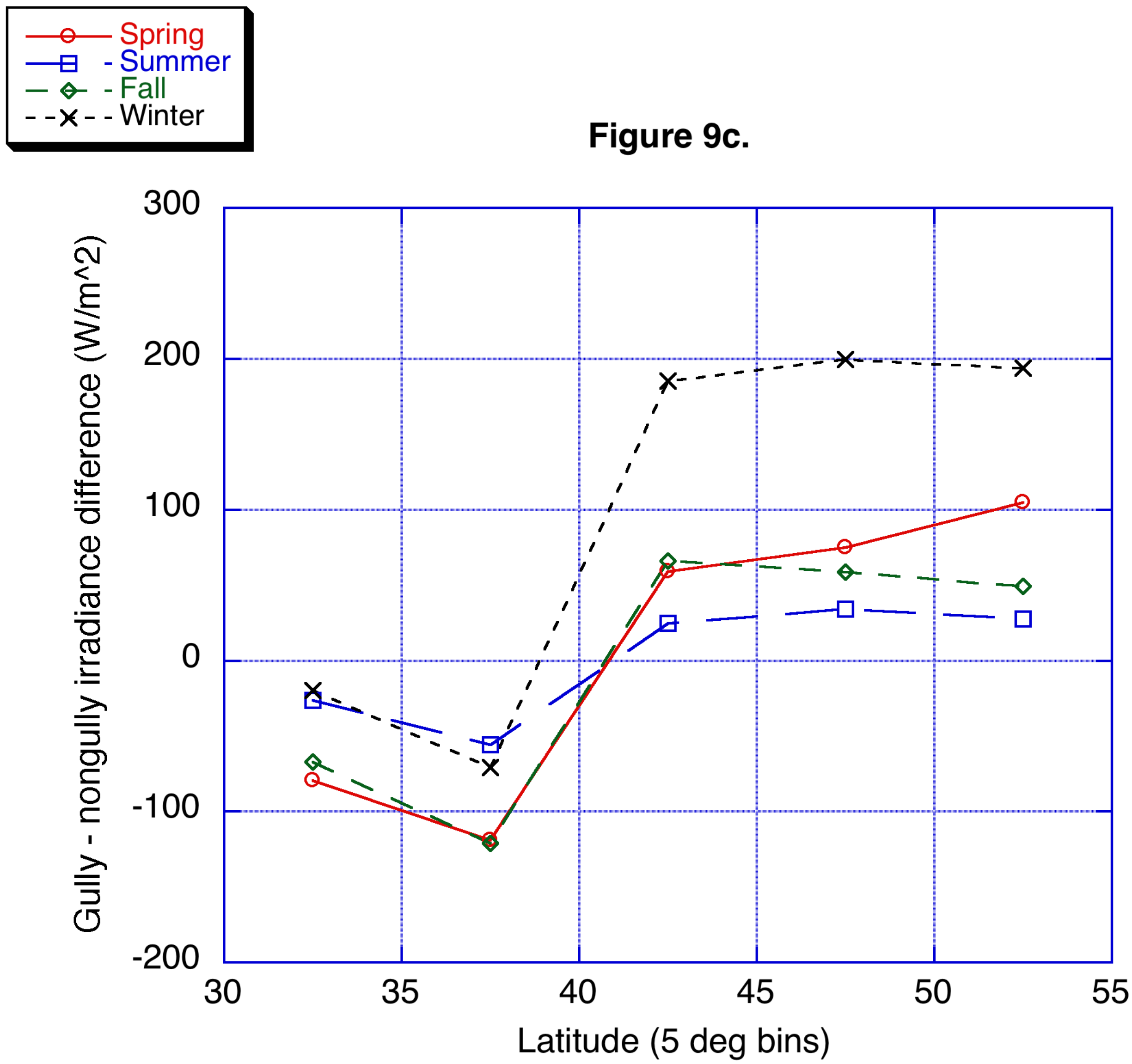
Spring
- Summer
- Fall
- - - Winter
Figure 9c.
300
200
100
0
-100
-200
Gully - nongully irradiance difference (W/m^2)
30
35
40
45
50
55
Latitude (5 deg bins)

Figure 9d.

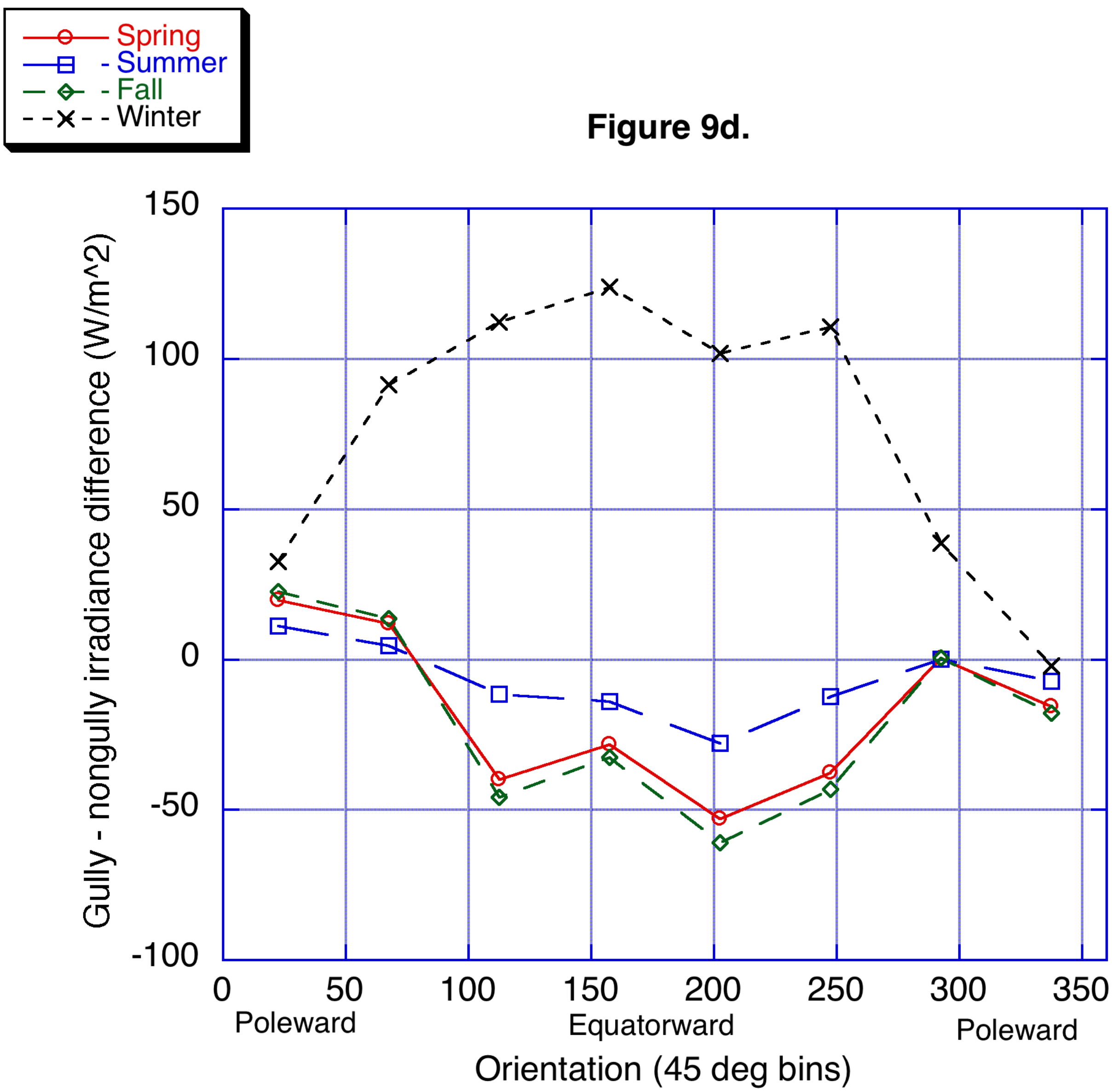

Spring
Summer
Fall
Winter
150
100
50
0
-50
-100
Gully - nongully irradiance difference (W/m^2)
0
50
100
150
200
250
300
350
Poleward
Equatorward
Poleward
Orientation (45 deg bins)

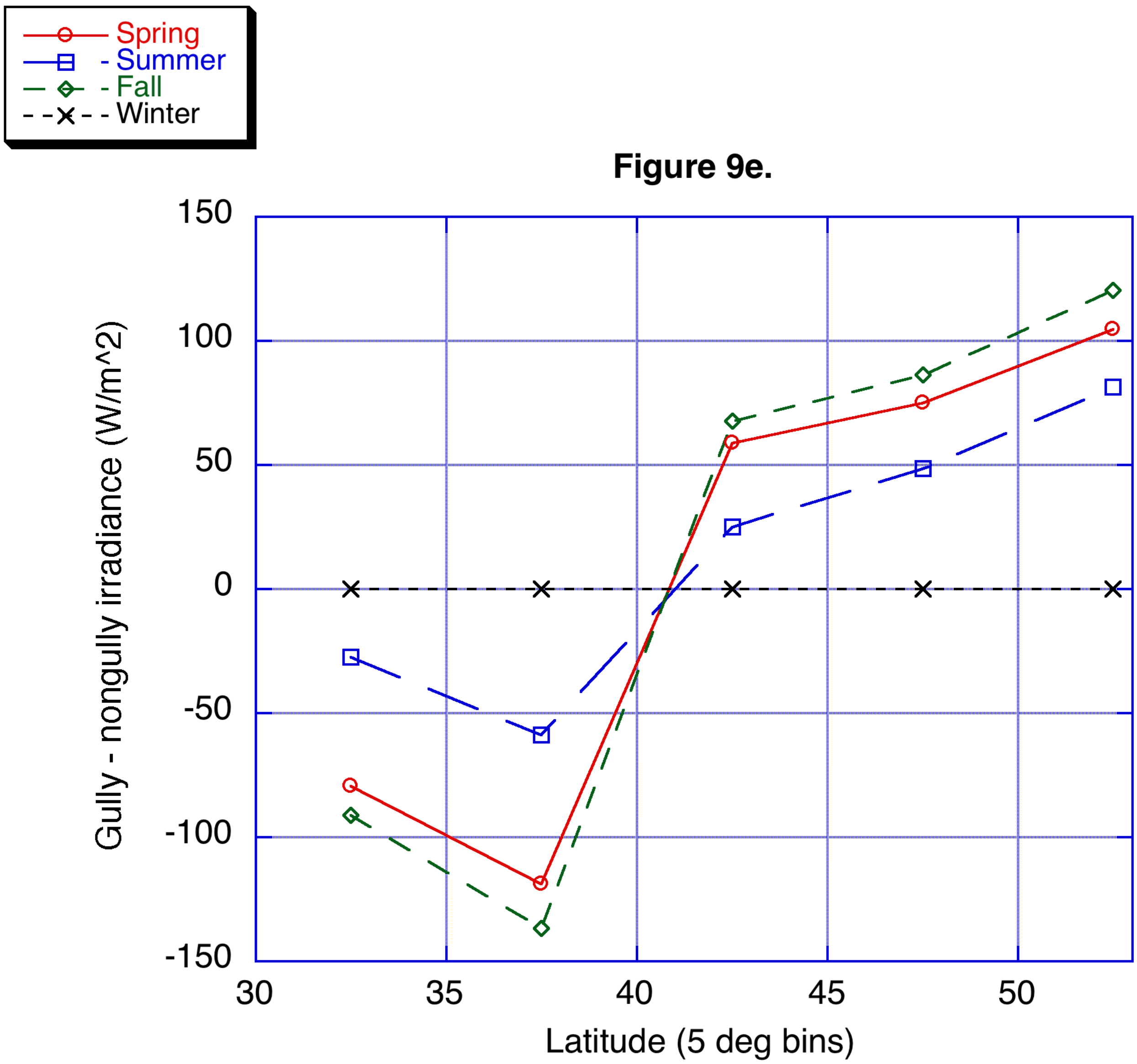
Spring
- Summer
- Fall
- - Winter
Figure 9e.
150
100
50
0
-50
-100
-150
30
35
40
45
50
Gully - nongully irradiance (W/m^2)
Latitude (5 deg bins)

Figure 9f.

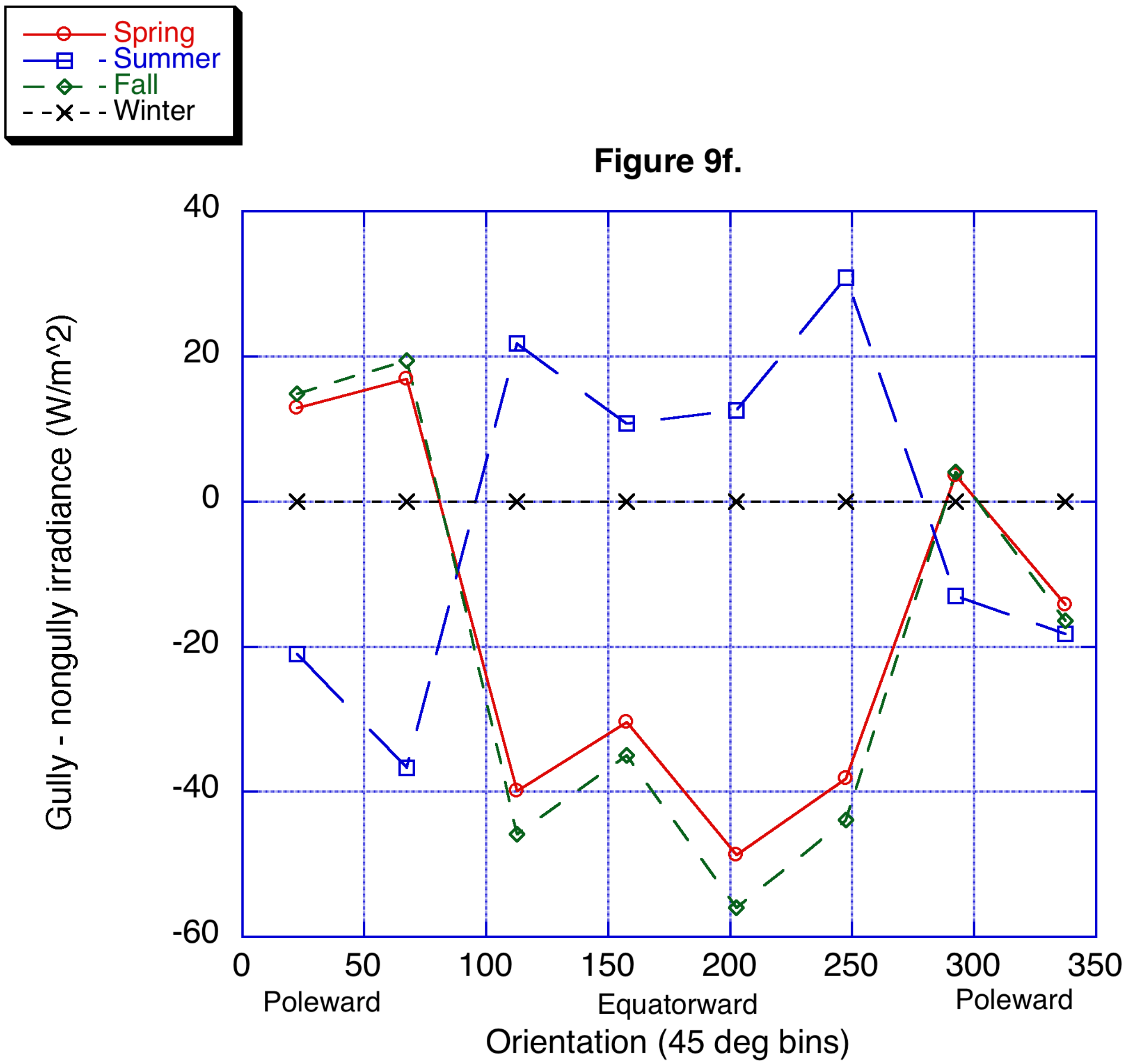

Spring
- Summer
- Fall
Winter
40
20
0
-20
-40
-60
Gully - nongully irradiance (W/m^2)
0
50
100
150
200
250
300
350
Poleward
Equatorward
Poleward
Orientation (45 deg bins)

Figure 10a.

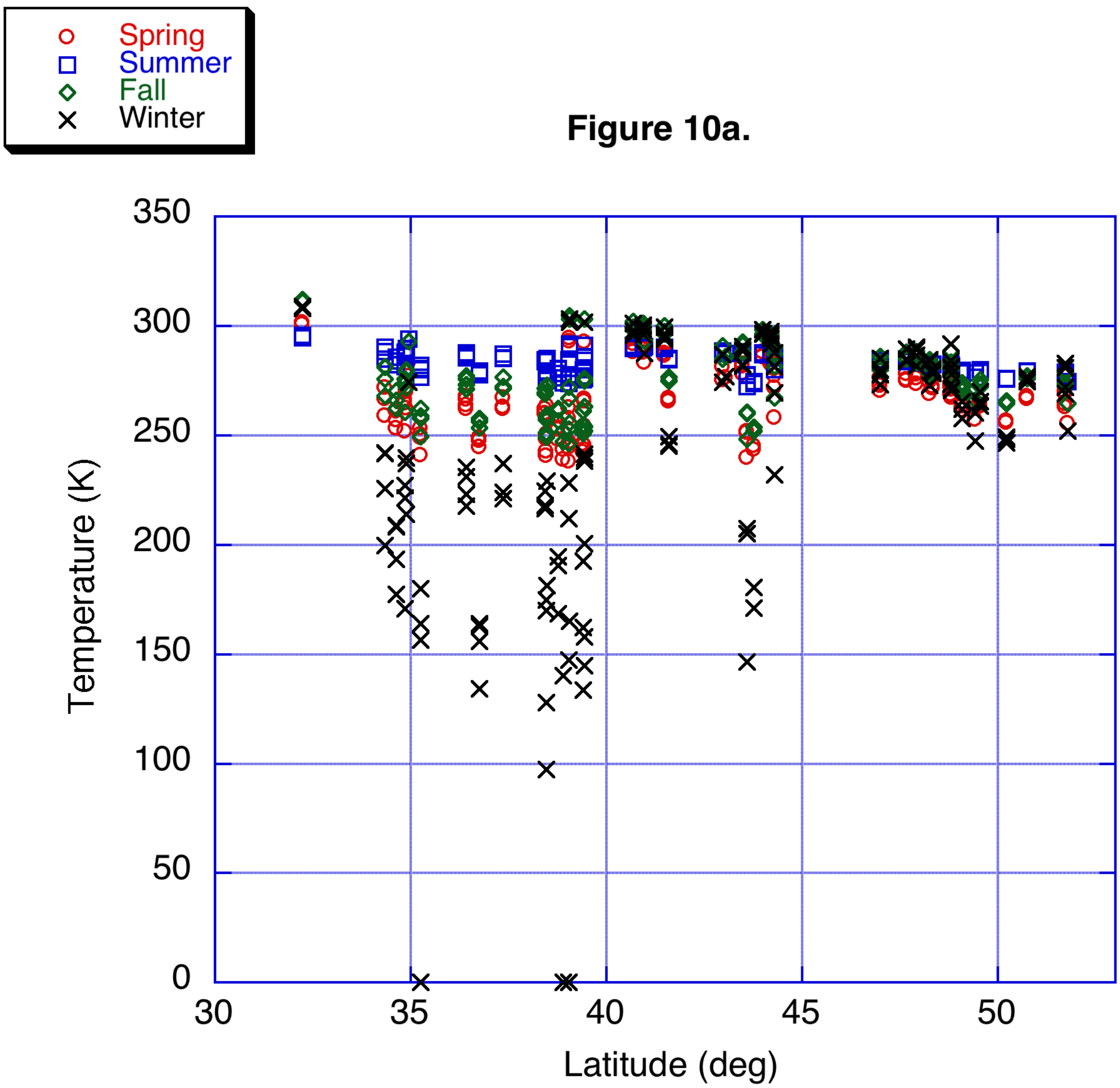

Spring
Summer
Fall
Winter
350
300
250
200
150
100
50
0
Temperature (K)
30
35
40
45
50
Latitude (deg)

Figure 10b.

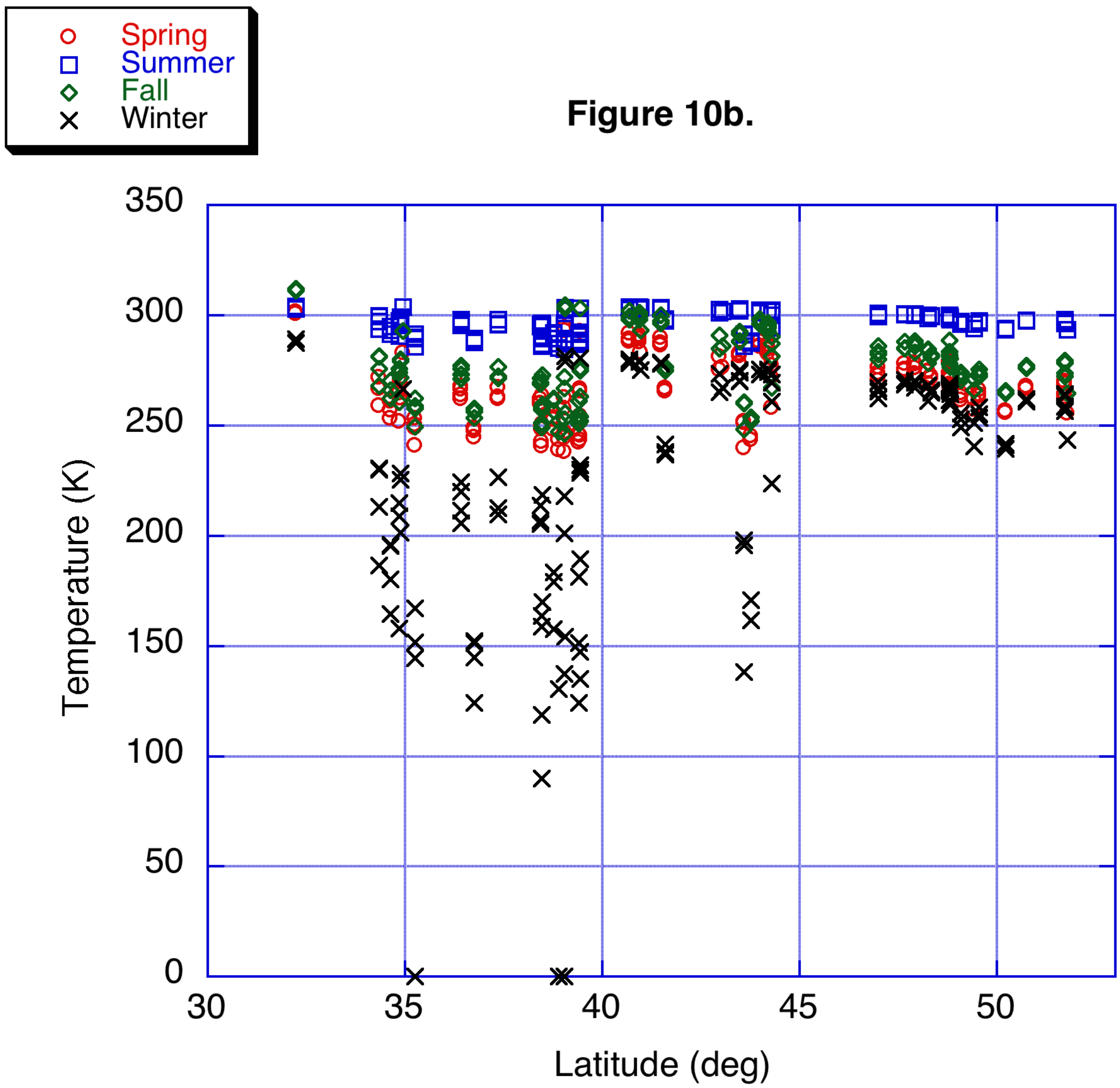

Spring
Summer
Fall
Winter
350
300
250
200
150
100
50
0
Temperature (K)
30
35
40
45
50
Latitude (deg)

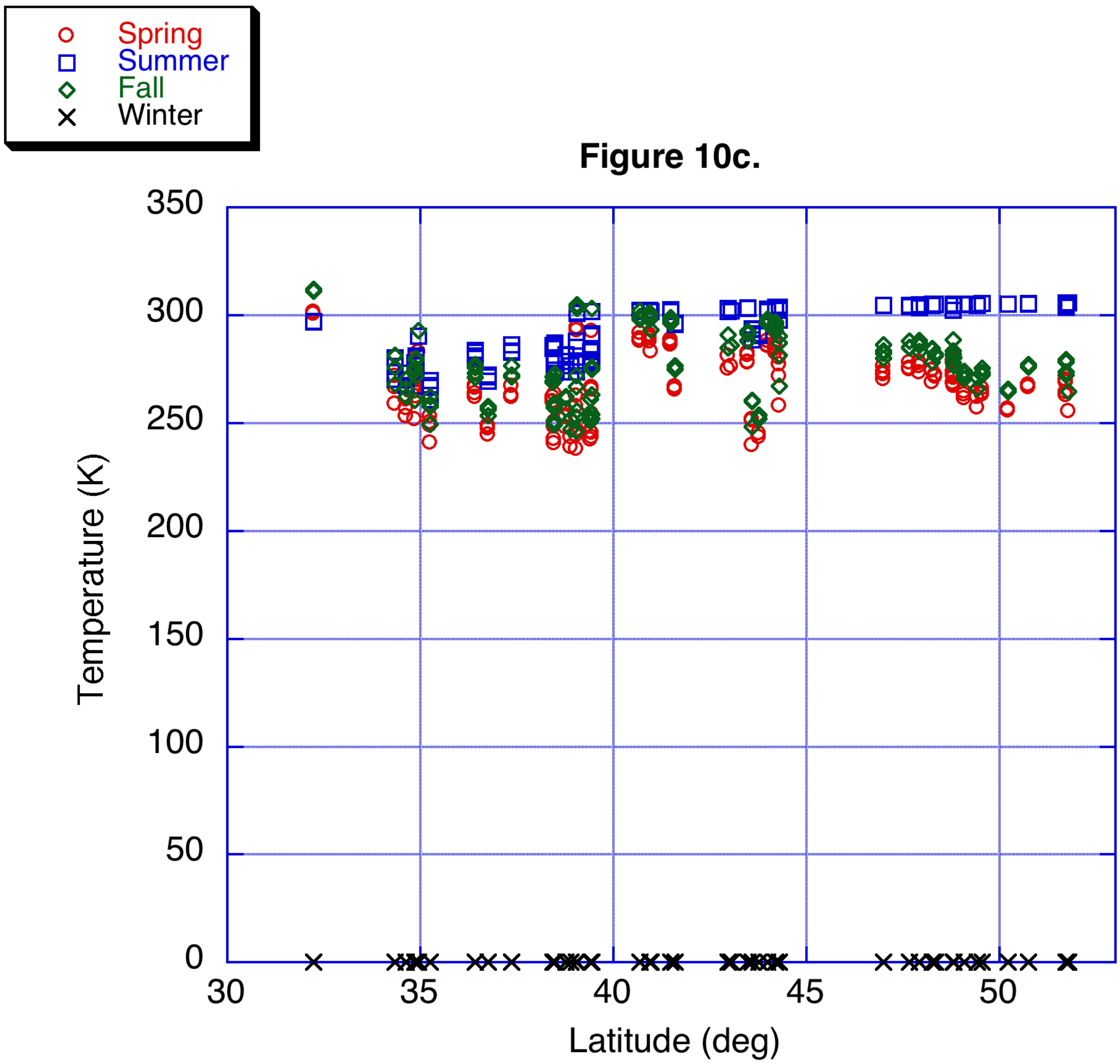
Spring
Summer
Fall
Winter
Figure 10c.
Temperature (K)
350
300
250
200
150
100
50
0
30
35
40
45
50
Latitude (deg)

Figure 10d.

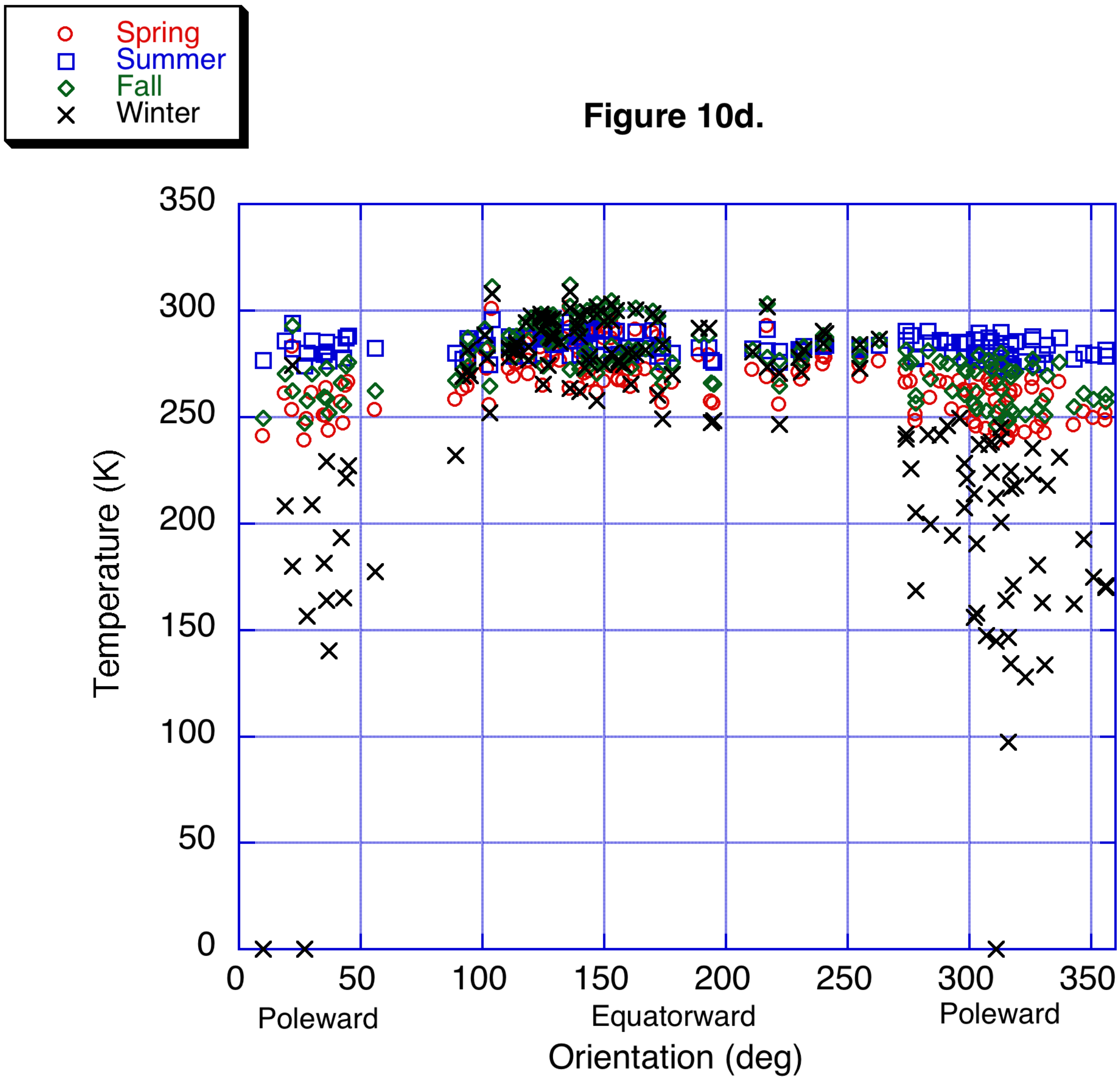
Spring
Summer
Fall
Winter
Temperature (K)
350
300
250
200
150
100
50
0
0
50
100
150
200
250
300
350
Poleward
Equatorward
Poleward
Orientation (deg)

Figure 10e.

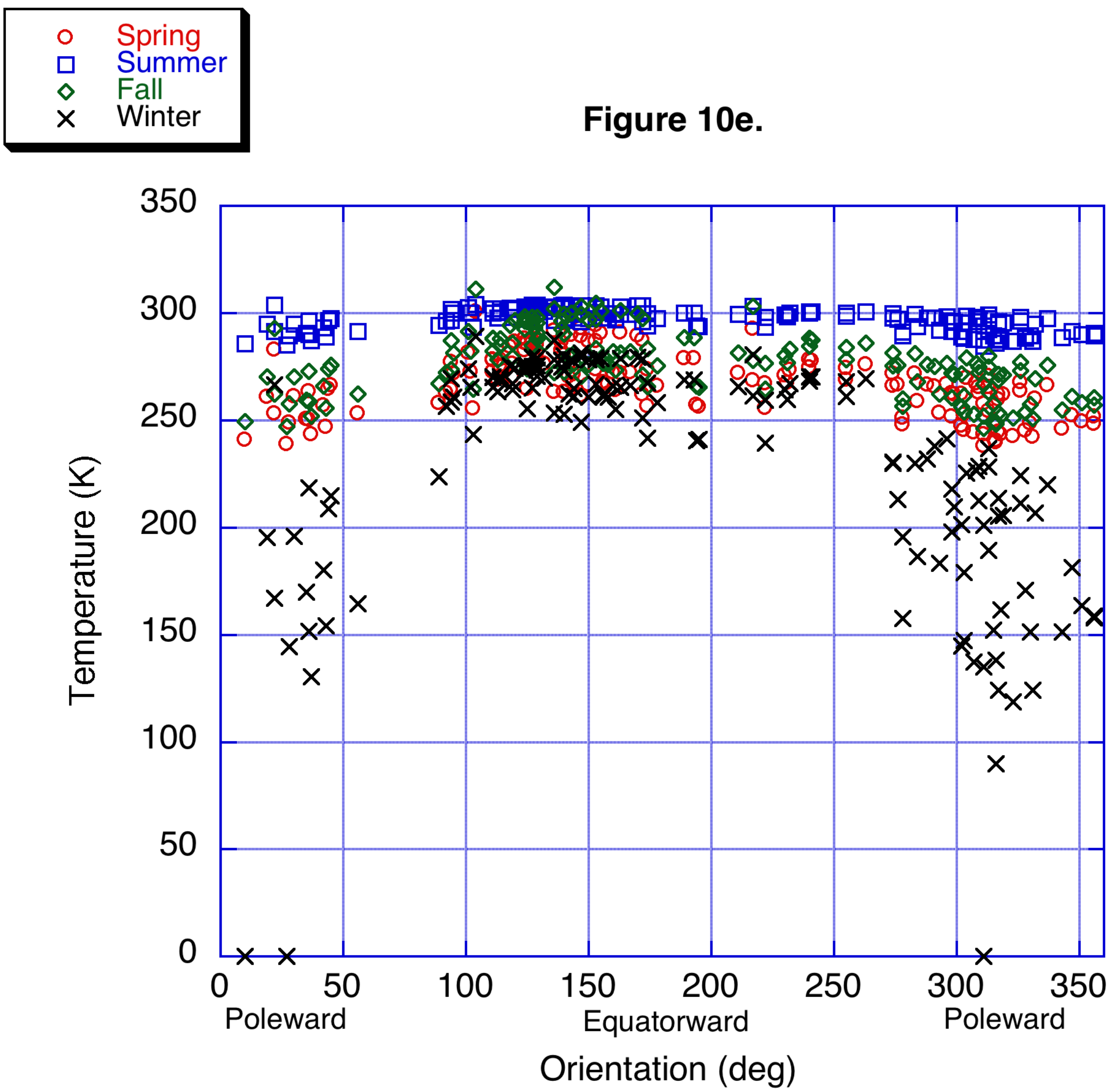

Spring
Summer
Fall
Winter
350
300
250
200
150
100
50
0
Temperature (K)
0
50
100
150
200
250
300
350
Poleward
Equatorward
Poleward
Orientation (deg)

Figure 10f.

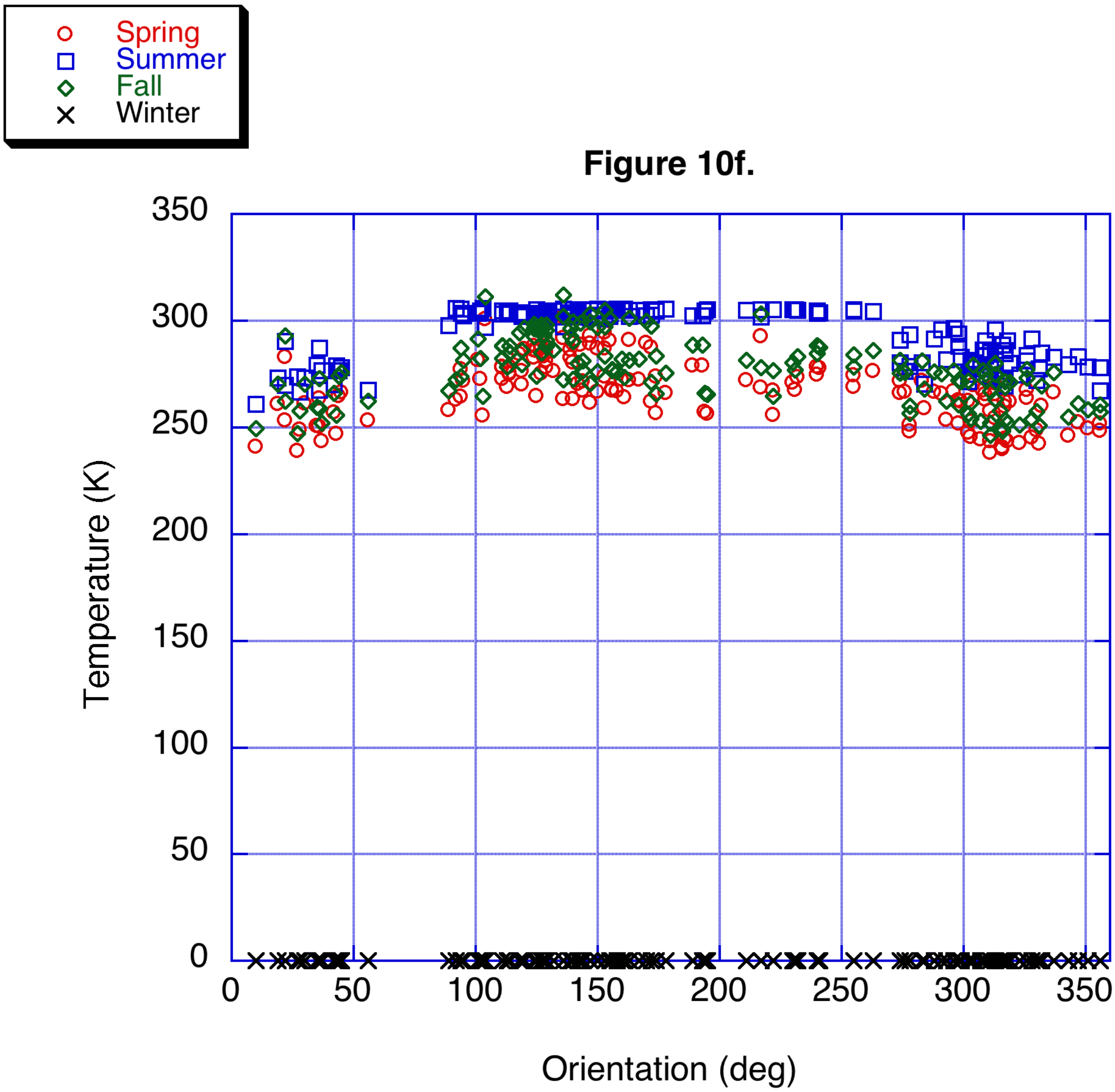

Spring
Summer
Fall
Winter
350
300
250
200
150
100
50
0
Temperature (K)
0
50
100
150
200
250
300
350
Orientation (deg)

Figure 11a.

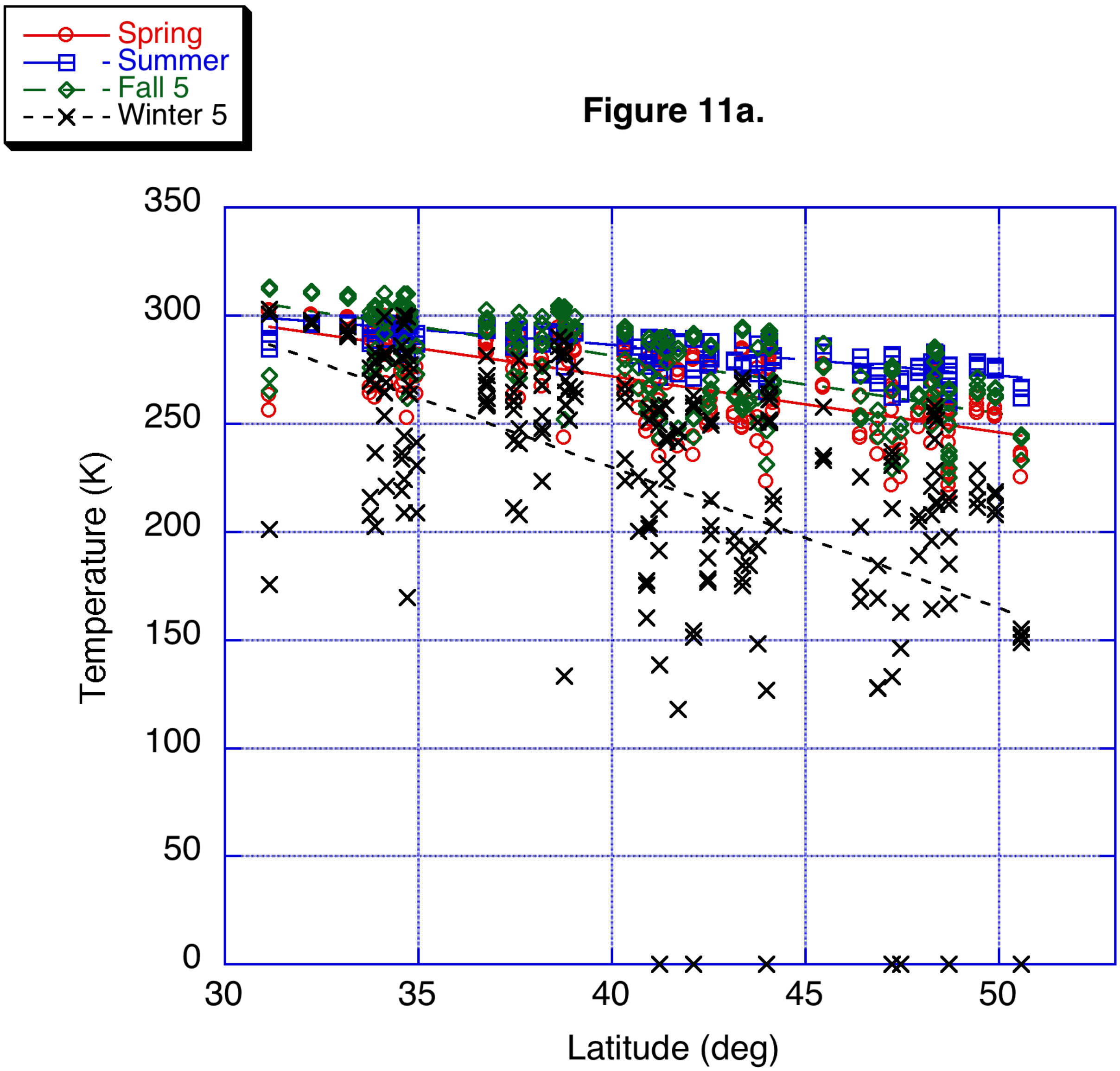

Spring
- Summer
- Fall 5
- - Winter 5
Temperature (K)
350
300
250
200
150
100
50
0
30
35
40
45
50
Latitude (deg)

Figure 11b.

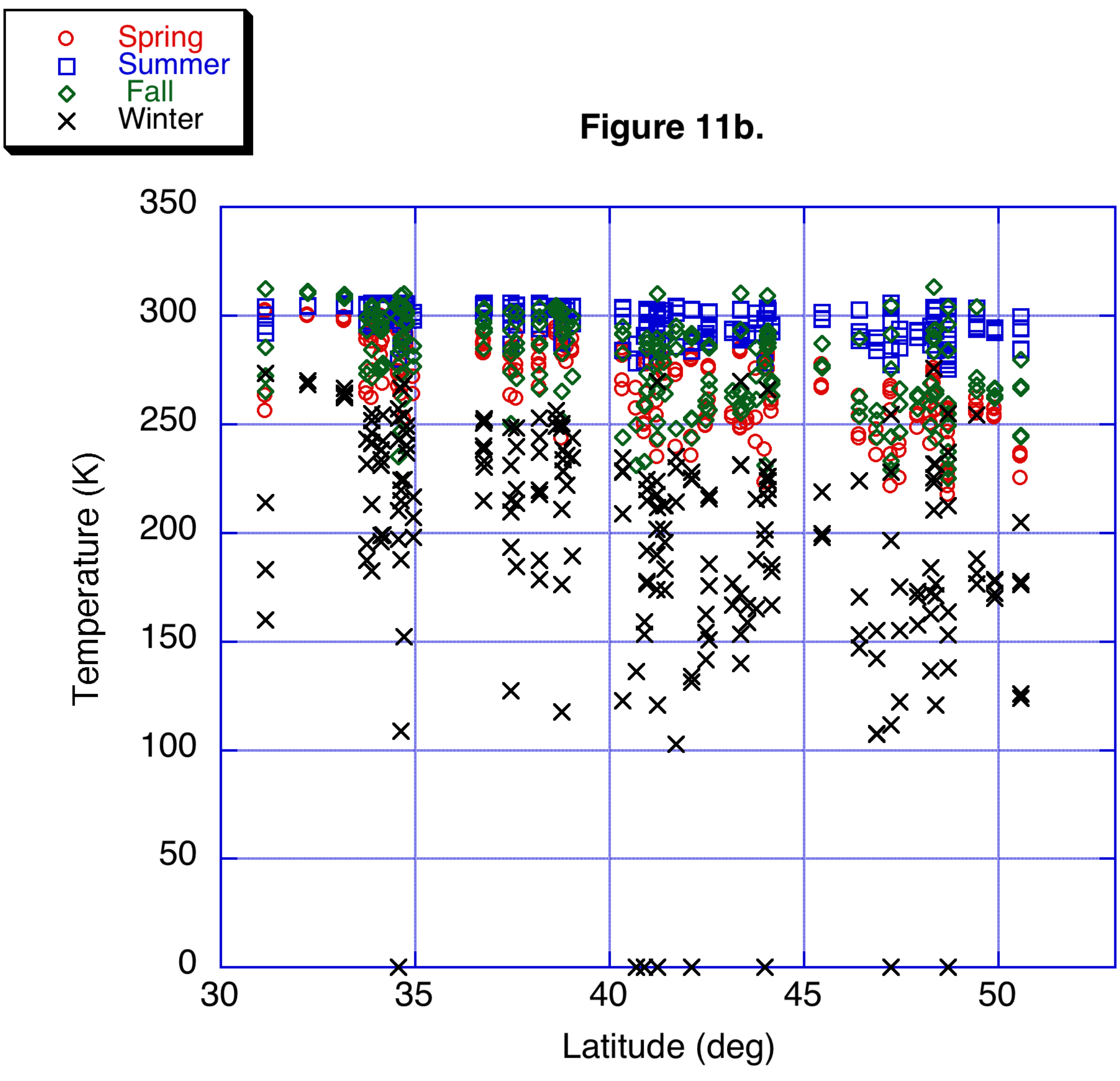

Spring
Summer
Fall
Winter
350
300
250
200
150
100
50
0
30
35
40
45
50
Temperature (K)
Latitude (deg)

Figure 11c.

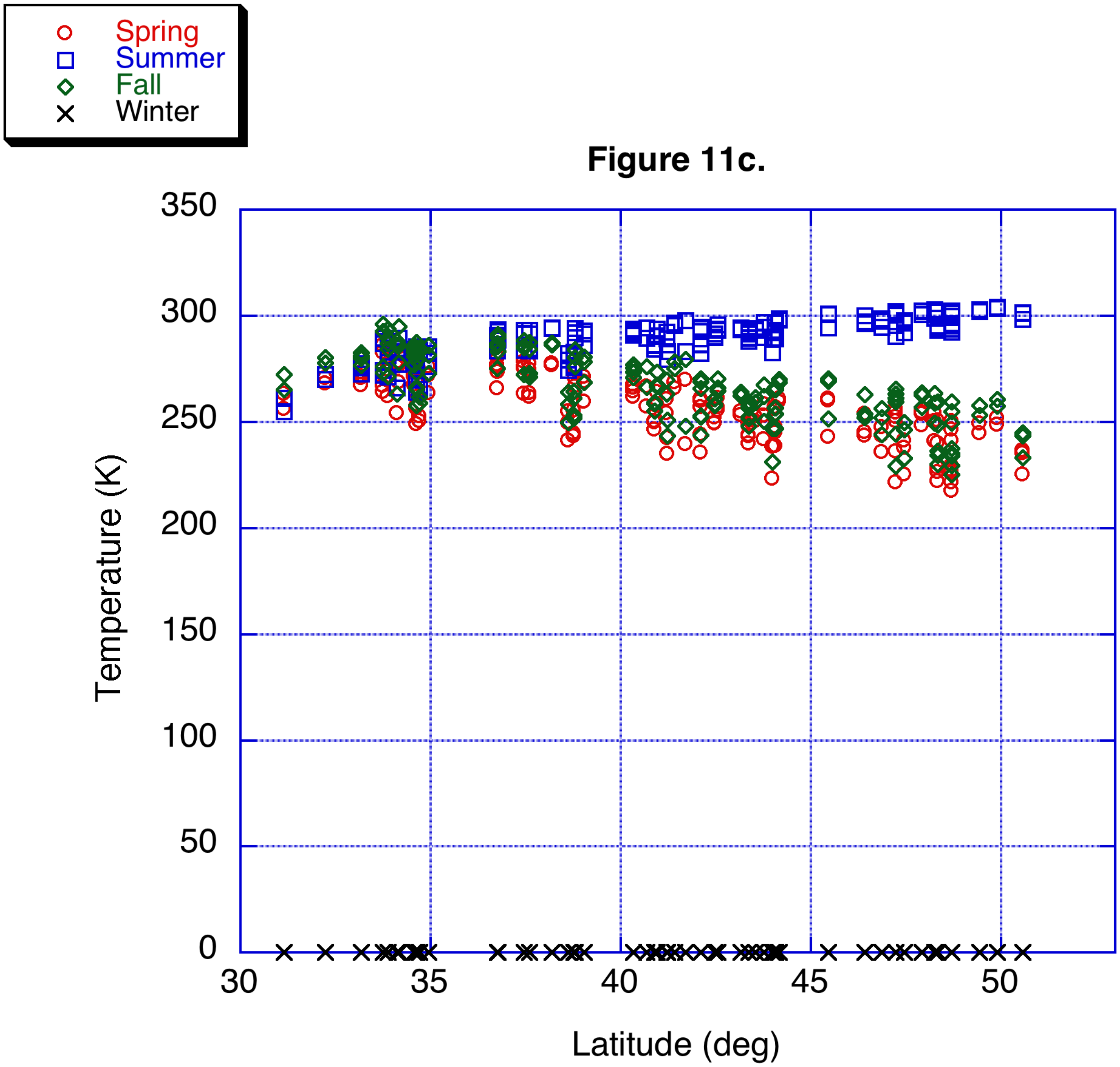
Spring
Summer
Fall
Winter
350
300
250
200
150
100
50
0
Temperature (K)
30
35
40
45
50
Latitude (deg)

Figure 11d.

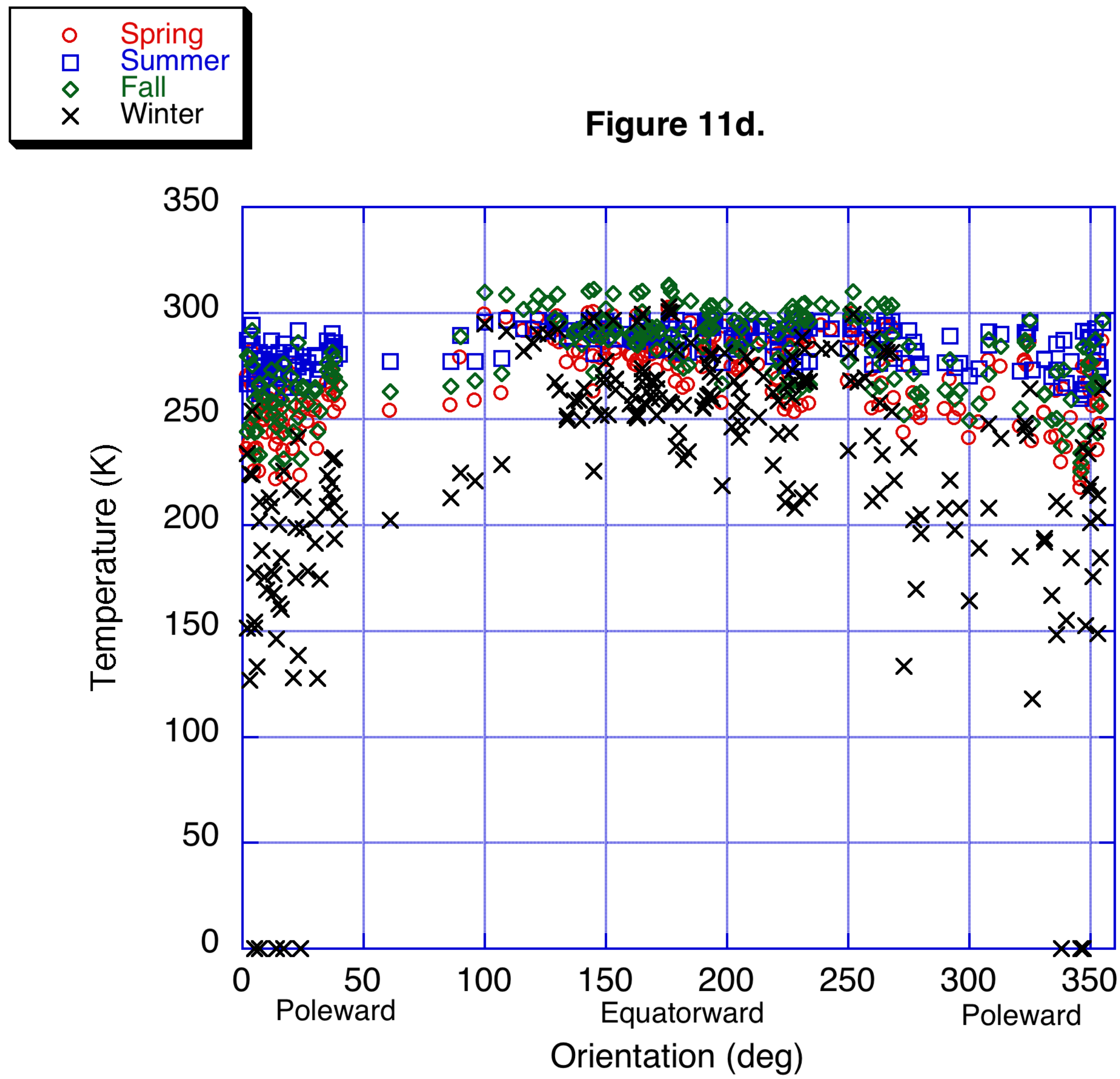
Spring
Summer
Fall
Winter
350
300
250
200
150
100
50
0
Temperature (K)
0
50
100
150
200
250
300
350
Poleward
Equatorward
Poleward
Orientation (deg)

Figure 11e.

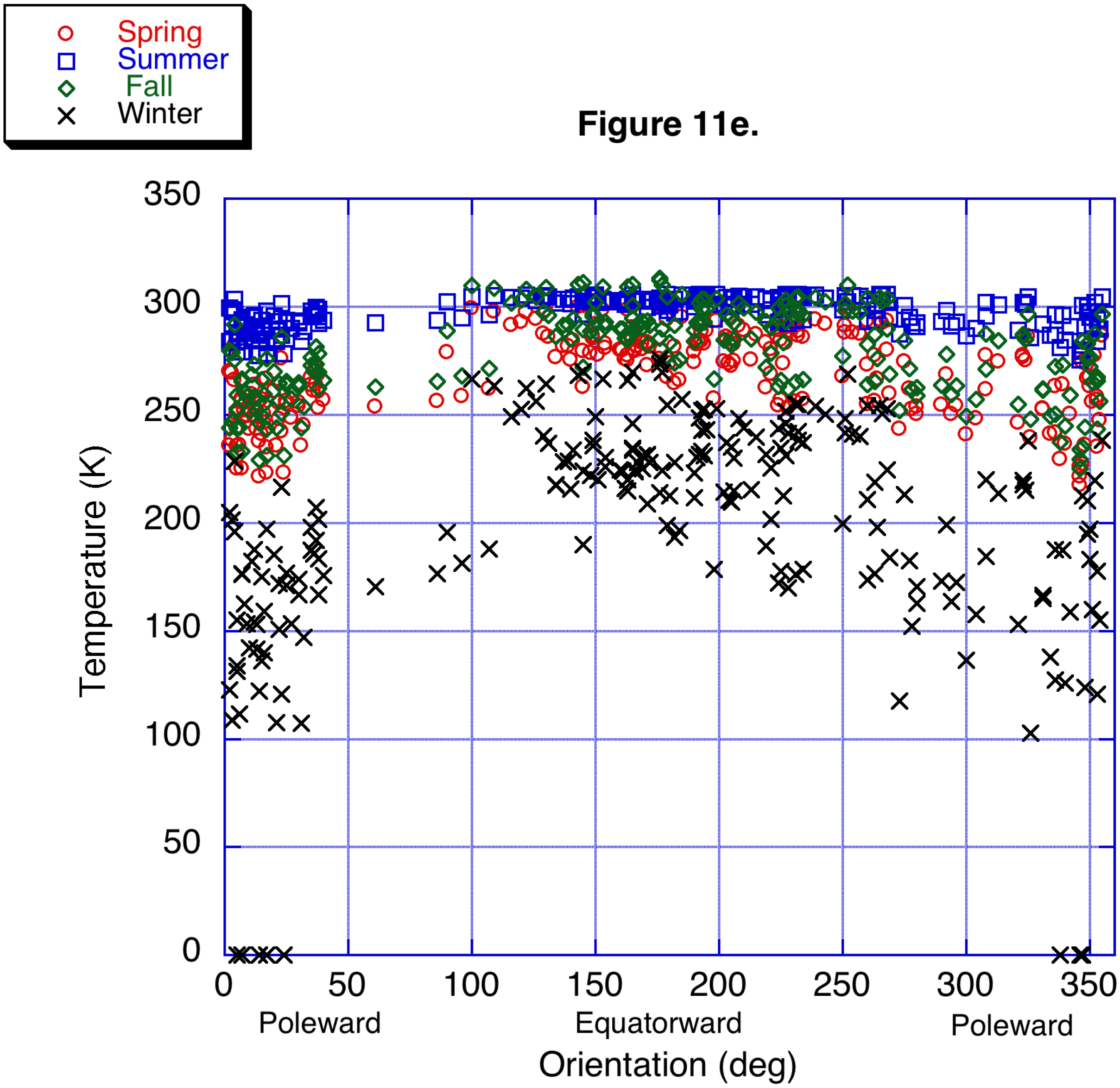

Spring
Summer
Fall
Winter
350
300
250
200
150
100
50
0
Temperature (K)
0
50
100
150
200
250
300
350
Poleward
Equatorward
Poleward
Orientation (deg)

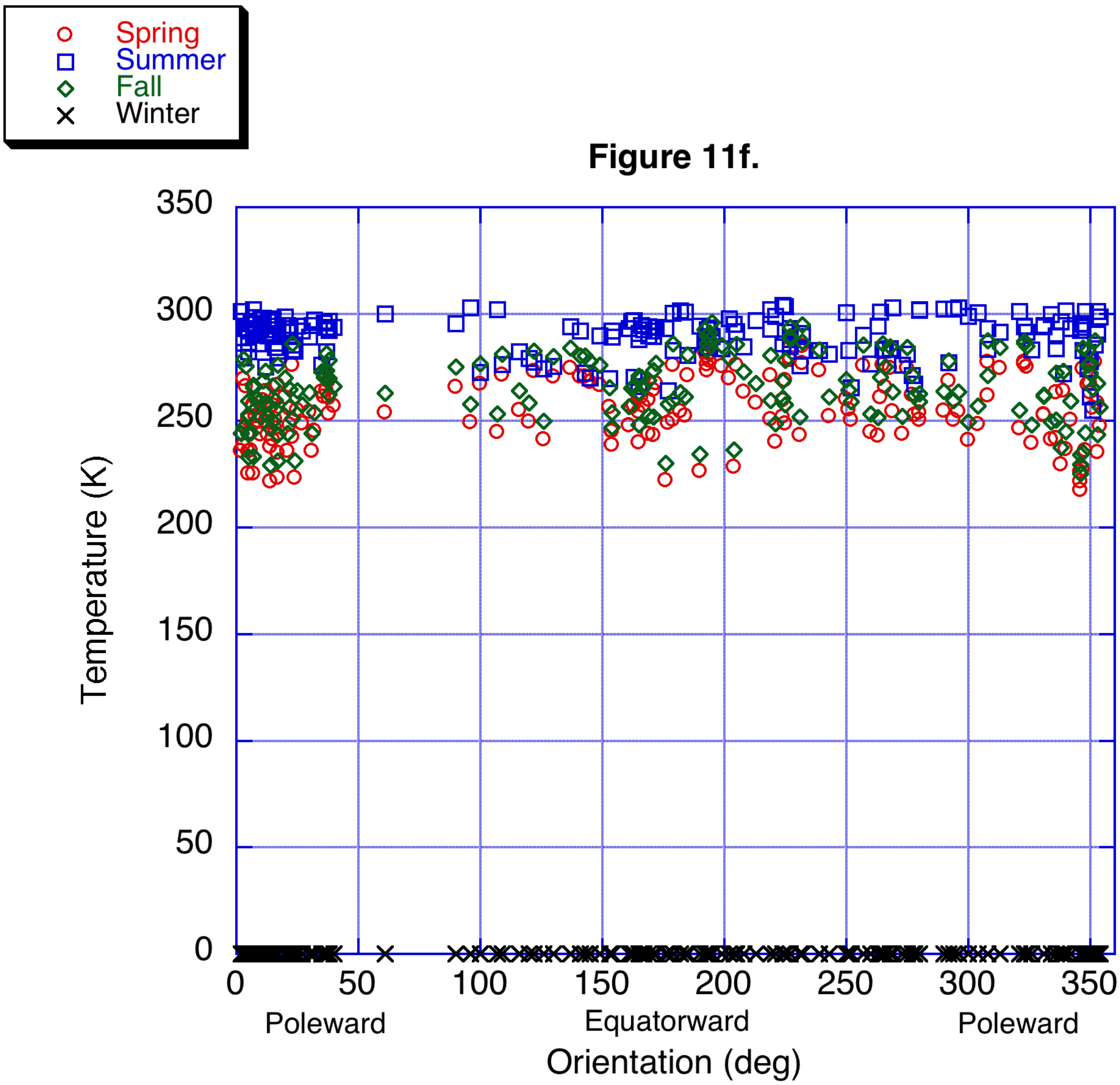

Spring
Summer
Fall
Winter
Figure 11f.
Temperature (K)
350
300
250
200
150
100
50
0
0
50
100
150
200
250
300
350
Poleward
Equatorward
Poleward
Orientation (deg)

Figure 12a.

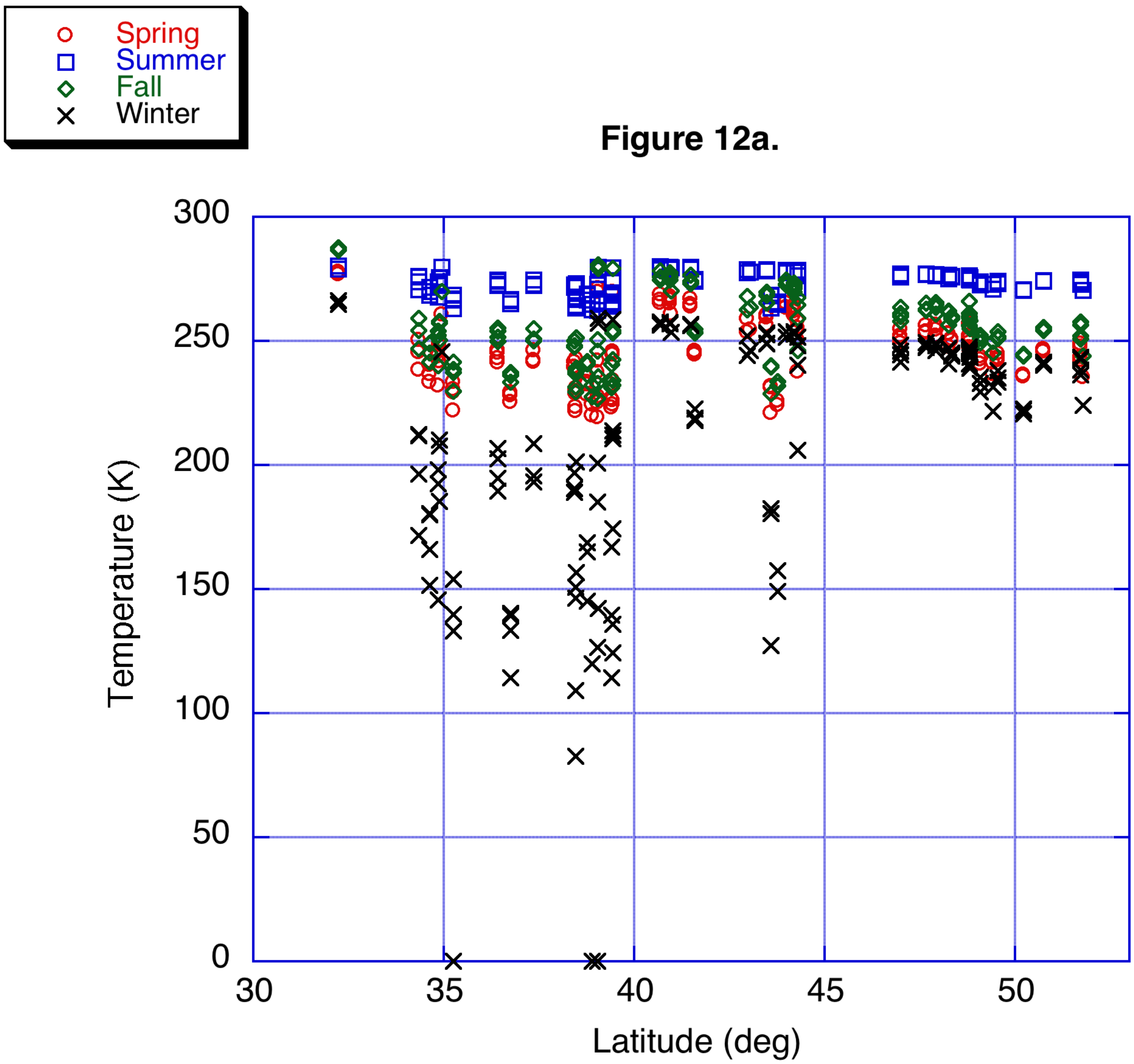
Spring
Summer
Fall
Winter
300
250
200
150
100
50
0
Temperature (K)
30
35
40
45
50
Latitude (deg)

Figure 12b.

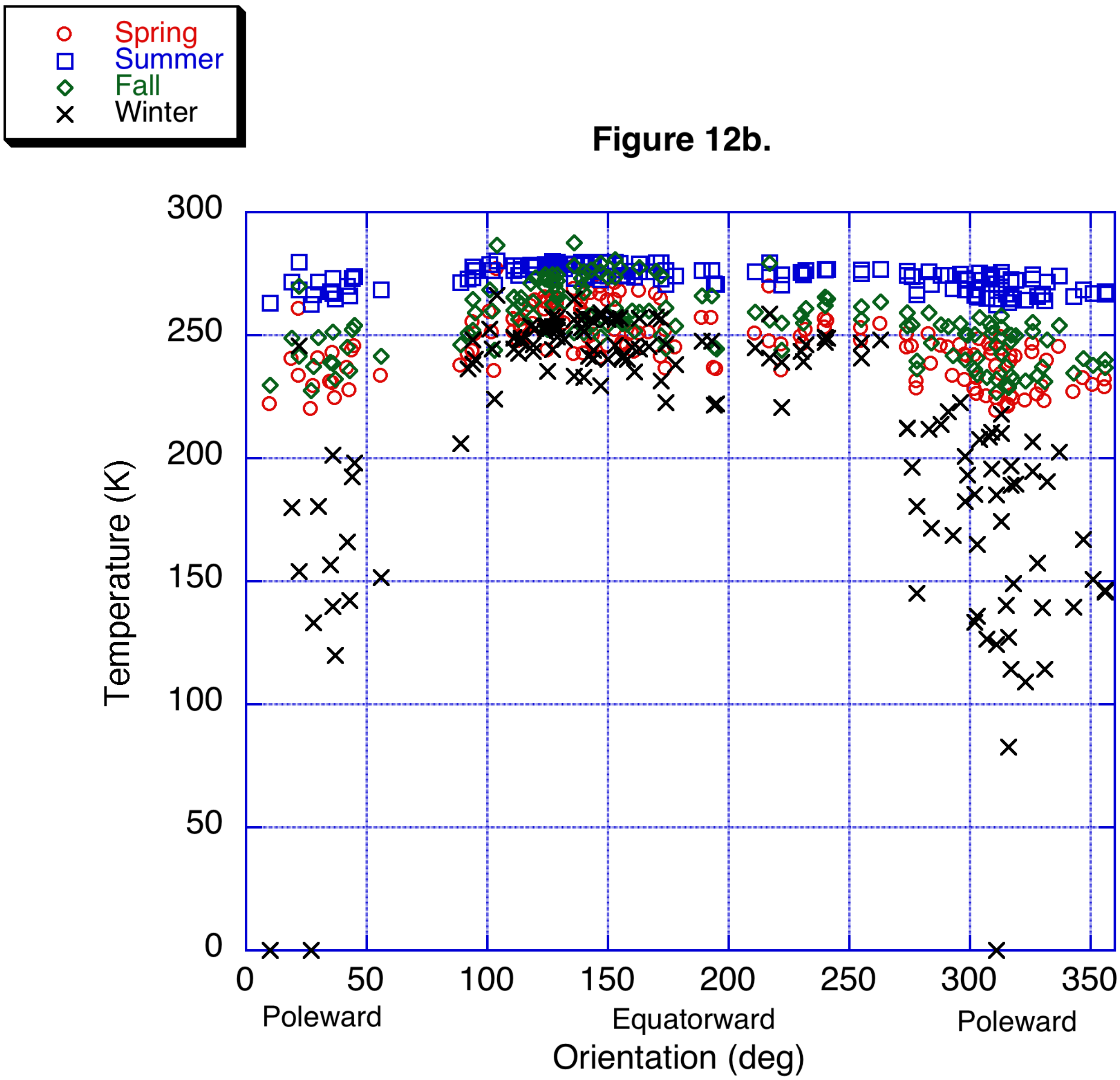
Spring
Summer
Fall
Winter
300
250
200
150
100
50
0
Temperature (K)
0
50
100
150
200
250
300
350
Poleward
Equatorward
Poleward
Orientation (deg)

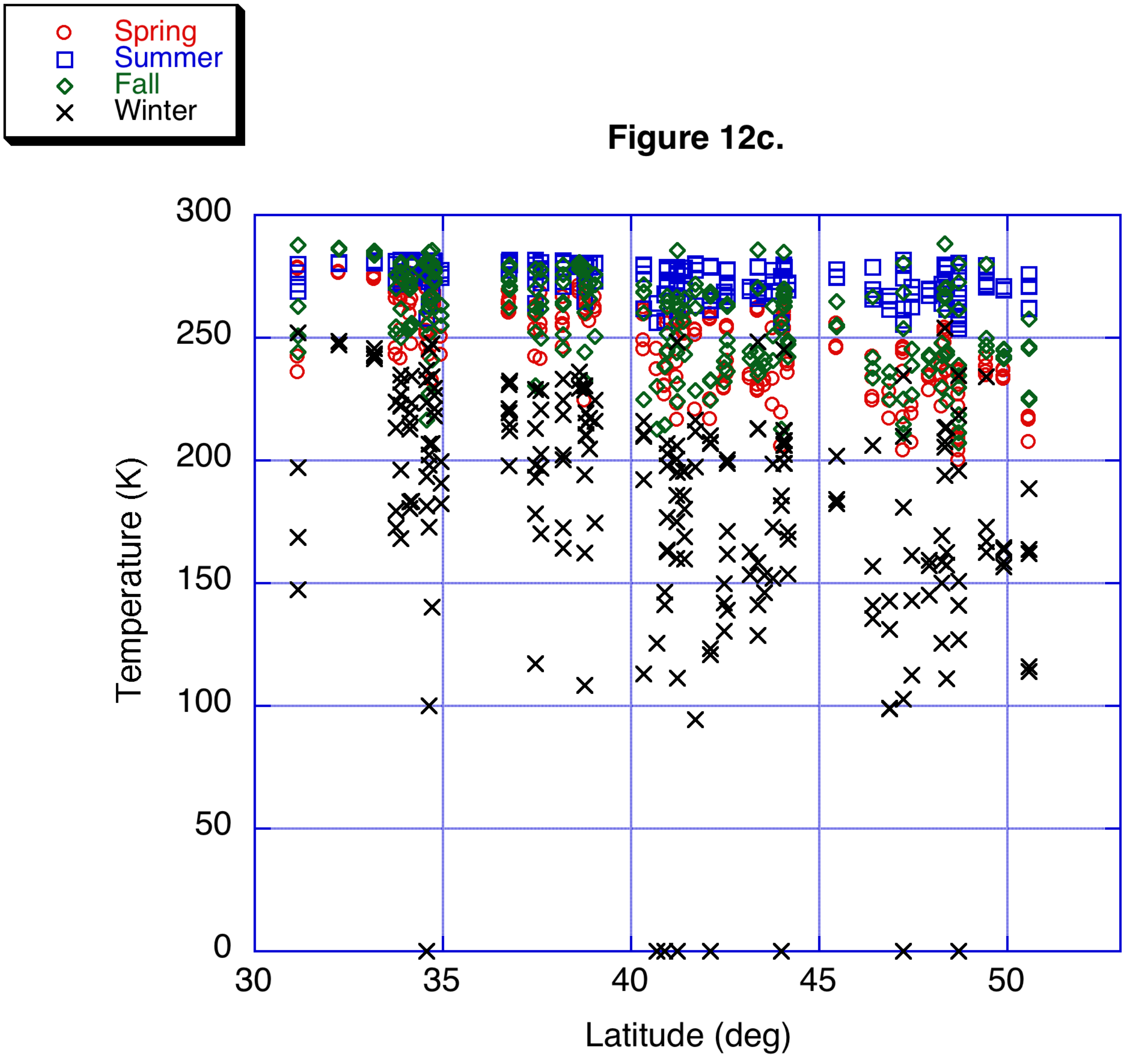
Spring
Summer
Fall
Winter
300
250
200
150
100
50
0
Temperature (K)
30
35
40
45
50
Latitude (deg)

Figure 12c.

Figure 12d.

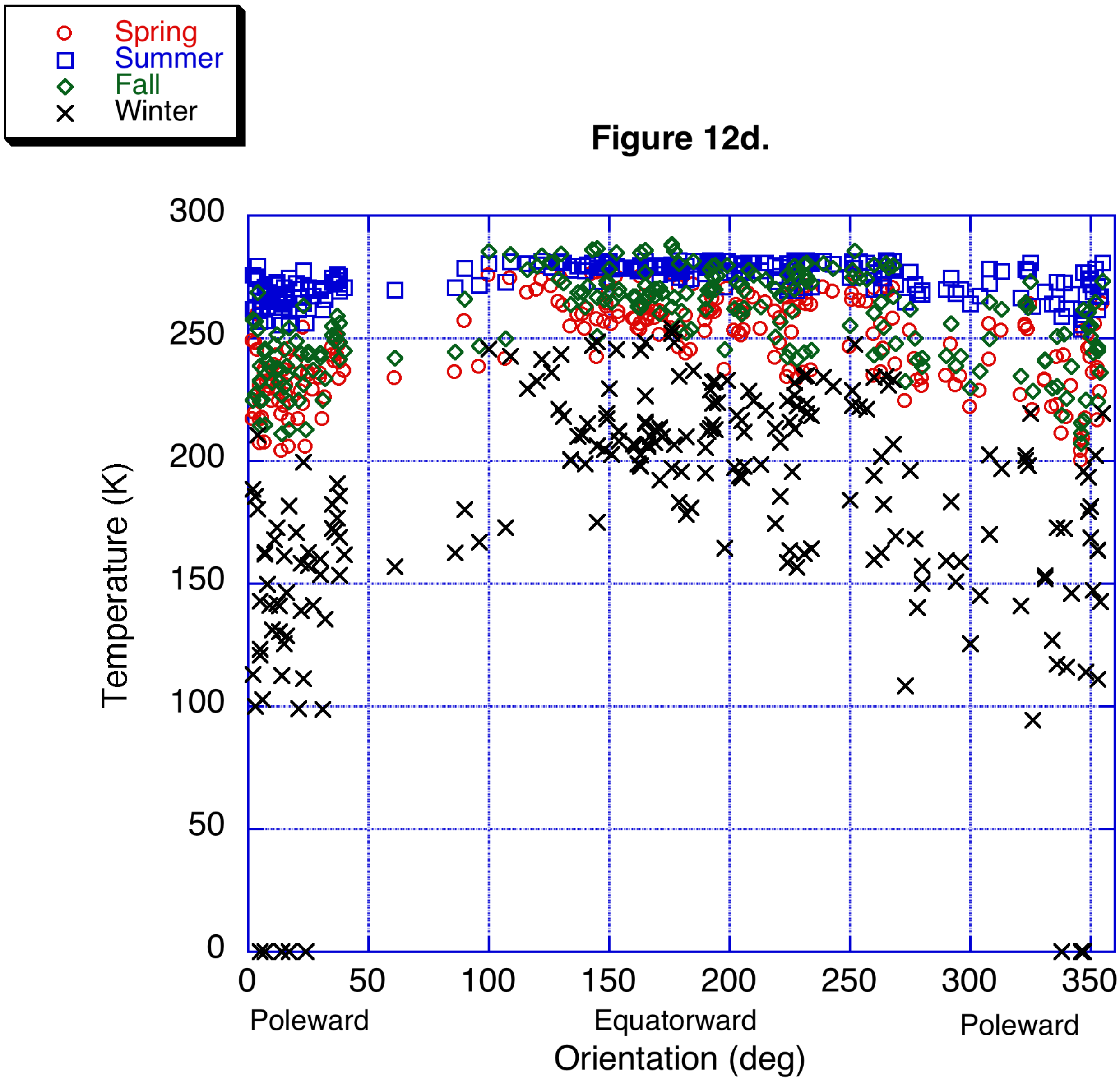

Spring
Summer
Fall
Winter
300
250
200
150
100
50
0
Temperature (K)
0
50
100
150
200
250
300
350
Poleward
Equatorward
Poleward
Orientation (deg)

Figure 13a.

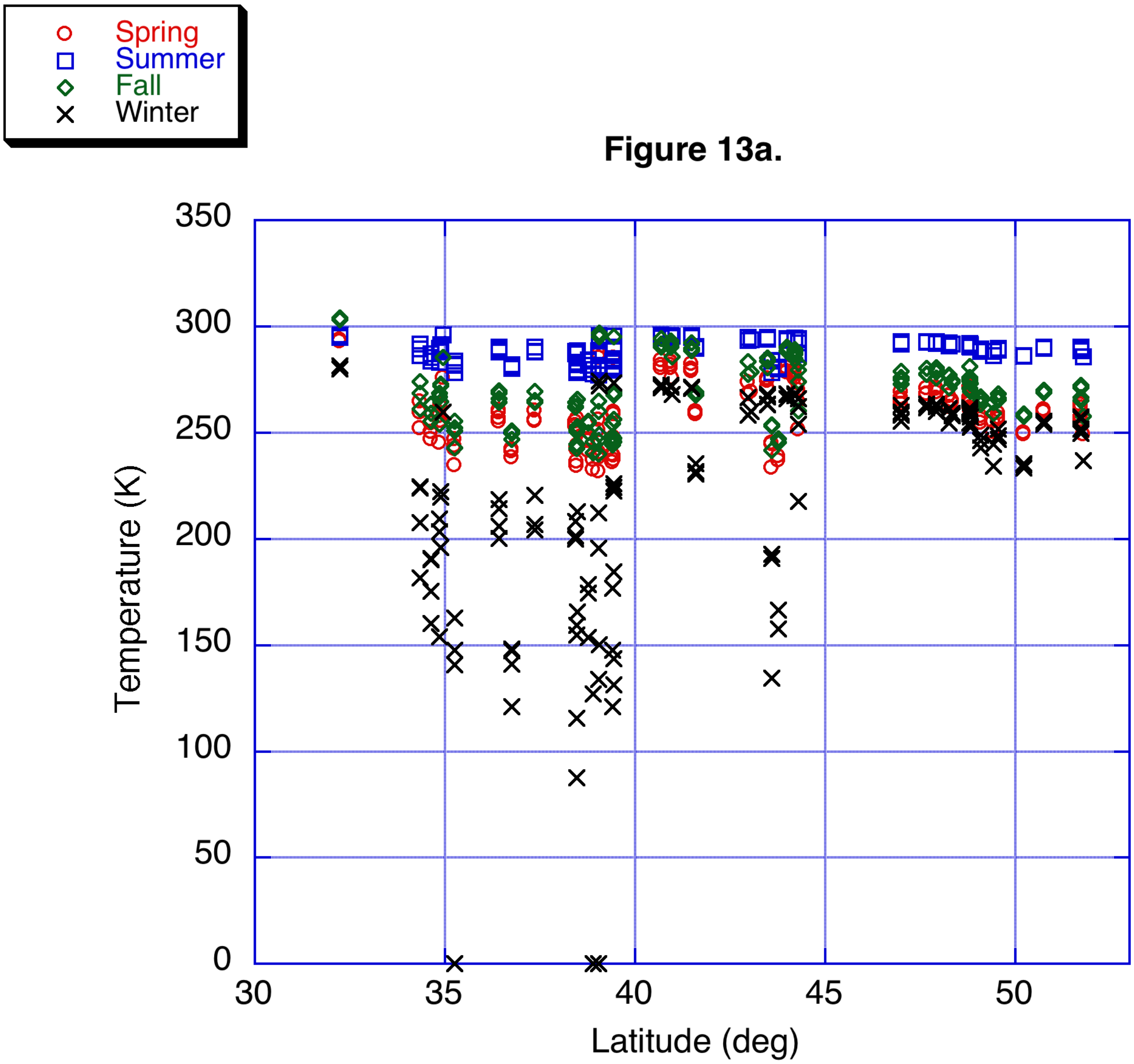

Spring
Summer
Fall
Winter
350
300
250
200
150
100
50
0
30
35
40
45
50
Temperature (K)
Latitude (deg)

Figure 13b.

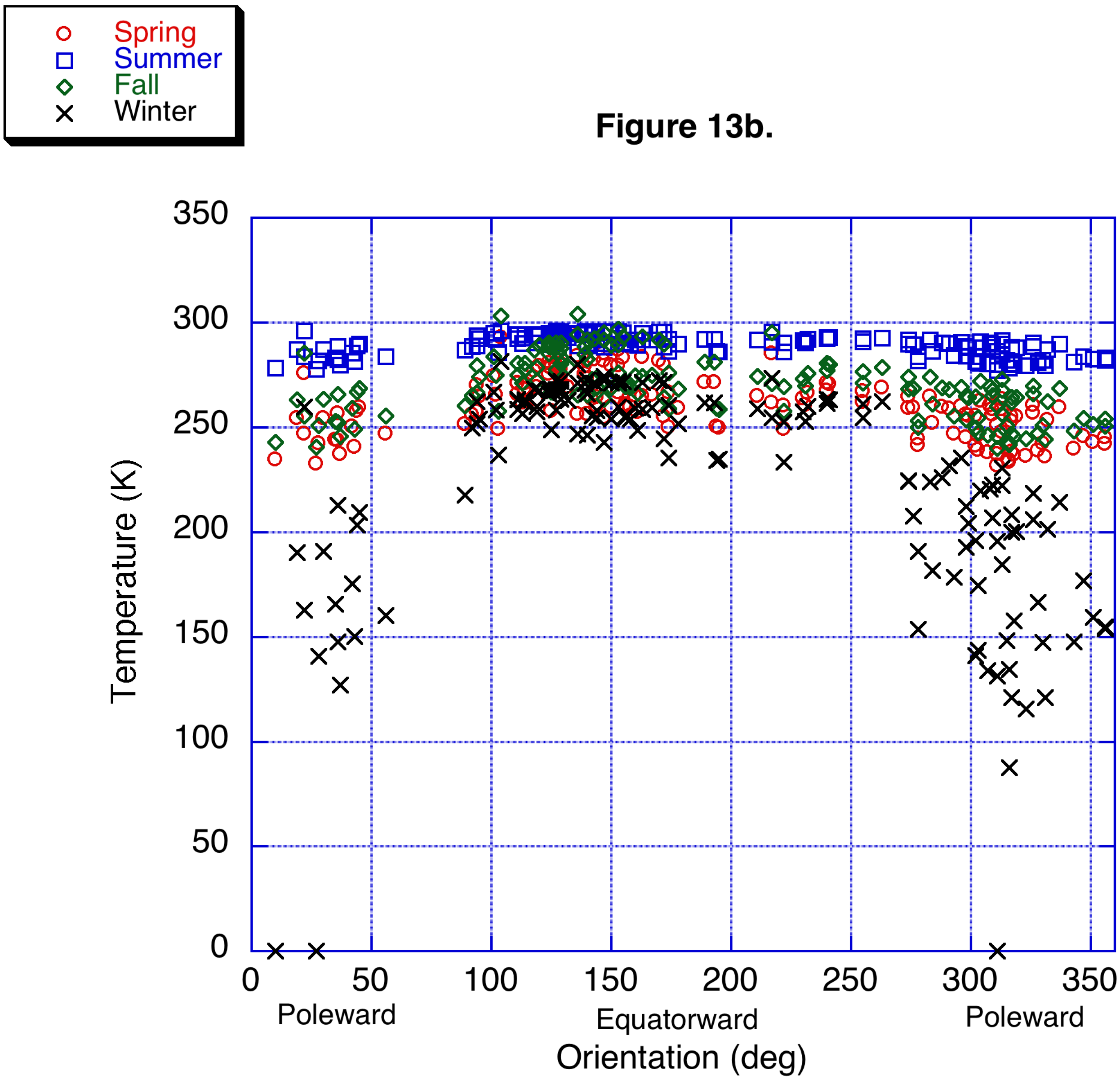

Spring
Summer
Fall
Winter
350
300
250
200
150
100
50
0
Temperature (K)
0
50
100
150
200
250
300
350
Poleward
Equatorward
Poleward
Orientation (deg)

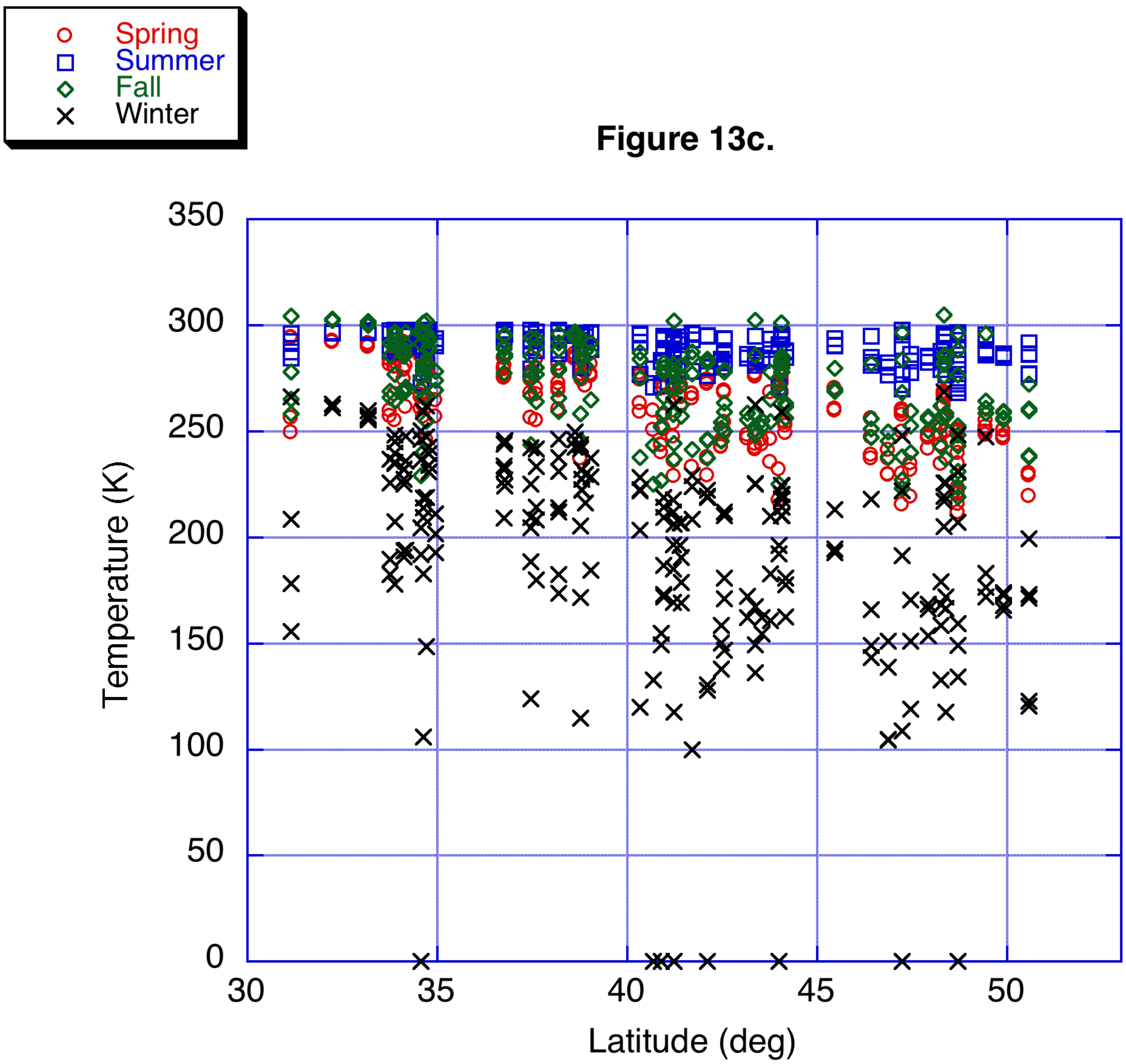

Spring
Summer
Fall
Winter
Figure 13c.
350
300
250
200
150
100
50
0
Temperature (K)
30
35
40
45
50
Latitude (deg)

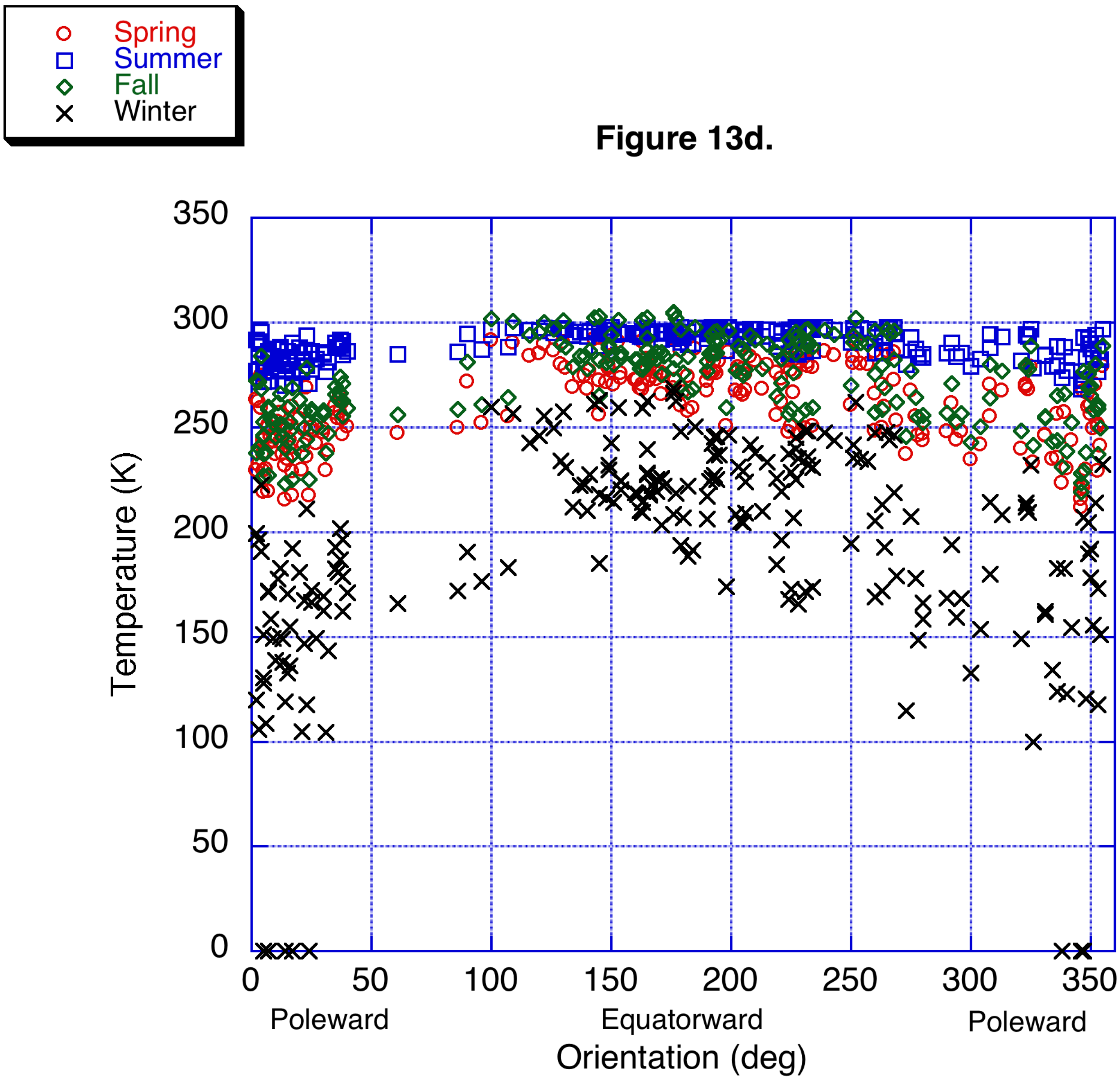

Spring
Summer
Fall
Winter
350
300
250
200
150
100
50
0
Temperature (K)
0
50
100
150
200
250
300
350
Poleward
Equatorward
Poleward
Orientation (deg)

Figure 13d.

Figure X1.

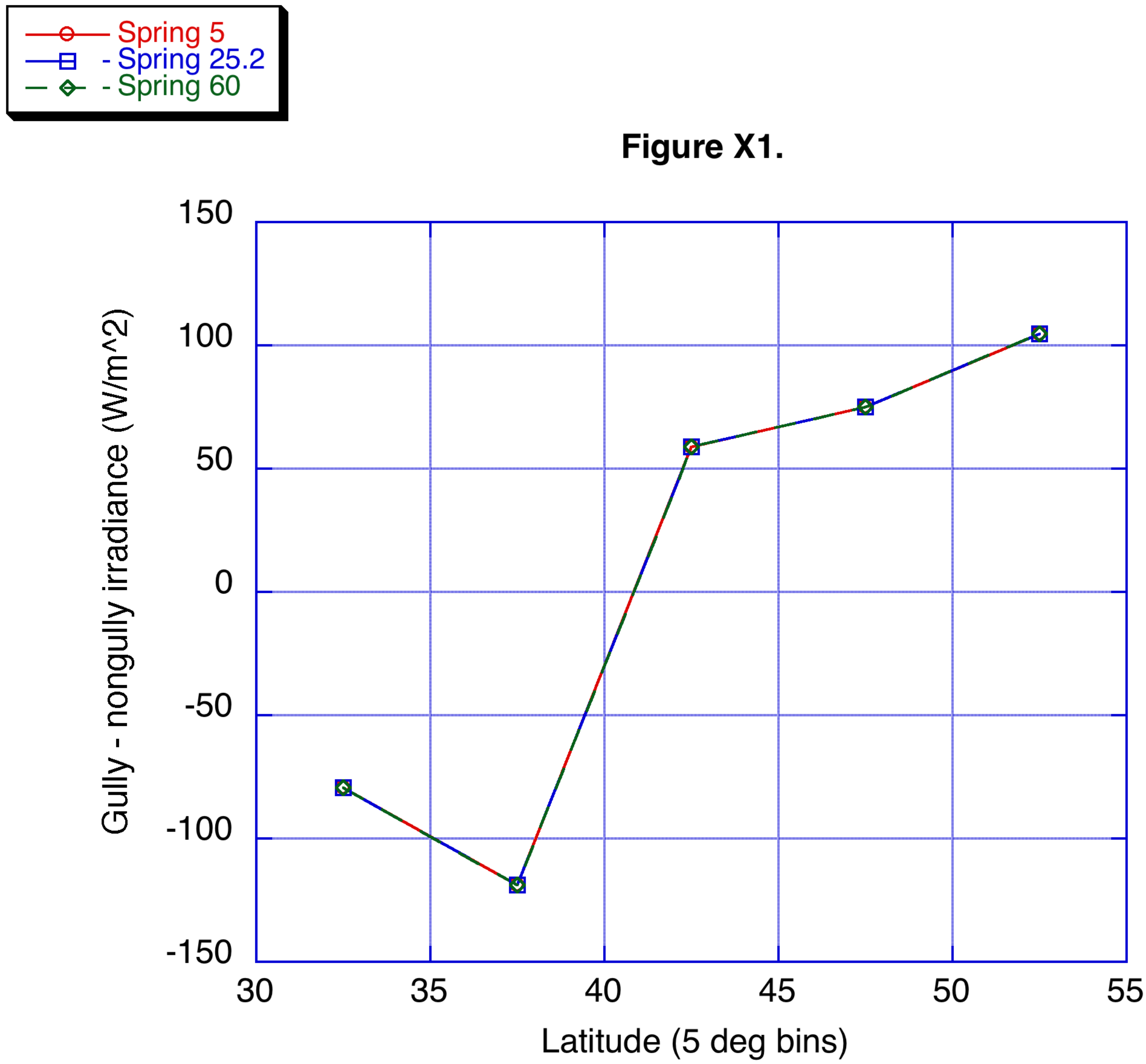

Spring 5
- Spring 25.2
- Spring 60
150
100
50
0
-50
-100
-150
30
35
40
45
50
55
Gully - nongully irradiance (W/m^2)
Latitude (5 deg bins)

Figure X2.

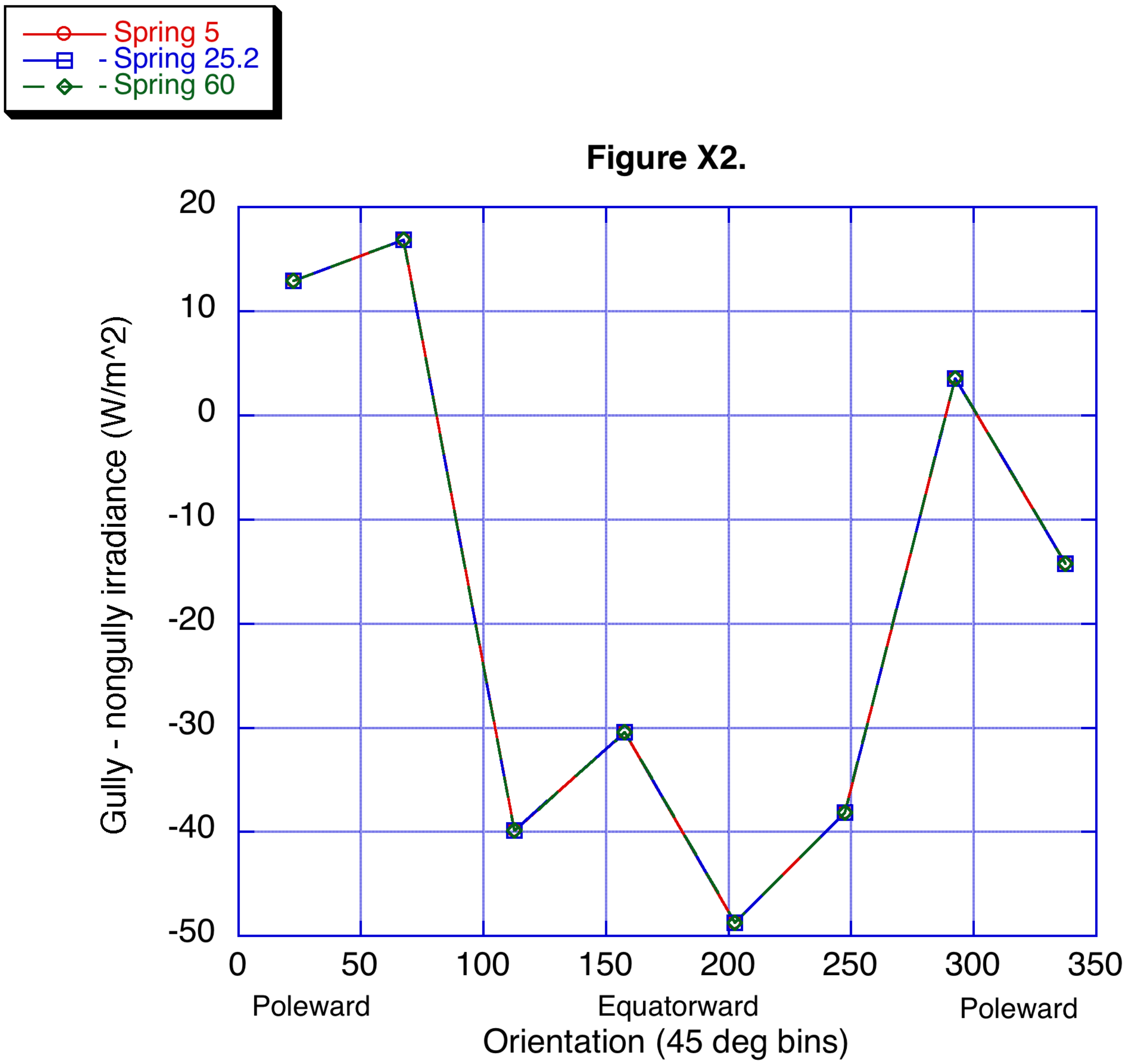

Spring 5
- Spring 25.2
- Spring 60
20
10
0
-10
-20
-30
-40
-50
Gully - nongully irradiance (W/m^2)
0
50
100
150
200
250
300
350
Poleward
Equatorward
Poleward
Orientation (45 deg bins)

Figure X3.

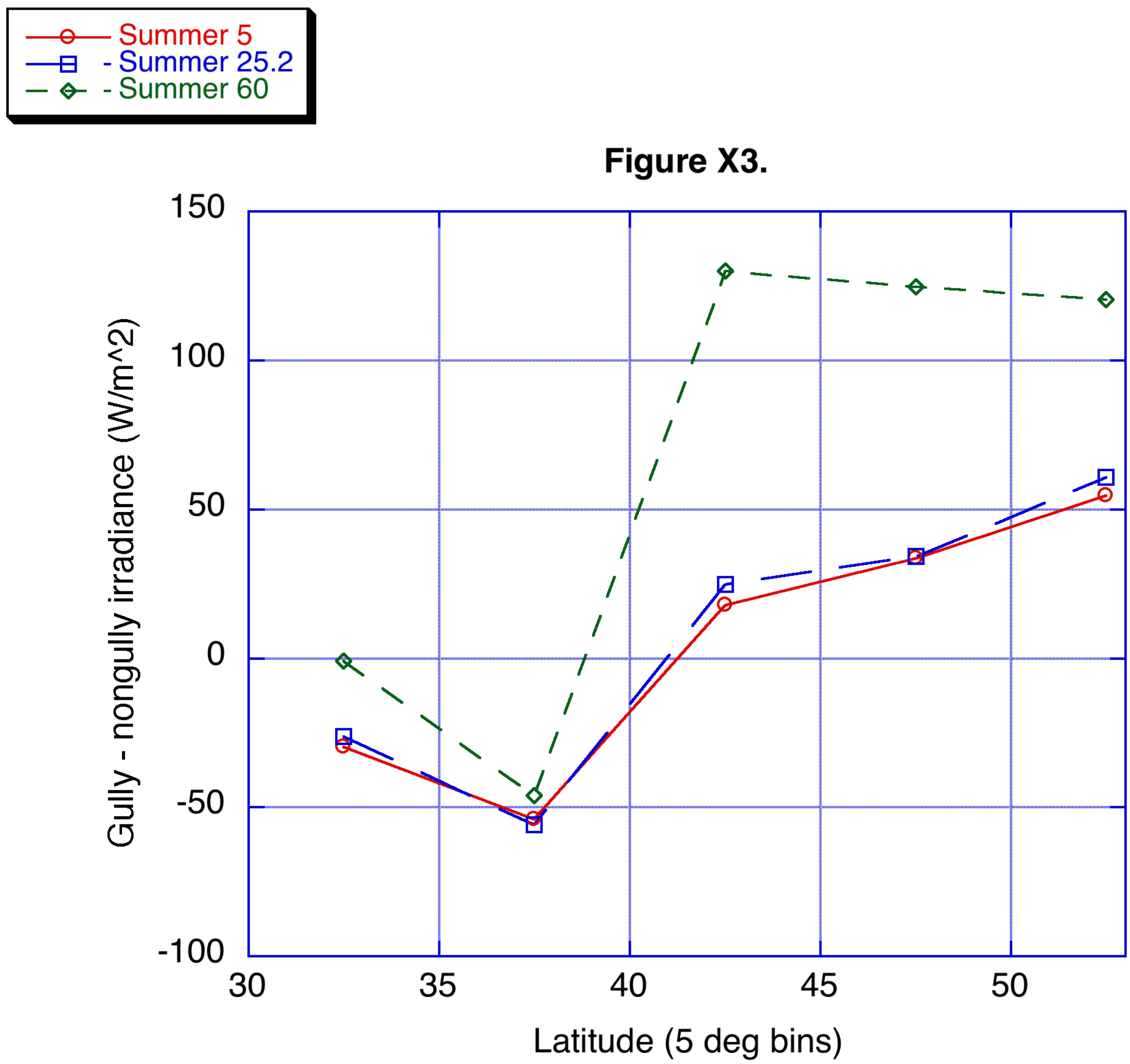

Summer 5
- Summer 25.2
- Summer 60
150
100
50
0
-50
-100
30
35
40
45
50
Gully - nongully irradiance (W/m^2)
Latitude (5 deg bins)

Figure X4.

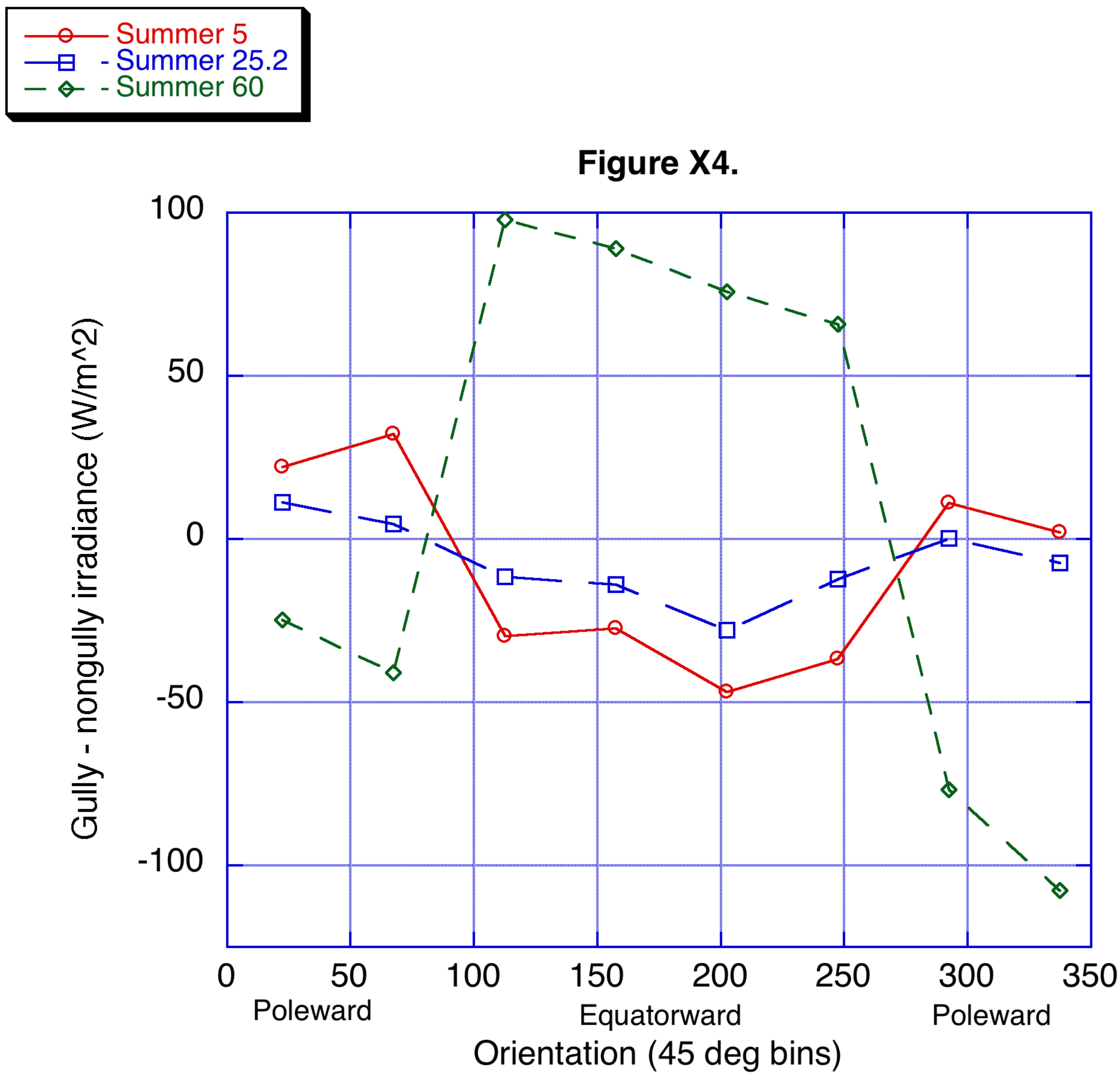
Summer 5
- Summer 25.2
- Summer 60
100
50
0
-50
-100
Gully - nongully irradiance (W/m^2)
0
50
100
150
200
250
300
350
Poleward
Equatorward
Poleward
Orientation (45 deg bins)

Figure X5.

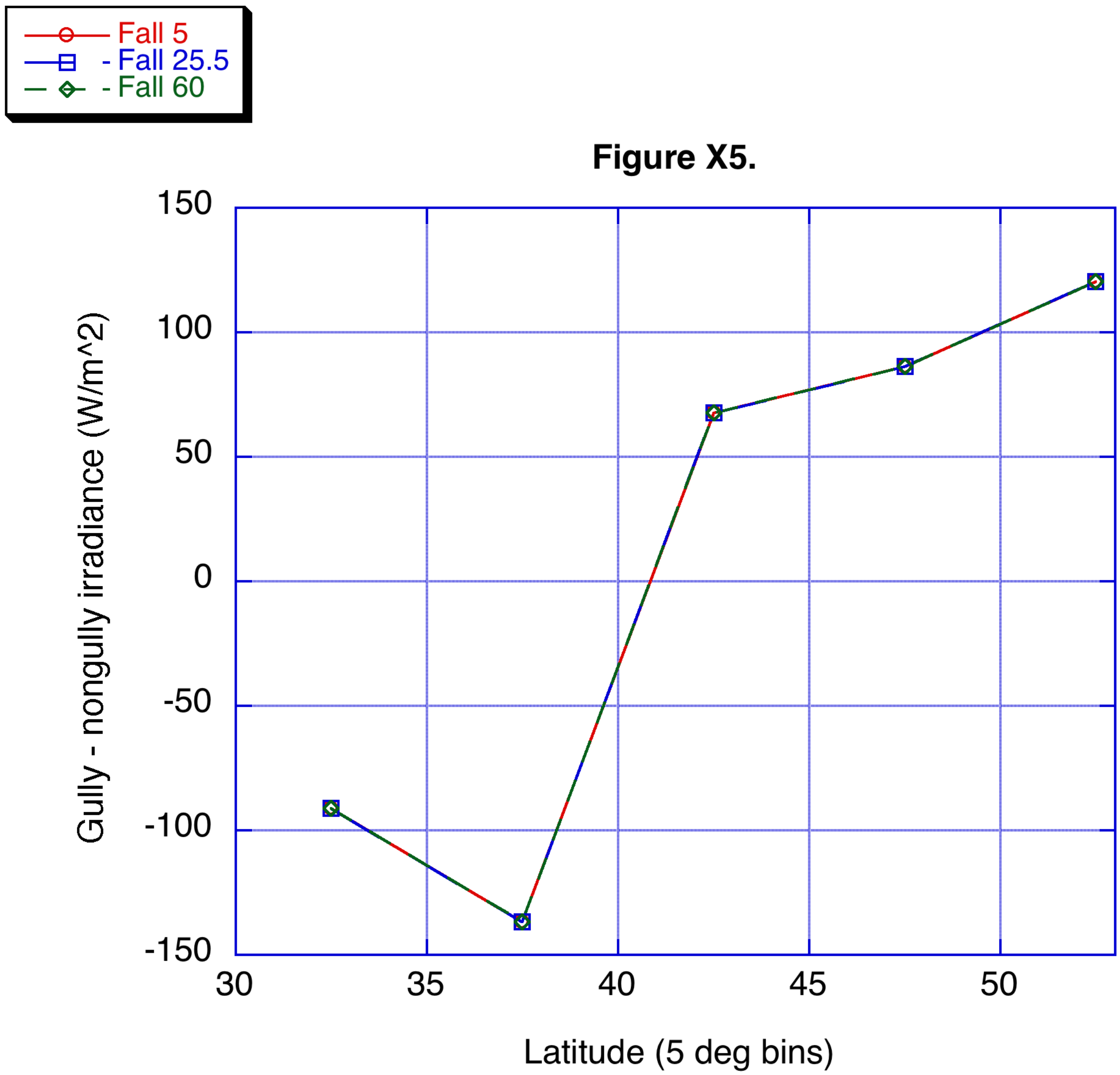

Fall 5
- Fall 25.5
- Fall 60
150
100
50
0
-50
-100
-150
30
35
40
45
50
Gully - nongully irradiance (W/m^2)
Latitude (5 deg bins)

Figure X6.

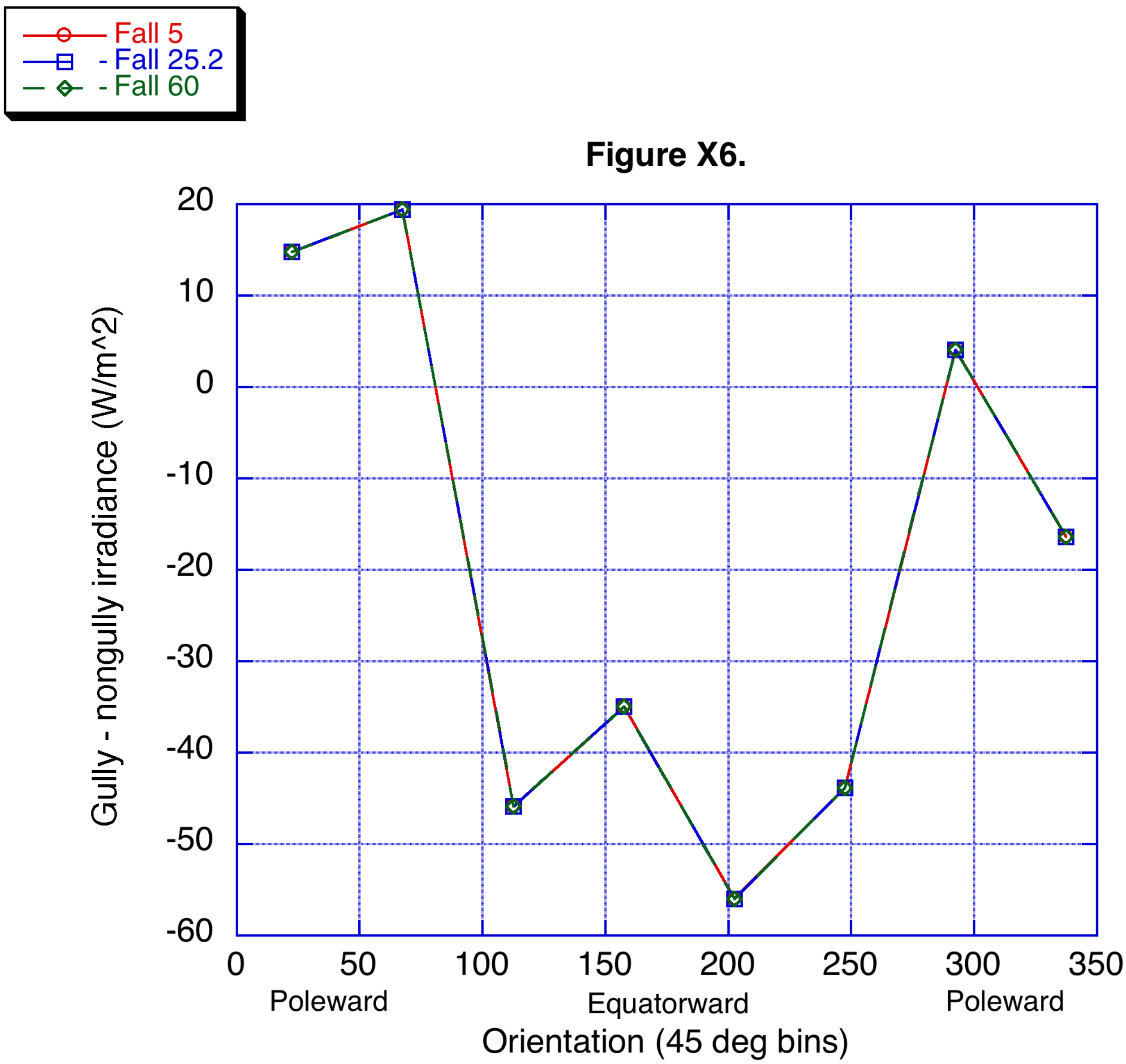

Fall 5
- Fall 25.2
- Fall 60
20
10
0
-10
-20
-30
-40
-50
-60
Gully - nongully irradiance (W/m^2)
0
50
100
150
200
250
300
350
Poleward
Equatorward
Poleward
Orientation (45 deg bins)

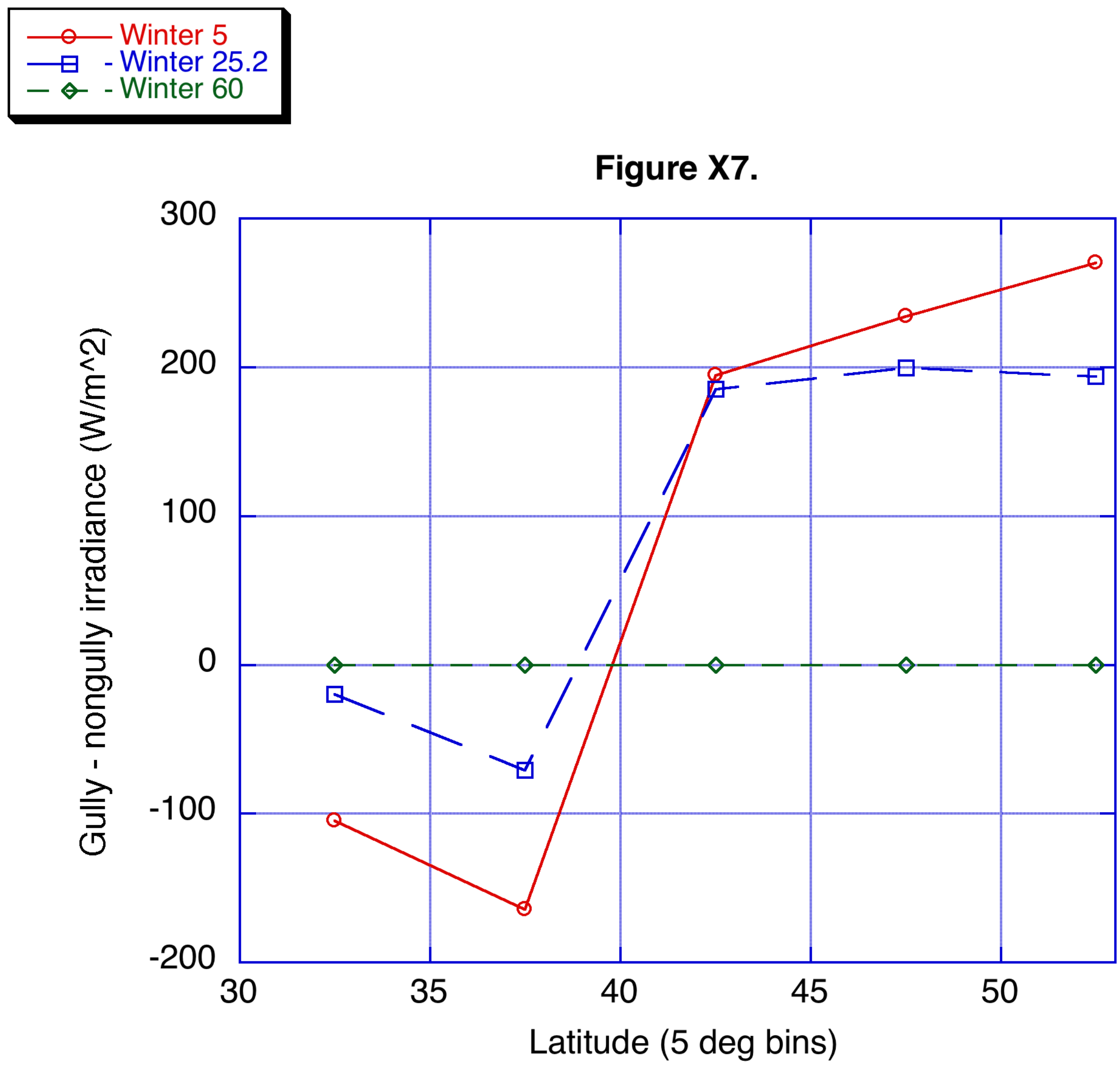

Winter 5
- Winter 25.2
- Winter 60
Figure X7.
300
200
100
0
-100
-200
30
35
40
45
50
Gully - nongully irradiance (W/m^2)
Latitude (5 deg bins)

Figure X8.

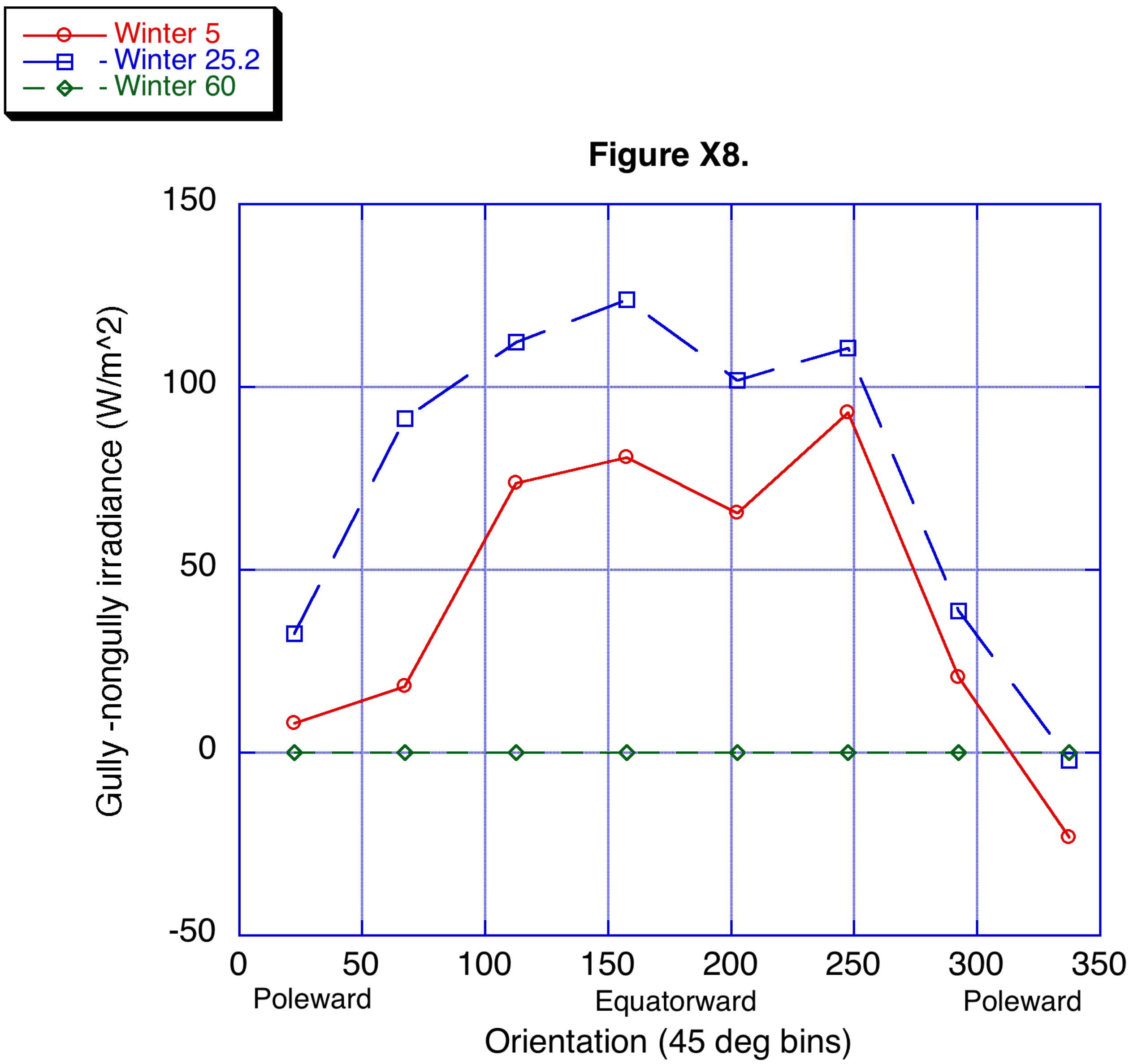

Winter 5
- Winter 25.2
- Winter 60
150
100
50
0
-50
Gully -nongully irradiance (W/m^2)
0
50
100
150
200
250
300
350
Poleward
Equatorward
Poleward
Orientation (45 deg bins)

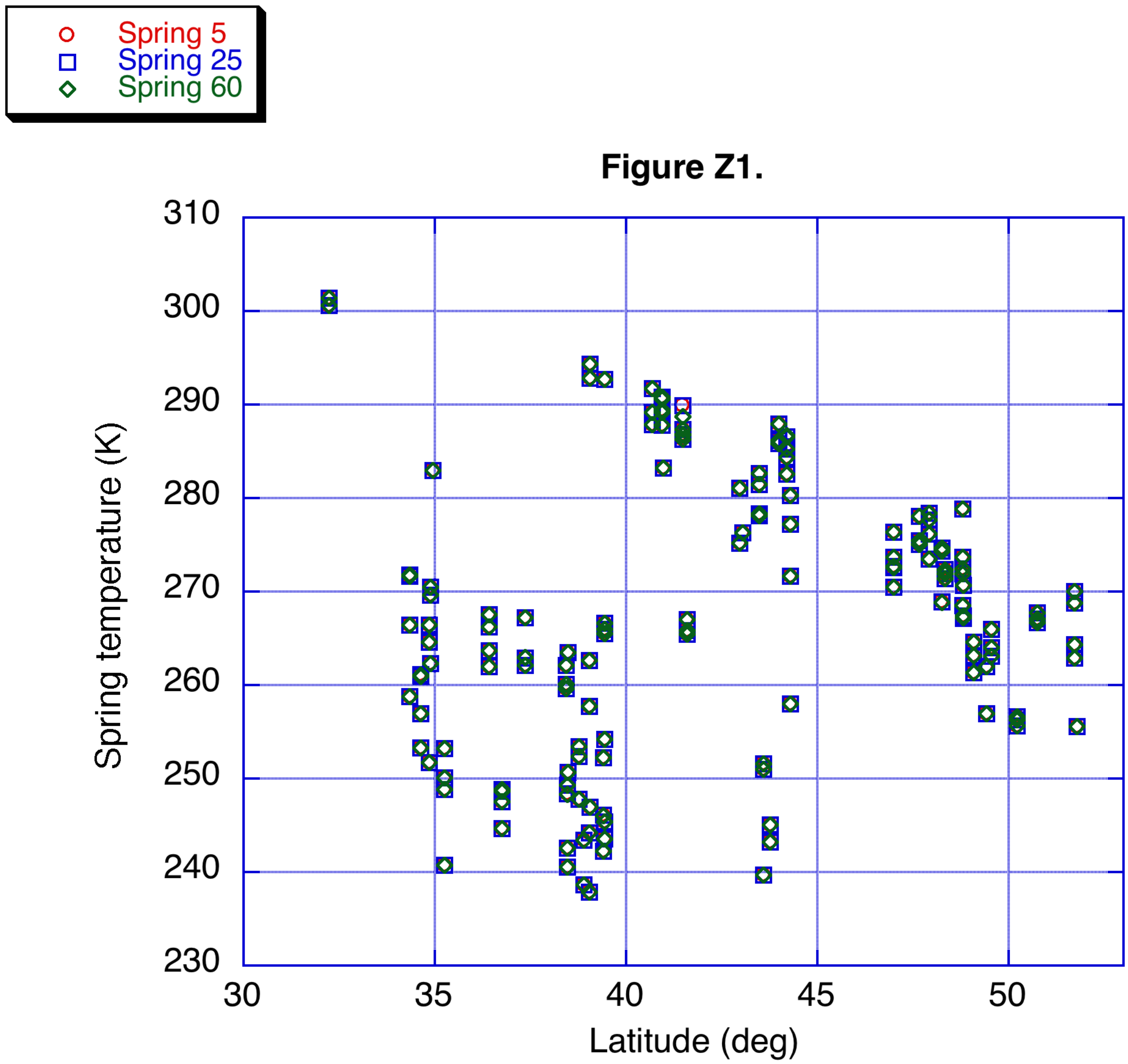

Spring 5
Spring 25
Spring 60
Spring temperature (K)
Latitude (deg)
310
300
290
280
270
260
250
240
230
30
35
40
45
50

Figure Z1.

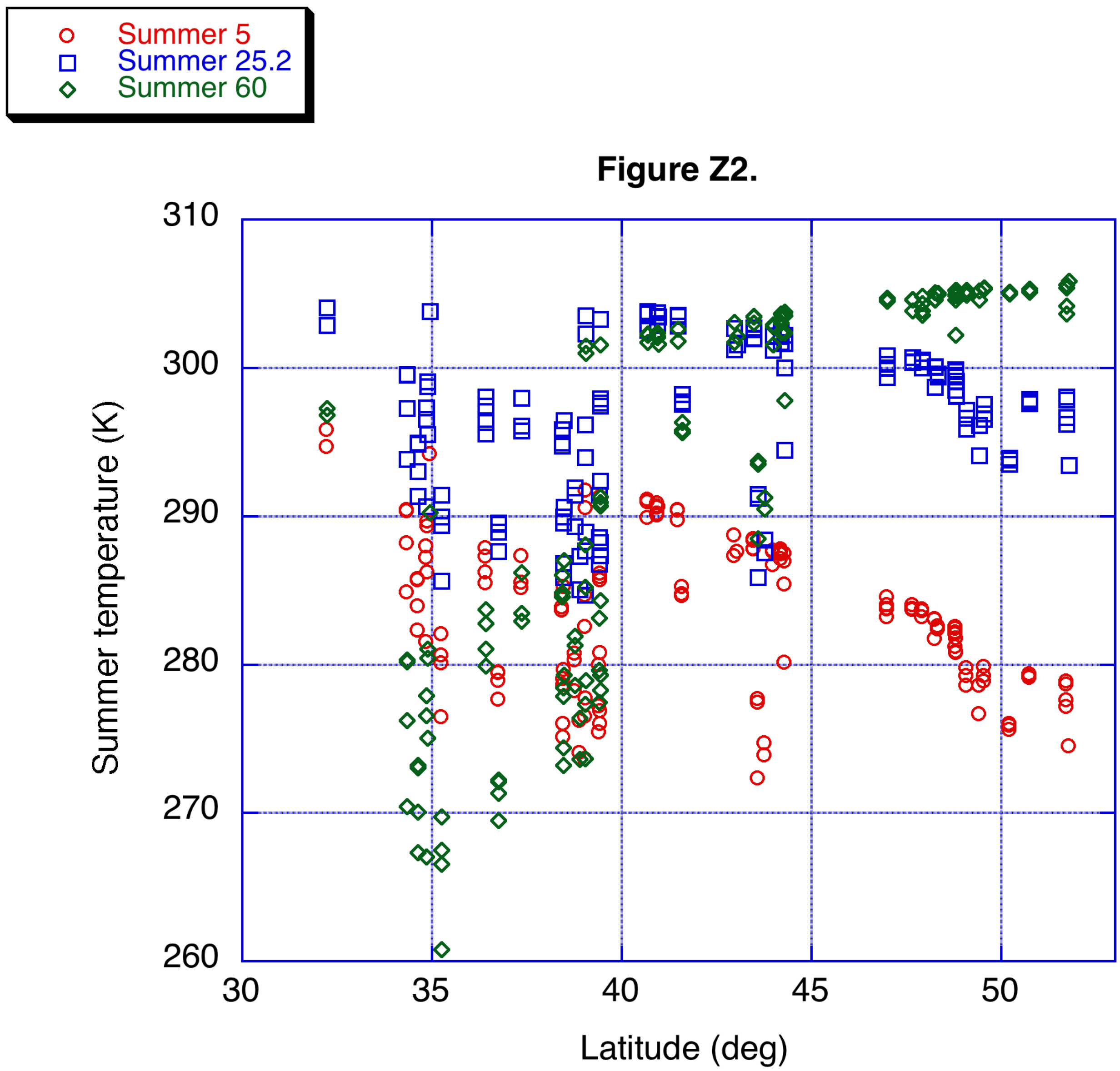

Summer 5
Summer 25.2
Summer 60
Figure Z2.
310
300
290
280
270
260
30
35
40
45
50
Summer temperature (K)
Latitude (deg)

Figure Z3.

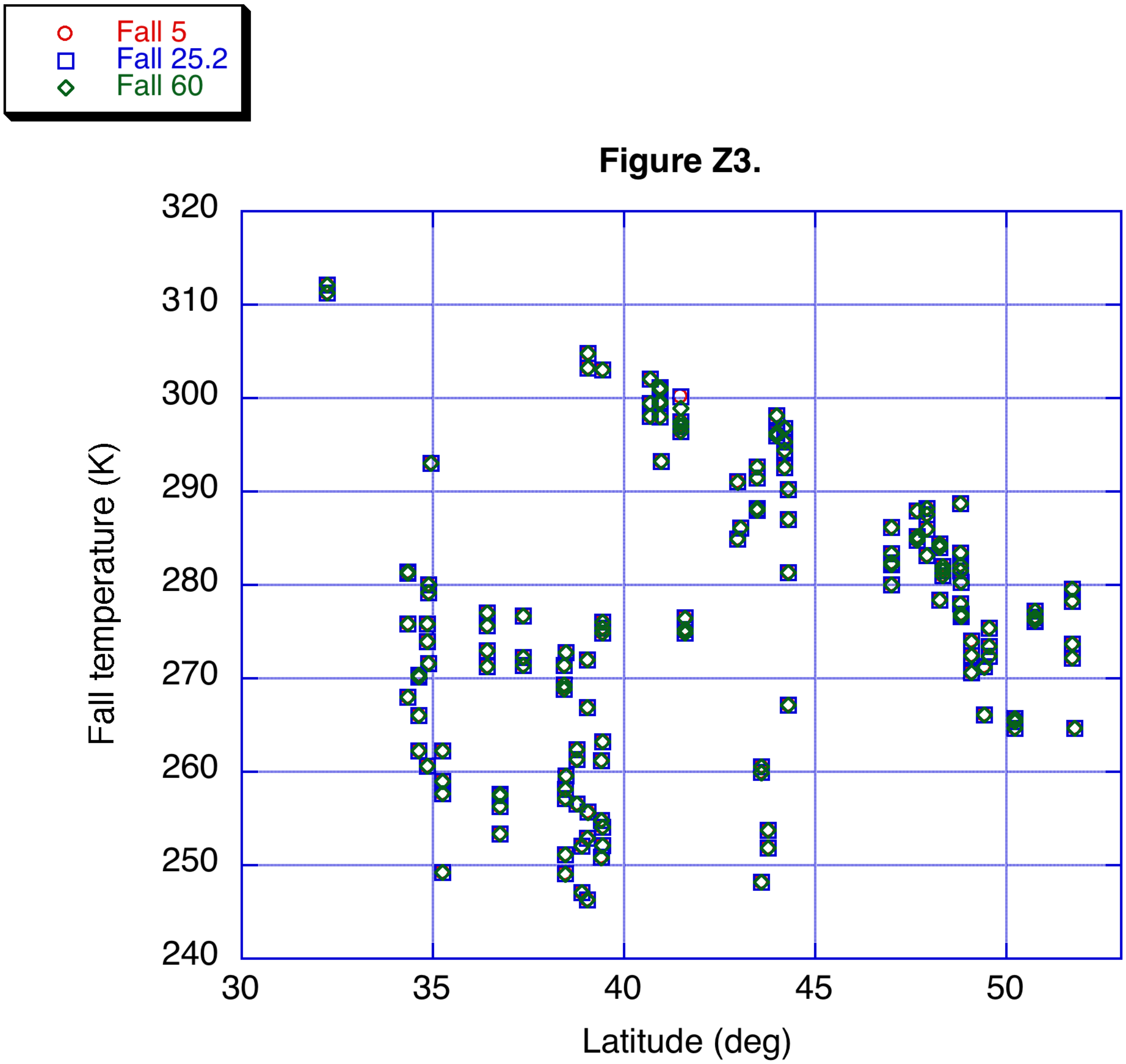

Fall 5
Fall 25.2
Fall 60
320
310
300
290
280
270
260
250
240
30
35
40
45
50
Fall temperature (K)
Latitude (deg)

Figure Z4.

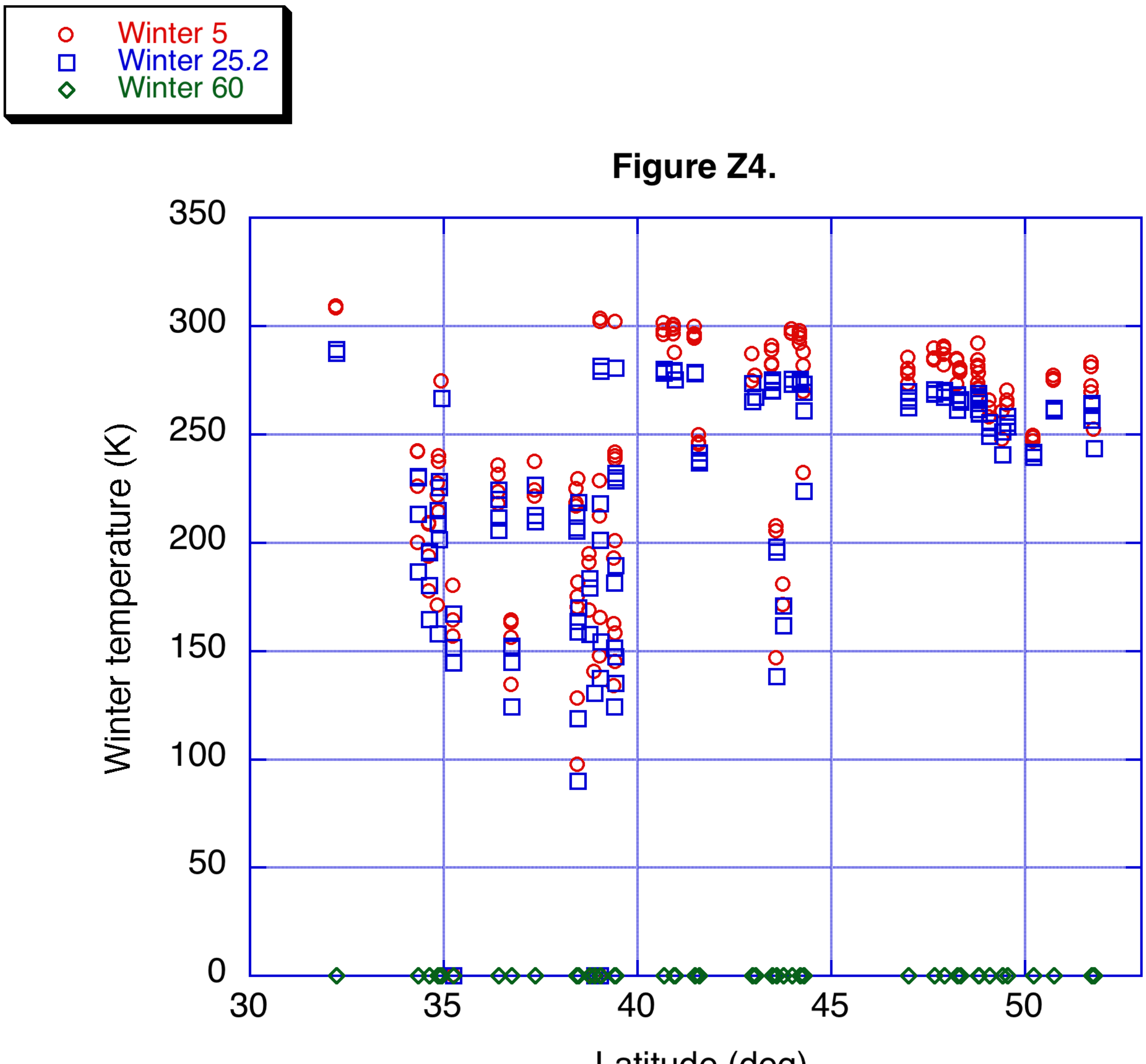
Winter 5
Winter 25.2
Winter 60
350
300
250
200
150
100
50
0
30
35
40
45
50
Winter temperature (K)
Latitude (deg)

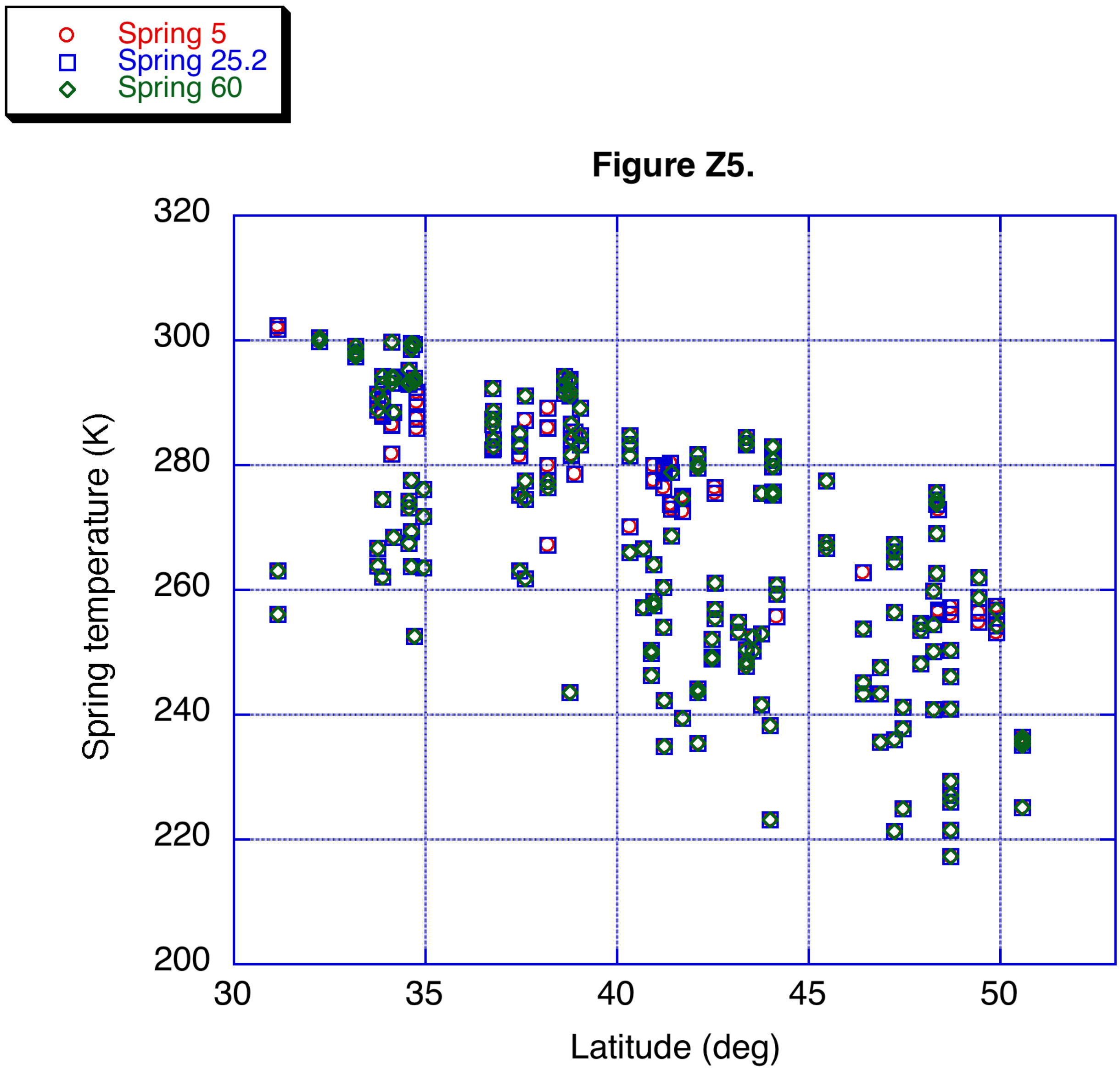
Spring 5
Spring 25.2
Spring 60
320
300
280
260
240
220
200
30
35
40
45
50
Spring temperature (K)
Latitude (deg)

Figure Z5.

Figure Z6.

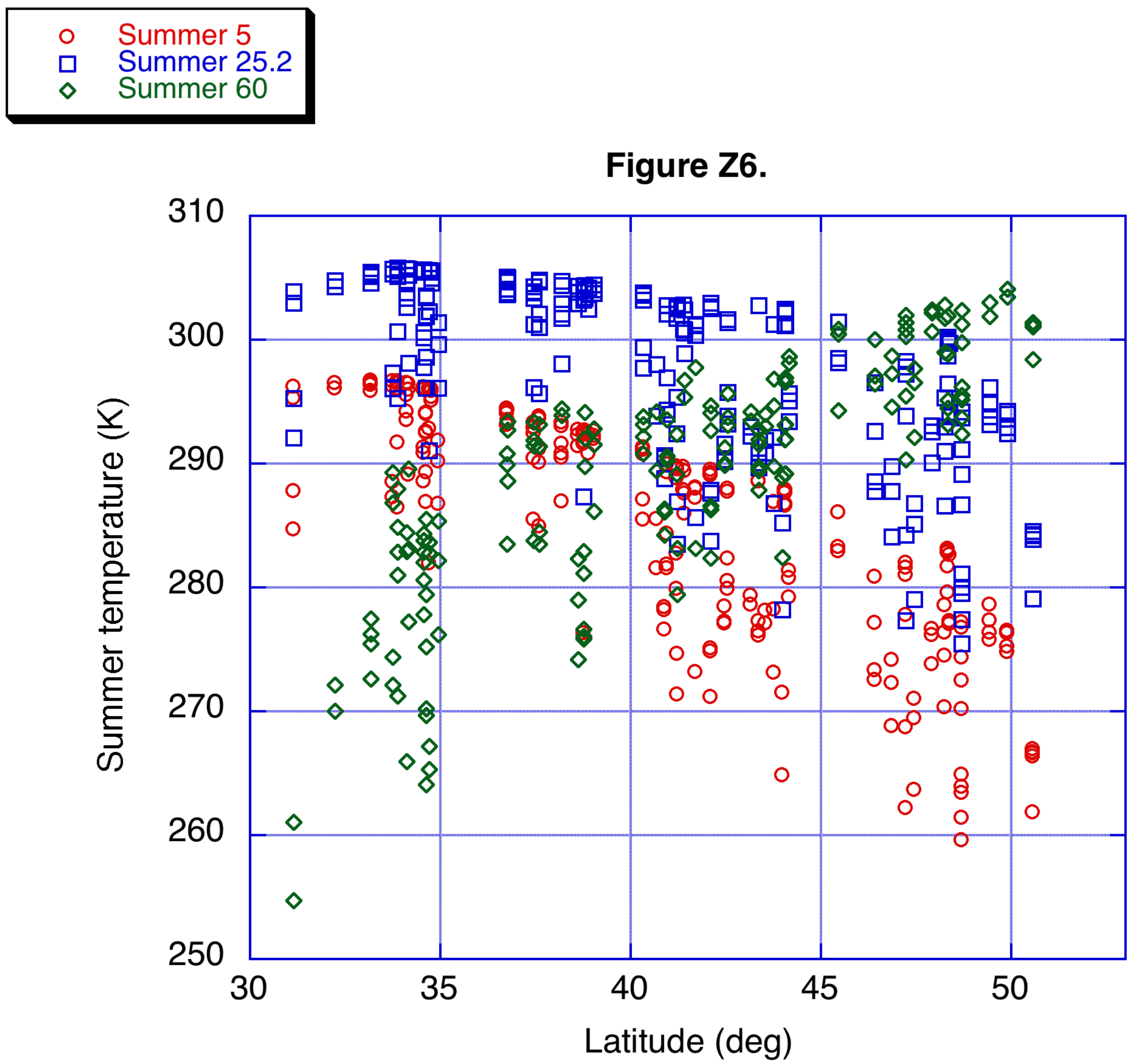

Summer 5
Summer 25.2
Summer 60
310
300
290
280
270
260
250
30
35
40
45
50
Summer temperature (K)
Latitude (deg)

Figure Z7.

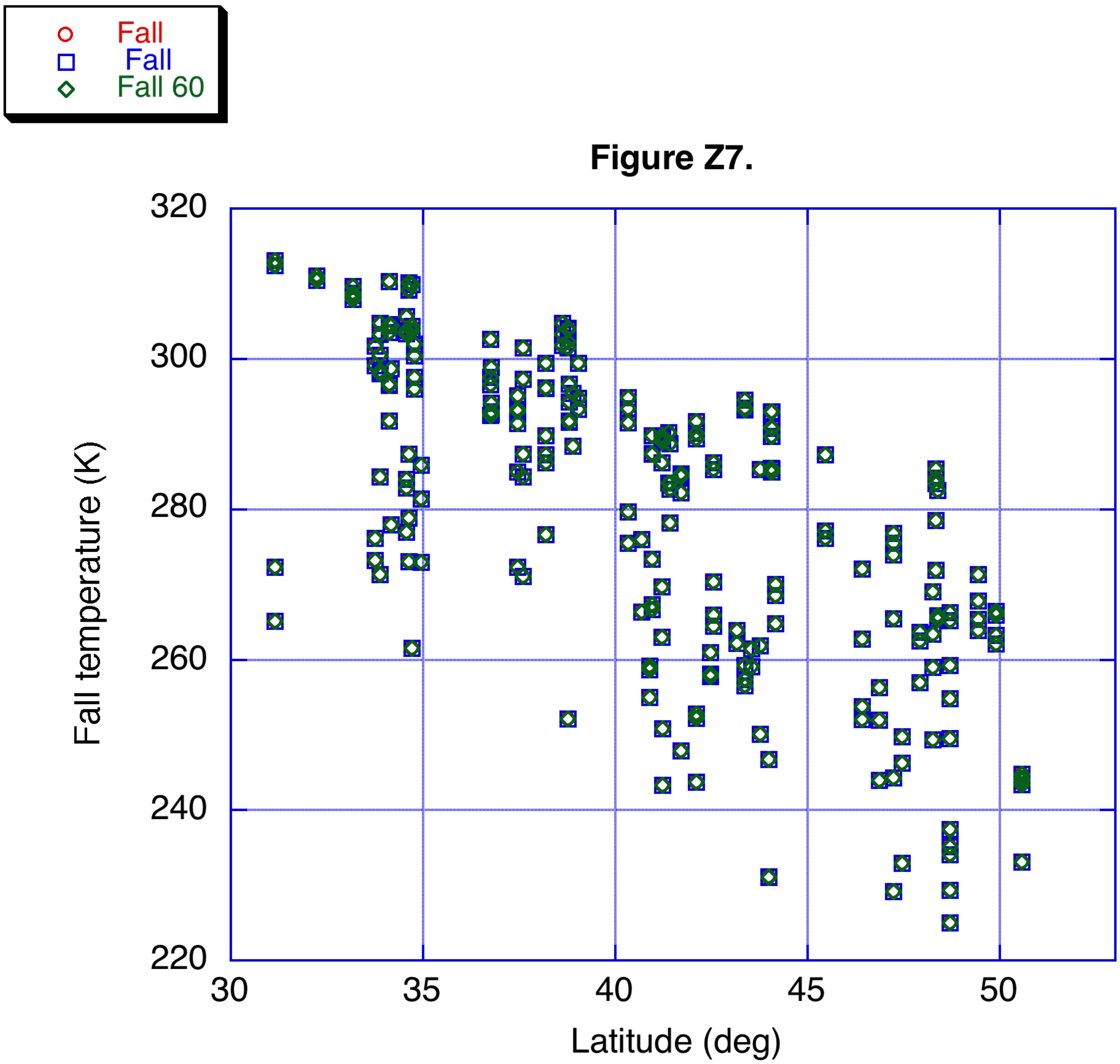

Fall
Fall
Fall 60
320
300
280
260
240
220
30
35
40
45
50
Fall temperature (K)
Latitude (deg)

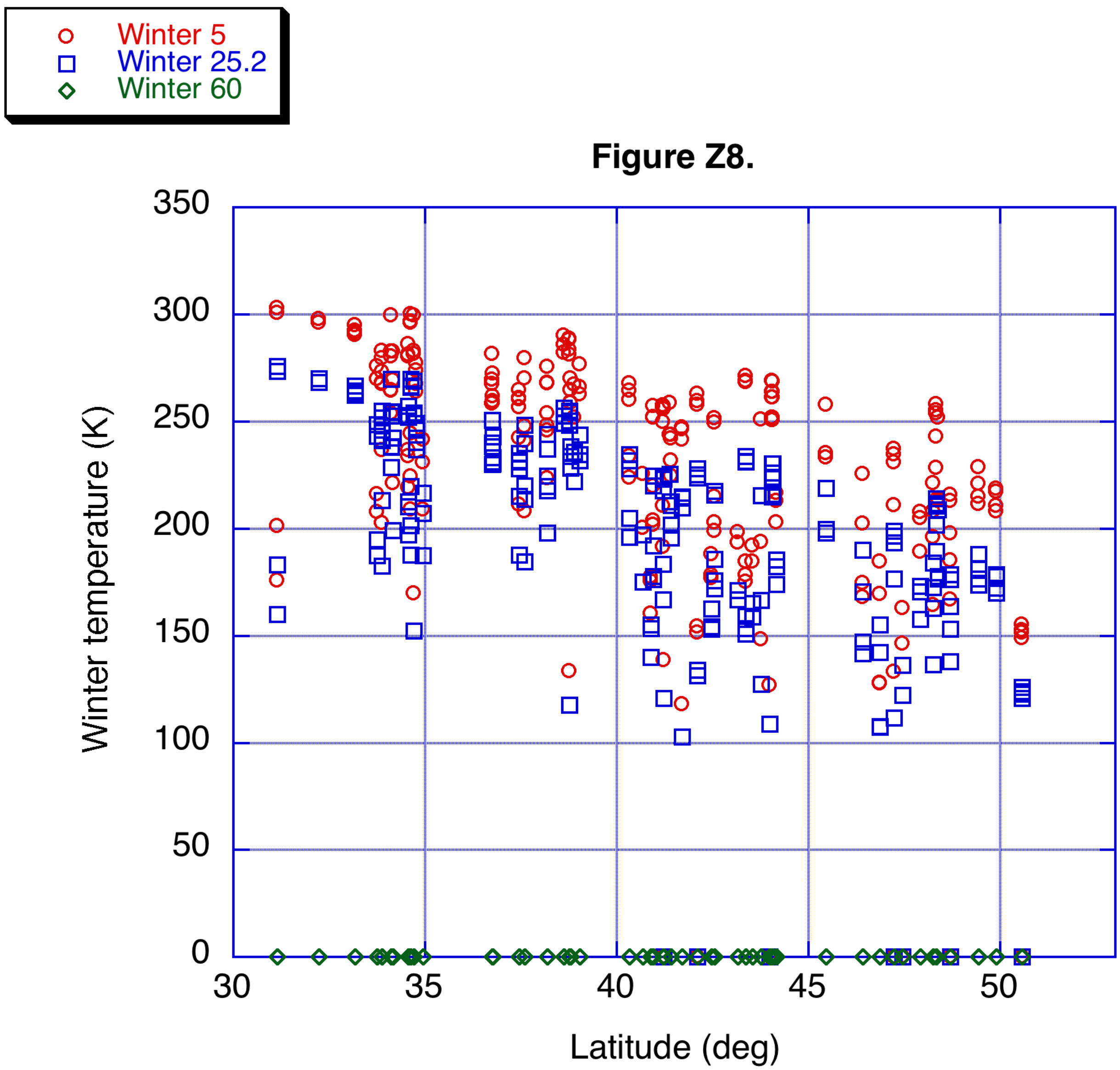
Winter 5
Winter 25.2
Winter 60
Figure Z8.
350
300
250
200
150
100
50
0
30
35
40
45
50
Winter temperature (K)
Latitude (deg)